



Corso di Laurea Magistrale in Ingegneria Biomedica
Tesi di Laurea Magistrale

Design and Testing of a Tendon-Like Orthosis Actuated by
Shape Memory Alloy Wires and Controlled by Myoelectric Signals

Relatore:
Prof. Marco Gazzoni

Candidato:
Elsebeth Nagels

Correlatore:
Dott. Ric. Giacinto Luigi Cerone

Anno accademico 2018/2019

Table of content

TABLE OF CONTENT	3
ABSTRACT	5
1 INTRODUCTION	7
1.1 ANATOMY OF THE HUMAN HAND	9
1.1.1 <i>Bones and Joints</i>	10
1.1.2 <i>Muscles</i>	11
1.1.3 <i>Tendons and Ligaments</i>	13
1.2 ARTIFICIAL MUSCLES	15
1.3 STATE OF THE ART	17
1.3.1 <i>Pneumatic and hydraulic gloves</i>	20
1.3.2 <i>Electric motors (DC)</i>	24
1.3.3 <i>Shape Memory Alloy (SMA) driven actuators</i>	29
1.4 SHAPE MEMORY ALLOYS	32
1.4.1 <i>Austenite and martensite transformation</i>	32
1.4.2 <i>Mechanical behavior</i>	34
1.4.3 <i>Pseudo-elasticity</i>	35
1.4.4 <i>Shape memory effect</i>	36
1.4.5 <i>Application technologies</i>	37
1.4.6 <i>Technical specifications</i>	38
2 DESIGN GOALS AND REQUIREMENTS.....	40
2.1 CURRENT SITUATION.....	41
2.1.1 <i>Functional design requirements</i>	43
2.1.2 <i>Technical specifications</i>	46
2.2 SYSTEM'S ARCHITECTURE	51
2.2.1 <i>SMA driver</i>	51
2.2.2 <i>SMA wire modules</i>	52
2.2.3 <i>EMG system</i>	52
2.2.4 <i>Software</i>	53
3 DESIGN AND PROTOTYPING	56
3.1 PROTOTYPING OF SMA-WIRE MODULE	56
3.1.1 <i>First prototype</i>	57
3.1.2 <i>Second prototype</i>	60
3.1.3 <i>Final design</i>	65
3.2 PROTOTYPING OF GLOVE	66
3.2.1 <i>Tendon system</i>	66
4 TESTS.....	68
4.1 FINAL TEST ON DUMMY HAND.....	68
4.1.1 <i>Test protocol</i>	68
4.1.2 <i>Test results</i>	72
4.2 FINAL TEST ON SUBJECT	78
4.3 EMG TEST	84
5 CONCLUSION AND RECOMMENDATIONS.....	87
5.1 CONCLUSIONS	87
5.2 RECOMMENDATIONS	89
ACKNOWLEDGEMENTS.....	92
BIBLIOGRAPHY	93

Abstract

This thesis is part of a project concerning the development of a tendon-like orthosis actuated by shape memory alloys wires which function as artificial muscles to compensate the hand weakness in post-stroke patients. The wearable device uses Nitinol wires for mechanical actuation of the orthosis, while the motion transmission to the affected hand is realized through a tendon-like, joint-less system attached to a soft glove.

Surface electromyographic (EMG) signal is measured on the subjects' forearm and integrated into the control system of the artificial muscles. Optimizations in the software have been implemented to improve actuator control functions.

With the use of shape memory alloys and 3D-printing techniques, a functional prototype is constructed which is adjustable to different subjects due to its size adjustment possibility, modularity and universal linkage to the glove for any of the finger motions.

Tests have been conducted on a dummy hand and on four subjects to gather data to confront the range of motion and repeatability of the motion. A final test shows the functionality of the system by actuating the subjects' right arm in a mirror motion due to control by the EMG signal measured on the left arm.

Sommario

Questa tesi fa parte di un progetto riguardante lo sviluppo di un'ortesi tendon-like azionato da fili di leghe a memoria di forma che funzionano come muscoli artificiali per compensare la mancanza di forza nella mano nei pazienti post-ictus. Il dispositivo indossabile utilizza fili in Nitinol per l'attuazione meccanica dell'ortesi, mentre la trasmissione del movimento alla mano interessata viene realizzata attraverso un sistema tendon-like e jointless a un guanto morbido.

Il segnale elettromiografico superficiale (EMG) viene misurato sull'avambraccio dei soggetti e integrato nel sistema di controllo dei muscoli artificiali. Ottimizzazioni nel software sono state implementate per migliorare le funzioni di controllo dell'attuatore.

Con l'uso di leghe a memoria di forma e tecniche di stampa 3D, viene costruito un prototipo funzionale che è regolabile per diversi soggetti grazie alla possibilità di regolazione delle dimensioni, alla modularità e al collegamento universale al guanto per qualsiasi movimento delle dita.

I test sono stati condotti su una manichino e su quattro soggetti per raccogliere dati per affrontare il Range of Motion e la ripetibilità del movimento. Un test finale mostra la funzionalità del sistema azionando il braccio destro dei soggetti in un movimento a specchio a causa del controllo del segnale EMG misurato sul braccio sinistro.

Chapter 1: Introduction

The human hand is a complex organ capable of doing many different tasks. Unfortunately, many people have difficulties in executing even the most basic tasks, like opening the hand and grasp objects. Often hand disabilities occur with diseases such as spinal cord injury, Cerebral Palsy, Parkinson's Disease, and stroke. For most of these cases, loss of hand functionality is observed, which can cause difficulties during activities of daily living (ADL) and thus impact one's quality of life [1]. For these people, a robotic hand orthosis can offer a solution.

Brain stroke and other injuries of the central nervous system are one of the most frequent causes of disability, involving sensory loss, weakness, poor movement coordination, or impaired execution of motor commands. Every year about 15 million people are affected by stroke [2], and approximately 80% of them experience long term reduced manual functionality [3]. Only in Italy, 913.000 people had a stroke and survived. There are approximately 200,000 cases every year, of which 80% are new episodes and 20% relapse [4]. Approximately one year after the acute event, one-third of the survivors of a stroke - regardless of whether it is ischemic or hemorrhagic - has a high degree of disability, so much so that they can be defined as totally dependent.

Physical rehabilitation therapy, such as repeating isolated movements, promotes motor recovery. In this way, the brain can reorganize itself by making new neural connections, also called neuroplasticity [5]. Therapists make patients repeat exercises and thus use neuroplasticity to re-map motor function in the brain. The grade of recovery depends a lot on the ability of the patient to attend therapy, which can be discouraged by the frequency, duration, or cost of the therapy. Robotic devices could be used in rehabilitation to restore and relearn motor functions, as shown in previous research [6]. It provides a high-intensity, repetitive, task-specific, and interactive treatment. For more realistic and task-oriented training, a portable device like a hand exoskeleton would be highly valuable, giving the possibility to interact with physical objects in daily life.

Usually, patients begin rehabilitation immediately after a stroke, with the first phase taking place in the hospital under the supervision of a physiotherapist. After leaving the hospital, the patient is usually provided a set of physiotherapy exercises, mostly to perform unaided and unsupervised at home. The reason for the unsupervised rehabilitation is the lack of resources available such as a shortage of physiotherapists. The priority is the recovery of the motion of the trunk and lower body, such as walking through gait relearning. While relearning the gait, also the upper arm recovery takes place. Hand rehabilitation after stroke has a lower priority than gait recovery. Thus, when rehabilitation of the hand begins, it is often after the best (begin) phase when the treatment has the highest potential for recovery [7]. If this

opportunity is missed, hand function rehabilitation is not as advanced as it could be. Using a robotic rehabilitation glove might improve the process of regaining the hand function by using it from the start of the rehabilitation period, and more importantly, throughout the day while executing activities of daily living, thus avoiding time constraining rehabilitation sessions. An orthosis that supports recovery rehabilitation would be a very useful instrument to reduce the social costs of the disease and increase the effectiveness of rehabilitation itself, reducing recovery time.

The aim of this thesis is to improve an existing exoskeleton prototype for hand rehabilitation using the NiTiNOL shape memory alloy as a mechanical actuator [8], [9]. The current prototype is capable of performing a one-finger flexion movement, possibly controlled by an EMG signal. The next step for improvement is to make the orthosis wearable and eventually extending the movements to more fingers.

The idea of this device started from these fundamental points to develop rehabilitation support and uses the principle of shape memory function of Nitinol wires which is characterized by a high ratio of developed force/thread weight, low stimulation current and the absence of an external motor that moves the wires. The effectiveness of these wires and the possibility of miniaturization of the device defines a system that is light and easy to wear.

1.1 Anatomy of the human hand

Designing a hand exoskeleton which is tightly coupled with the hand when it is worn, requires an understanding of hand anatomy and biomechanics to ensure safe and effective operation. Specifically, considering the degrees of freedom (DOF, number of planes within which a joint can move) and range of motion (ROM) of each joint is essential for the design of a mechanically safe structure.

The human hand is the most distal portion of the upper limb. Distal and proximal are medical terms referring to the distance of a body part in regards to its proximity from the center of the body. It is characterized by complex functions with a high number of DOF, which allow it to move in three dimensions quickly through neuromuscular control. The cutaneous receptors and muscles allow precise control of the hand in subtle and rough movements, managing to regulate variables like force, range of movement, and position in space. The movements that can be performed include: extension, flexion, adduction, abduction, see *Figure 1-1* [10] for a visual representation. For each kind of movement, the coordination uses certain specific muscles and joints.

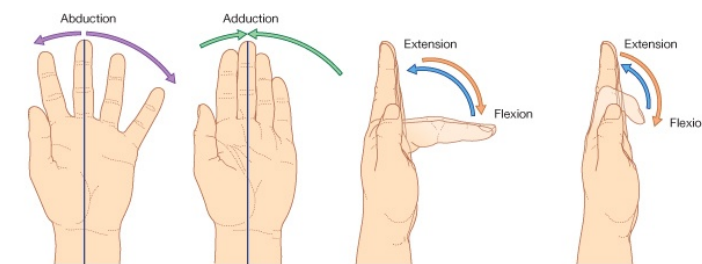


Figure 1-1 Visual representation of flexion/extension and abduction/adduction movements

The human hand consists of 27 bones divided into carpus, metacarpus, and phalanges. The bone segments are connected to each other through the joints, which guarantee the coordination between the various segments. Each articulation consists of a joint capsule, synovial fluid, and cartilage. The ligaments hold the bone segments together allowing movement relative of the same and giving the hand 23 DOF and a certain ROM.

1.1.1 Bones and Joints

The bones of the hand are naturally grouped into carpus bones and digits. Carpus bones are a group of eight bones which make up the wrist and root of the hands. The fingers are each composed of metacarpal and phalangeal segments [11]. The five digits are named as follows from the radial to the ulnar side: thumb, index finger, middle finger, ring finger, and little finger. Each finger ray is composed of one metacarpal and three phalanges, except for the thumb (which has only two phalanges). So in total there are 19 bones and 14 joints distal to the carpals, as shown in *Figure 1-2* [11].

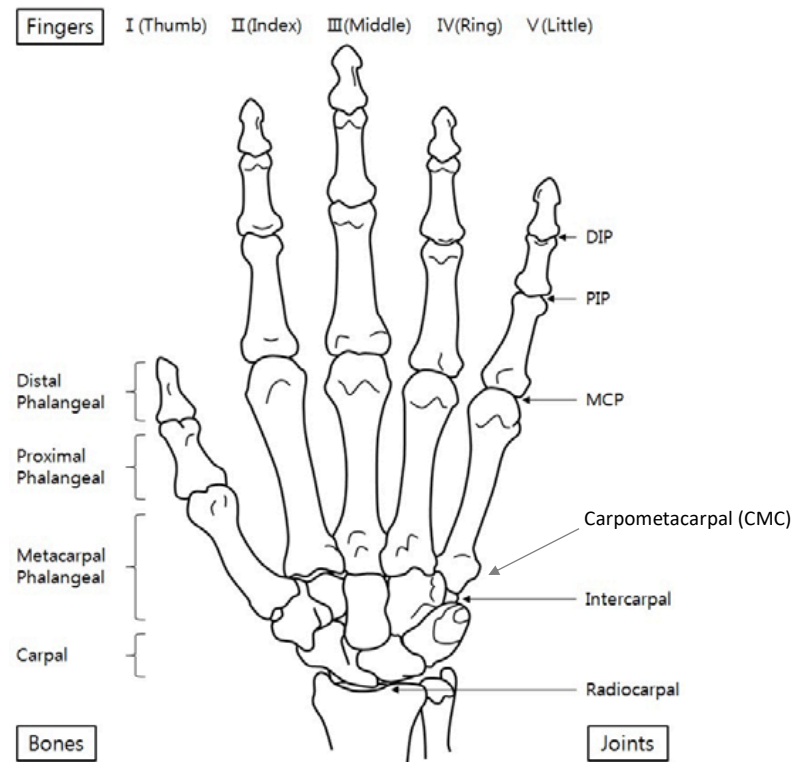


Figure 1-2 Bones and joints of the human hand

The group of carpal bones is arranged in two rows, those in the more proximal row (more close to the center of the body) articulate with the radius and ulna bones of the forearm. Between the two rows of carpal bones is the intercarpal articulation. Each finger is connected with a specific carpal bone at the carpometacarpal (CMC) joint. Not every CMC joint has the same degrees of freedom. The joint of the thumb is a sellar joint, showing two degrees of freedom with flexion/extension and abduction/adduction. The CMC joints of the fingers are classified as plane joints with one degree of freedom, while the fifth CMC joint of the little finger is often classified as a semi-saddle joint with conjugal rotation.

The next joint of each finger links the metacarpal bone to the proximal phalanx at the metacarpophalangeal (MCP) joint. MCP joints have two degrees of freedom, permitting flexion/extension and abduction/adduction movements. Further, between the phalanges of the fingers, the proximal interphalangeal (PIP) and distal interphalangeal (DIP) joints are

found. Although the IP joints are frequently modeled and assumed as having a single axis of rotation for simplicity, in fact, they do not remain constant during flexion and extension. Later is shown why this causes difficulties in the design process of a rigid exoskeleton.

As seen not all fingers have the same kind of joints and thus not the same amount of degrees of freedom. Also, the orientation of the thumb and the unique configuration of its CMC joint provide this digit with a large range of motion and greater flexibility [12]. For now, the thumb is too complex to include in the design for the exoskeleton prototype and will be considered later.

The resting posture is a position of balance without active muscle contraction. The MCP joints are flexed approximately 45° , the PIP joints are flexed between 30° and 45° , and the DIP joints are flexed between 10° and 20° at the resting posture. Flexion of the MCP joints is approximately 90° , and the little finger is the most flexible (at about 95°), while the index finger is the least flexible (at about 70°) [11]. The extension varies widely among individuals. For PIP and DIP joints, flexion of about 110° and 90° occurs. Extension beyond the zero position is regularly observed and depends mainly on the ligamentous laxity.

1.1.2 Muscles

The hand has about 40 muscles which can be divided according to the position as intrinsic or extrinsic muscles.

- **Extrinsic:** The extrinsic muscles originate from the arm and forearm, and they are responsible for flexion and extension of the digits. There are nine extrinsic muscles. Three muscles of those perform finger flexion; the flexor digitorum superficialis, the flexor digitorum profundus, and the flexor pollicis longus. Five extrinsic muscles contribute to the extension of the fingers, while the abduction of the thumb is carried out by the abductor pollicis longus.
- **Intrinsic:** The intrinsic muscles are located entirely within the hand, and they permit the independent action of each digit. The dorsal interossei muscles (DI) and palmar interossei muscles (PI) are groups of muscles originating from between the metacarpals and attached to the base of the proximal phalanges or the extensor assembly. The interosseous muscles flex the MCP joint and extend the PIP and DIP joints. They are also effective abductors and adductors and produce some rotations of the MCP joint.

Forearm muscles

The muscles responsible for closing the hand are:

- deep flexor of the fingers;
- superficial flexor of the fingers;
- lumbrical;

- palmar and dorsal interosseous;
- long flexor of the thumb (which is neglected in this phase);

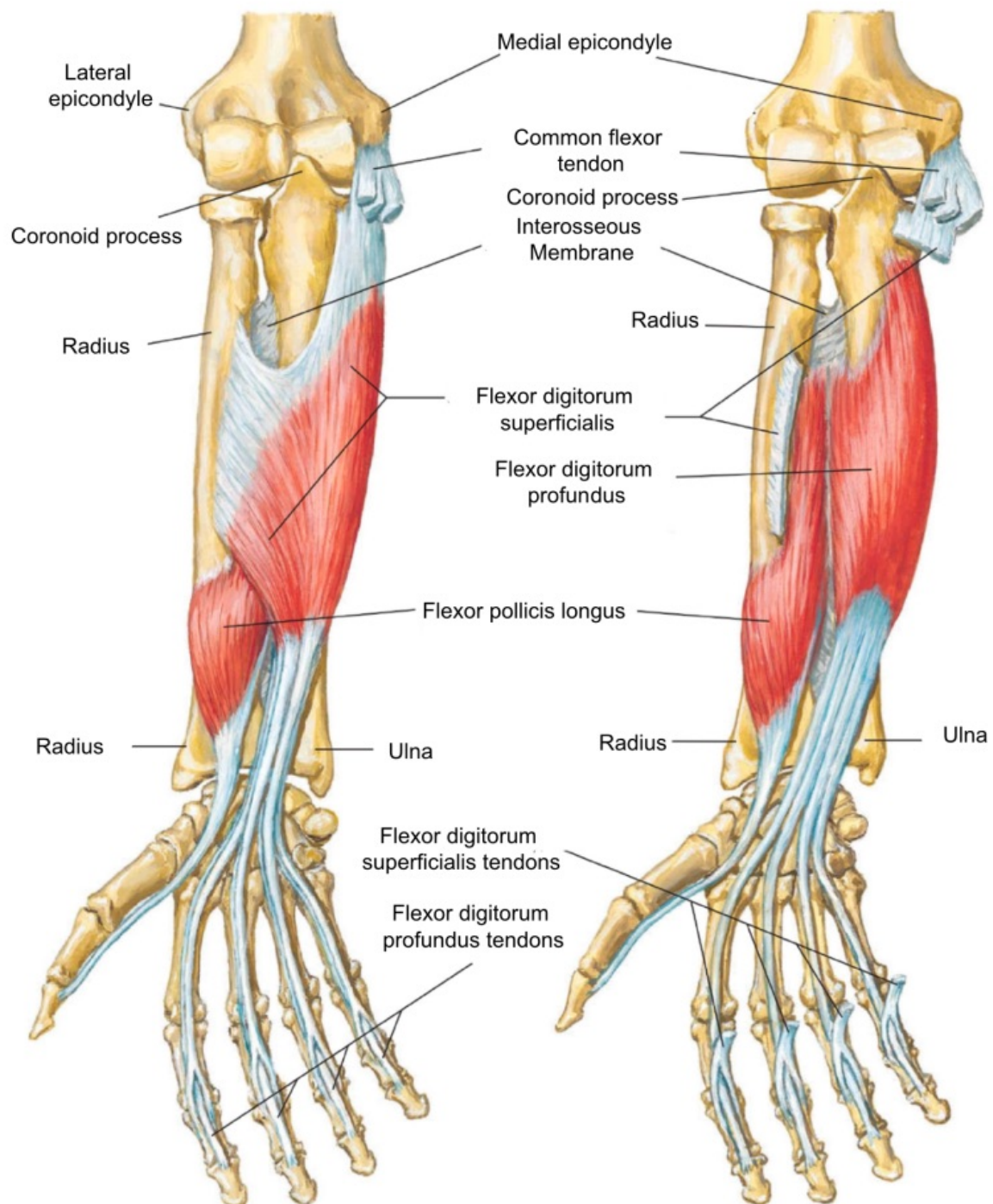


Figure 1-3 Anatomical figure of the arm [13]

The muscle signals in the forearm can be measured to obtain a useful EMG signal for orthosis control.

1.1.3 Tendons and Ligaments

As a digit moves, each tendon in the finger slides a certain distance. This excursion takes place simultaneously in the flexor and extensor tendons. The relationships between the movement of the finger tendons and the angular displacements of the MCP, PIP, and DIP joints have been reported to be both linear and nonlinear. The excursions are larger in the more proximal joints. Also, the excursion of the flexor tendons is larger than that of the extensor tendons, and the excursion of the extrinsic muscle tendons is larger than that of the intrinsic tendons. There are several important extracapsular and capsular ligaments that support and stabilize the hand. The most important extracapsular ligament is the transverse intermetacarpal ligament (TIML). It is stretched across the entire width of the hand at the level of the metacarpal heads. The capsular collateral ligaments provide important joint stability to all of the finger and thumb joints.

The PIP and DIP joint collateral ligaments attach completely to the bones. They are concentrically placed and are of equal length; therefore, these ligaments are maximally tensed throughout their range of motion.

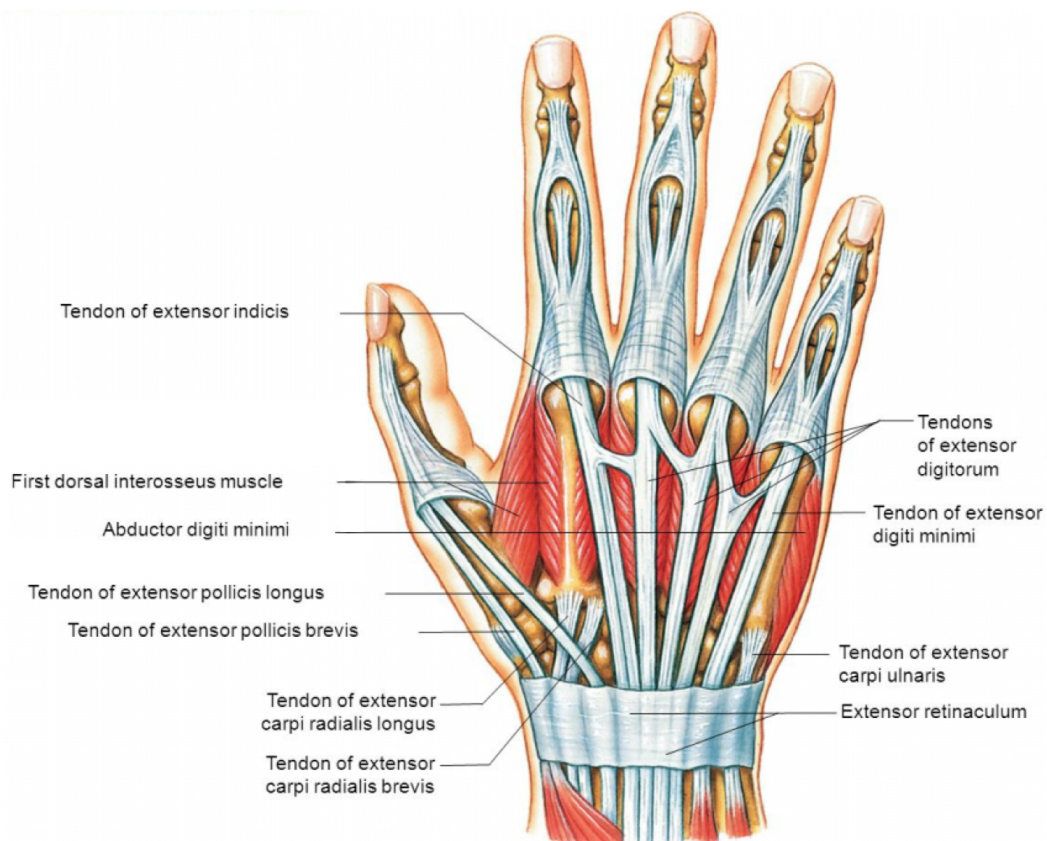


Figure 1-4 Muscles and tendons on the dorsal side of the human hand, Pearson Education 2012

The tendons of the last three fingers are connected to the same extrinsic muscle in the forearm, the extensor digitorum. If the hand is clenched into a fist, and one of the last three fingers extends, automatically the other two fingers also extend. The extensors are located on the back of the forearm and are connected in a more complex way than the flexors at the

dorsal side of the fingers. Tendons come together with interosseous and lumbrical muscles to form the extension mechanism.

Furthermore, the index finger is equipped with an extra extensor, used for example to indicate. The extensors are located within six separate spaces.

On a functional level, the hand can perform the following types of movement:

- Finger grip with sub-terminal opposition: it is obtained by opposing the thumb to the other four fingers.
- Finger grip with sub-terminal-lateral opposition: this is obtained when the fingertip of the thumb presses on the lateral surface of the index.
- Three finger grip: using the thumb, index, and the middle finger in the grip.
- Five finger grip: it is obtained when all the fingers are involved in the grip. It is used for grabbing small objects.
- Diagonal palm grip: the object is held between the thumb and the other four fingers, it is in contact with the palm and its axis is diagonal to that of the hand.
- Cross palm grip: the object is held between the thumb and the other four fingers, is in contact with the palm and its axis is transversal to that of the hand.
- Spherical palm grip: the object is held between the thumb and the other four fingers, it is in contact with the palm. The sphericity of the object leads to a different flexion of the fingers.

The forces exerted by the hand during a two-finger grip can reach 100 N while the power grips, where the whole hand is used, also reach 500 N in young subjects and 300 N in elderly subjects [14].

According to another study of NASA [15], on average the population reaches a maximum force, in the cross palmar grip, of 260 N and in the digital grip of 60 N. The forces in play decrease when the test execution time lengthens, in fact, the same grips sustained over time have the following forces: 155 N and 35 N.

Although the hand can exert strong forces, during the gestures performed in daily routine, the forces employed are a few Newton at the tip of each finger. In literature, the exoskeletons are calibrated and limited not to exert forces greater than 15 N on each finger.

To grasp a small bottle of water (522 grams, diameter 57mm) using a cross palm grip, the forces on the five fingers, starting from the thumb and ending with the little finger, are 1.3 N, 1.0 N, 0.9 N, 0.8 N, and 0.4 N in static conditions [16] respectively. Naturally, the contact forces of the other phalanges and the palm also intervene. In general, the total contribution of the whole hand to maintain a grip on the bottle of water must be a force of 16.3 N.

It should also be noted that, in the flexion movement of a palmar grip, the force is not evenly distributed on the four fingers but the index finger effects 25% of the total, the middle finger 33.5%, the ring finger 25% and 16.5% by the little finger [14].

1.2 Artificial muscles

A natural muscle is a contractile organ with fibers that actuates force and motion in response to nervous stimulation. It works by the chemo-mechanical action of actin and myosin proteins. The joints of the body human are arranged in such a way that for each segment of articulation, a system of agonist and antagonist muscles is defined.

The development of artificial muscles that replace or support natural ones has led to the engineering of biomimetic actuators. They can be of different types and can work according to different sources of mechanical work.

- Pneumatic actuators
- Hydraulic actuators
- Electrical, such as servo-motors
- Shape Memory Alloys, such as NiTiNol

In the last forty years, many attempts have been made to construct artificial muscles based on the mechanism of natural ones. However, though the mechanism is similar, the differences between artificial and human muscles remain present. The artificial actuator cannot and should not be exactly like the natural muscle in all its aspects, for example not all of these properties are beneficial:

- Power source (the ability to convert chemical energy into work through the 'combustion' of sugars forms a dense reservoir of energy, about twice as high as batteries);
- Environmental conditions
- Materials and microstructure
- Response to stimulation
- Fatigue



Figure 1-5 McKibben artificial pneumatic muscle
<http://lucy.vub.ac.be/gendes/actuators/muscles.htm>

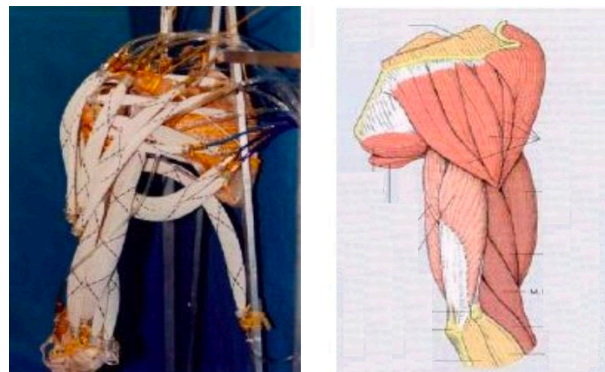


Figure 1-6 **Left:** McKibben muscle model of the shoulder musculature.
Right: Anatomical sketch of the shoulder musculature
 Anthroform Biorobotic Arm project of Washington's BioRobotics Laboratory (Hannaford et al., 1995)

Actuators should only reproduce those characteristics of muscle that are beneficial for the application. There are several attractive design features that could lead to great advantage.

- The gradual control of the force by numerous activated fibers in parallel, a process known as recruitment. It allows to optimize efficiency over a wide range of loads and contraction velocities, also enabling the control of acceleration and force;
- The relatively low stiffness of inactive muscle fibers which therefore not require significant forces to strain. In most of the artificial muscles, there is little ability to change the Young's modulus. Shape Memory Alloys do have this property of pseudo-elasticity.
- The ability to alternate stiffness in certain tasks, which are very important in the control strategy. This control could be imitated by artificial actuators in a fast feedback network, but would result in a considerable increase of complexity of the system;
- Another attractive feature of muscles is its integrated circulation system. It distributes the fuel (glucose and oxygen) and removes heat and waste. The capillary density and the efficiency of such a system would also be advantageous in biomechanical actuators;
- The ability of the muscles to operate for billions of cycles for a period of a hundred years or more, assured by the regeneration of proteins on site.

1.3 State of the art

An extended research in PubMed among any combination of different keywords (hand, orthosis, glove, robot, SMA, shape memory alloy, grasp, stroke, rehabilitation, ADL, soft glove, exoskeleton, design) has brought to light a vast variety of research- and design processes for the construction of wearable robotic hands. All of the papers found were systematically reviewed and marked for the most crucial information which could be of any use in the design process for this Shape Memory Alloy-based orthosis. Many of the papers describing a design process for hand rehabilitation orthosis were published in the last four year, which shows this is a recent trend.

All of the found designs can be divided based upon their actuation system:

- Pneumatic
- Hydraulic
- Electro-pneumatic
- Electric motors (DC)
- Shape Memory Alloy

These can all be combined with different transmission systems such as Bowden cables, belts linkage bars, and wires.

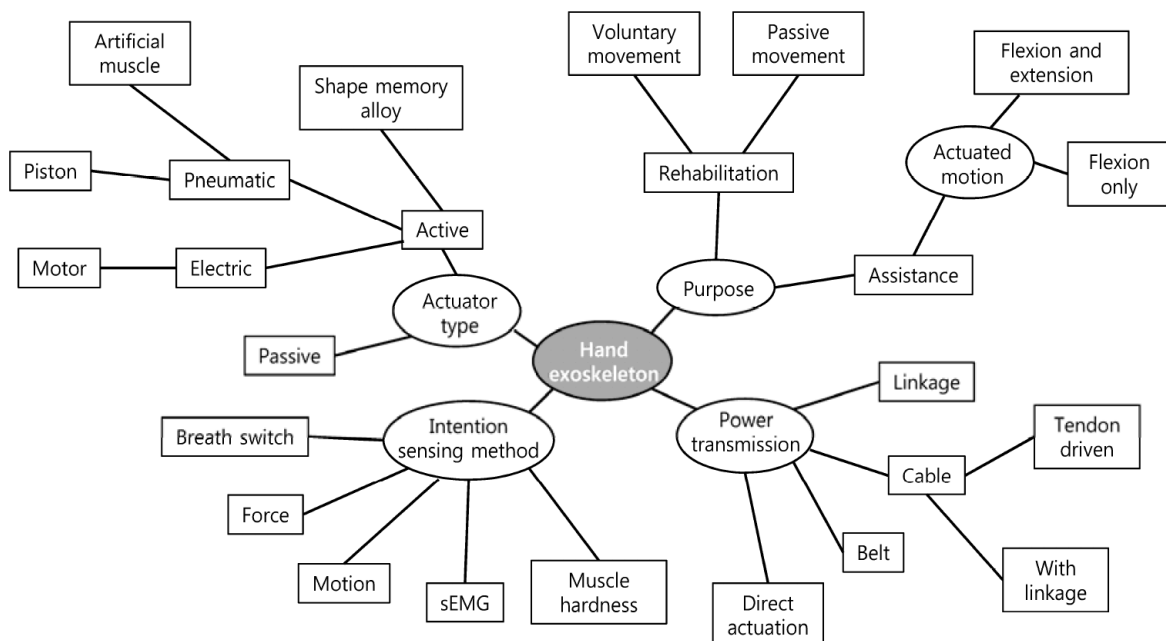


Figure 1-7 Classification of current hand exoskeleton technologies [11].

The state of the art of wearable rehabilitation devices for support during activities of daily living of people experiencing difficulties in developing strength and control of the hand, especially in the most delicate movements, is variegated. Cutting-edge technologies are used to restore the various functions of motion in the most similar way possible to the hand.

Usually, the devices are divided into two groups based on whether a mechanical linkage structure is used, or whether they are soft robotics with a joint-less and even tendon-like structure. In the first group, mechanical linkages are used to build an external anatomical structure which is attached to the users' hand to move it. The second group does not have a rigid structure with joints maintaining the original degrees of freedom, but uses the patients' skeleton as support. Often these are ergonomic soft gloves with a tendon-like structure or soft pneumatic actuators.

A tendon-like structure is a bioinspired design using a Bowden cable or a wired interface that separates the actuator from the joint complex of the hand. The absence of rigid parts removes constraints on non-actuated degrees of freedom and also reduces joint alignment issues, which could prevent joint damage. Additionally, soft robotics, in general, are lighter and have simpler designs, creating possibilities for at-home rehabilitation.

There are many prototypes on the market, and the evidence and data collected have formed a sound basis in the choice of materials, the order of magnitude of the system, and the mode of transmission. In almost all cases steel (Bowden) cables are used, rarely NiTiNol wires or a flexible shaft system.

Sensors that help control the system are generally of a few types: magnetic encoders, potentiometers, angle sensors, force and pressure load cells, cameras and reflecting markers, and EMG electrodes.

Also, in present designs the amount of actuated fingers varies. In many designs a complete hand motion such as flexion or extension of all fingers is realized. On the other hand, some devices were strategically designed to actuate only the digits absolutely necessary to perform specific tasks, such as pinching or grasping.

Systems can also be under-actuated when few actuators are used to manage the motion of all the fingers of the hand. It can be chosen for an economic reason or the weight/power ratio, reduced encumbrance, and ease of control: it does not affect the fluidity of the movements or the effectiveness of the system. Though excluding the possibility of defining motion relative to individual fingers, this has little influence on the normal function of the hand during rehabilitation.

All systems have advantages and disadvantages. Hydraulic or pneumatic systems have a problem of size that does not influence rehabilitation but limits its use in all daily activities.

Attached to a glove are soft pneumatic actuators that can be pressurized to support finger flexion or extension. DC motors are often contained in backpacks or exposed on the arm, located away from the hand. They give less but not negligible encumbrance by connecting them to the fingers by cables. Several examples of robotic rehabilitation arms that were found during the research will be discussed.

1.3.1 Pneumatic and hydraulic gloves

Most existing wearable robotic hand devices have been developed for rehabilitation purposes and consist mostly of rigid exoskeleton designs that are often heavy and can be challenging to align with the biological joints of the hand. Soft robotic devices, however, are made from easily deformable materials which conform to the contours of the human body. The lack of rigid components removes constraints on non-actuated degrees of freedom and also reduces joint alignment issues, which could prevent joint damage. Additionally, soft robotics may be lighter and have simpler designs, making them more likely to be portable and more comfortable to put on and off.

According to extended research of available soft robotic gloves for rehabilitation purposes, pneumatic actuators were the most common type of actuators used in soft robotic devices [17].

One of the most found designs is a glove with the hydraulic or pneumatic soft actuators wrapped around the dorsal side of the hand, resulting in an open-palm design. Often it is a construction with high encumbrance, thus making it difficult to use during activities of daily living.

Polygerinos hydraulic soft glove, 2015

Panagiotis Polygerinos wrote several papers on different designs of these wearable soft robotic gloves. Soft pneumatic actuators are directly attached to the hand with a glove. In these cases, the flexible or underactuated structure is adopted, and the wearer's hand provides a skeletal structure for the motion of the exoskeleton device.

The robotic glove [18] uses a combination of elastomeric and inextensible materials that align with the user's hand and distribute the forces along the finger in a safe way.

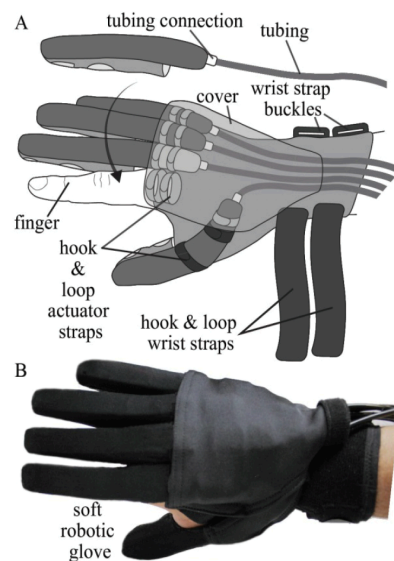


Figure 1-8 Polygerinos' soft robotic glove, 2015 [18]

These actuators consist of elastomeric tanks with fibers of anisotropic reinforcement that induce specific bending, twisting and extending trajectories under fluid pressurization. When the actuators are pressurized, they can generate motion paths that are kinematically similar to the motion of the human finger and thumb, yet require only the simple control input of pressurization. With this hydraulic choice, performances similar to human ones can be obtained, which can generate sufficient hand closing force to assist with activities of daily living. In some cases, it is combined with a user intent that is detected by monitoring gross muscle activation signals with surface electromyography (EMG) electrodes mounted on the user's forearm.

Polygerinos hydraulic soft glove, 2014

A similar design to the other hydraulic robotic soft glove is this device that utilizes inexpensive hydraulic soft actuators made from elastomeric materials with fiber reinforcements to control the fingers [19]. Integrated fluidic pressure sensors measure the internal pressure of soft actuators and allow control of finger flexion/extension. It is made with soft and compliant materials that do not resist finger motion when unpowered.

The total weight of the assembly with pressurized fluid weighs 285 g. In order to enable portability and minimize additional weight on the hand and arm, the device's hydraulic power supply and supporting electro-mechanical components were mounted on a waist belt pack of 3,3 kg. However, not all pneumatic gloves have this feature of portability regarding the fluid or air tank and pump which is needed to actuate the glove, normally being a big disadvantage respect to more portable solutions.

Figure 1-9 presents the components to assemble a fiber-reinforced soft bending actuator, which incorporates radial reinforcements to limit radial expansion and a strain-limiting layer to promote bending by inhibiting linear growth along a portion of the tubular body.

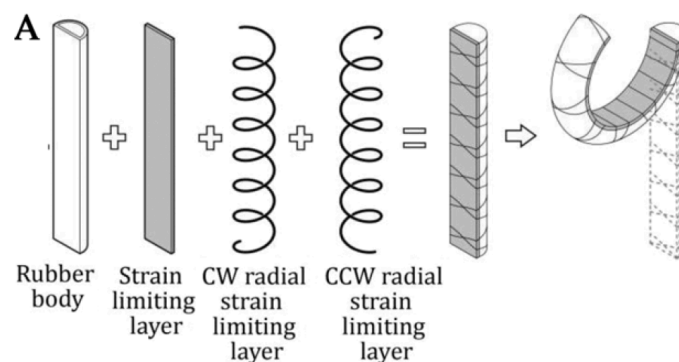


Figure 1-9 assembly of a fiber-reinforced soft bending actuator [19]

The soft, fiber-reinforced actuators used in the glove device are fabricated in four stages. First, the hollow geometry of the tubular body is defined; after that, reinforcements are applied. The third stage of the fabrication consists of encapsulating the tubular body and

reinforcements in a thin layer of rubber by using a 3D printer. This anchors the reinforcements during handling and operation. In the last stage, the open ends of the body are capped. The length of each actuator segment is empirically estimated such that when pressurized up to 345 kPa (50 psi), the deformation corresponds to the individual skin extension, joint angle

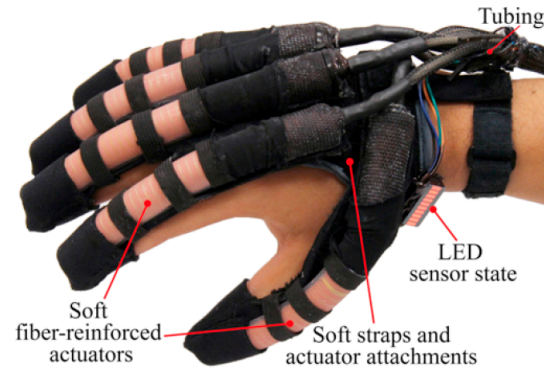


Figure 1-10 Polygerinos' robotic soft glove, 2014 [19]

and twisting joint angle of flexed biological fingers.

However, Polygerinos found that when the actuators were integrated into the glove and constrained by the hand anatomy, they could be pressurized up to 400 kPa (~60 psi) and provide comfortable forces to the wearer.

Pneumatic Soft robotic glove by Yap

A design and development of a soft pneumatic glove are made by Yap [20]. The actuators are made by silicon rubber which has an elastic modulus similar to human tissues.

For the actuators, they developed a new type of soft fabric-reinforced pneumatic actuator with a corrugated top fabric layer that could minimize the excessive budging and provide better bending capability compared to fiber-reinforced soft actuators developed in previous studies. This corrugated top fabric layer allows a small initial radial expansion to initiate bending and then constrains further undesired radial expansion. The elastic fabric can provide an estimated 4.5N of extension force to pull the fingers to the open hand state when the actuators are depressurized.



Figure 1-11 Pneumatic Soft robotic glove by Yap [20]

The total weight of the glove is only 180 grams, which is lower than Polygerinos' design [19]. The actuator works under air pressure inflation of the actuators, so it does not add a significant amount of extra weight to the hand, as compared to hydraulically actuated actuators. The total system weight is 1.26 kg, also lighter than the other designs. This design needs a lower range of operating pressure as well to achieve a similar output force, namely 120 kPa respect to 345 kPa at Polygerinos' research.

The choice of pneumatic over hydraulic allows the control system to be more portable and lightweight than the control system presented by Polygerinos, as it does not require a water reservoir. However, the limitation of the pneumatic system is that it is slower due to slow valve discharging speed and long response times when depressurizing.

Other designs

Pneumatic glove by Wang

Another design is made by Wang [21]. It is a skinny rehabilitation glove with five fingers which uses a bi-directional soft pneumatic bending actuator for both extension and grasping motion. It uses a higher pressure, 675 kPa, for the pneumatic actuators, delivering a force of 21.2 N in the fingers. All five fingers on the rehab glove are controlled independently with isolated solenoid valves, and a proportional valve regulates input air pressure.

Each finger is equipped with a force sensor to measure the pressure force at the fingertip and a bending sensor to record the angular displacement of the corresponding MCP joint.

Pneuglove

The PneuGlove [22] uses residual control of finger flexion that is observed in stroke survivors and, thus, assists only during digit extension.

The PneuGlove utilizes air pressure to assist in digit extension during grasp-and-release tasks. It consists of a custom-fabricated air bladder with five independent channels on the palmar side of the glove and a lycra backing on the dorsal side. Also, the dorsal side of the glove holds the flexion sensors to provide a measure of haptic feedback in addition to the assistance of finger extension. Extension of the fingers and thumb is essential for positioning the digits for grasp and for enabling the release of the object during the grasp-and-release task. Air pressure within a channel creates an extension force which pushes the digit further into extension. Each bladder channel is physically isolated from the others so that the assistance of each digit is achieved independently. When the air pressure is removed, the digit is free to flex (the deflated glove offers minimal impedance). Thus, it is possible to grab real objects with the PneuGlove.

1.3.2 Electric motors (DC)

These rehabilitation gloves are driven by a number of motors, located on the hand or further away to not let them obstruct any movements. Designs with an electric motor are in general heavier than the pneumatic or SMA-wire driven exoskeletons. The transmission can be executed by a linkage bar mechanism, cables, or a combination of both.

A cable transmission system actuated by electric motors located away from the hand can drastically reduce the excess volume caused by mechanical linkages and actuators. The glove contains cables which mimic the tendons in the human hand. The volume reduction is a great advantage compared to other types of electronic driven rehabilitation gloves since the collision-free workspace of the hand is improved.

Electric batteries which can power the motors are generally more compact than pressure pumps used by pneumatic and hydraulic actuators. Also, they can be quieter, cheaper, more durable, and require less maintenance. However, the mechanical transmission mechanisms mentioned before often suffer from low efficiency, mechanical complexity, alignment issues, and other problems.

Exo-Glove Poly

This is the new prototype of the previously developed Exo-Glove, only made with silicone to enable the necessary sanitation used in hospitals [23]. The previous prototype was made of fabric, thus absorbing sweat and difficult to clean in between uses. It is adjustable in size to make it wearable for different users. Also, the minimal coverage area on the hand enables more ventilation. It uses two motors, one to move the thumb and the other one to move the index and middle finger. It enables flexion and extension movements of the three fingers. The system uses under-actuation to permit the wearer to grasp various objects adaptively and to

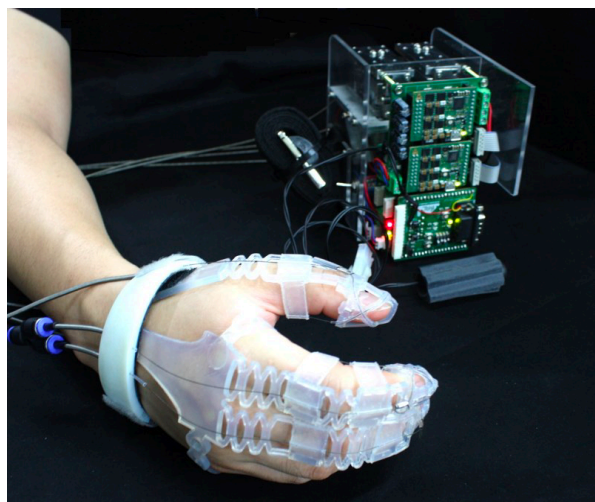


Figure 1-12 Exo-Glove Poly [23]

reduce the number of actuators needed. It is controlled with a simple button as input for control. It can execute a force of 29.5 N on a cylinder object.

The original Exo-Glove design, however, uses a flexible tendon routing system and an underactuated adaptive mechanism in a fabric glove. One of the problems of using a glove interface is that it stretches. The glove part of the system is compact and weighs 194 g. The results showed sufficient performance for the execution of daily life activities, namely a pinch force of 20 N. [24]

Based on the structure of the human hand, the Exo-Glove has two tendons for each finger and the thumb, several types of straps that together form the pulley. In order to generate an appropriate finger trajectory for different users, the tendon path of the routing system can be adjusted by changing the length and position of the fabric straps.

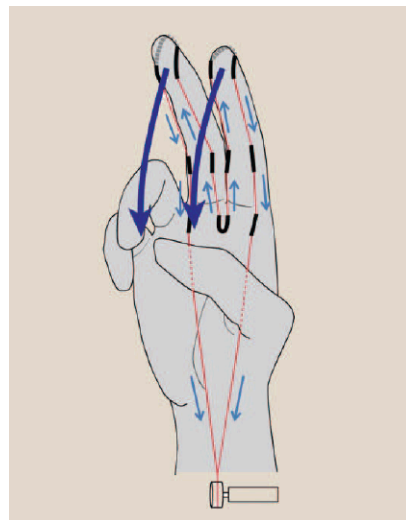


Figure 1-13 The tendon routing system of the Exo-Glove [24]

The Exo-Glove distributes the pulled length of the tendon to multiple fingers. A system of U-shaped tubes at the tips of the index and middle fingers and between the fingers distributes the tension of the tendon to both fingers. The mechanism, therefore, also enables adaptation when the glove is in contact with an uneven surface.

Regarding the control input, wrist motion has been considered because it is easy to detect, and people with a paralyzed hand are generally familiar with performing wrist motion to induce finger motion to grasp an object.

Graspy Glove (2017)

Graspy Glove [25] can perform both flexion and extension motions of the thumb and three fingers (excluding the little finger) due to bidirectional actuators. It is a soft glove, adjustable,

and leaves the palm free for object grasping and manipulation. Also, it is compact and light, the weight of the whole system being 340 g. The maximum pinch force provided by the device was experimentally measured to be 16 N, which gives a high power-to-weight ratio. The glove is capable of performing both a precision grip and a power grip.

Only a single motor per finger is used for flexion and extension, leading to a lighter glove. Also, only one cable was used for the transmission, which is guided along the central axis of the finger. Finally, the motors are placed directly on the dorsal side of the hand. These approaches decrease friction and therefore improve transmission efficiency.

The developed device consists of 2 to 4 layers, which are assembled into a single device. Firstly, a soft glove as an inner layer for comfort. A second layer is made up of stiff material onto which the actuators and cable guides are mounted. The third layer is the actual exoskeleton system (actuators and cables), which drives the fingers. The outer layer is optional and can be used to cover the actuators and cables of the exoskeleton.

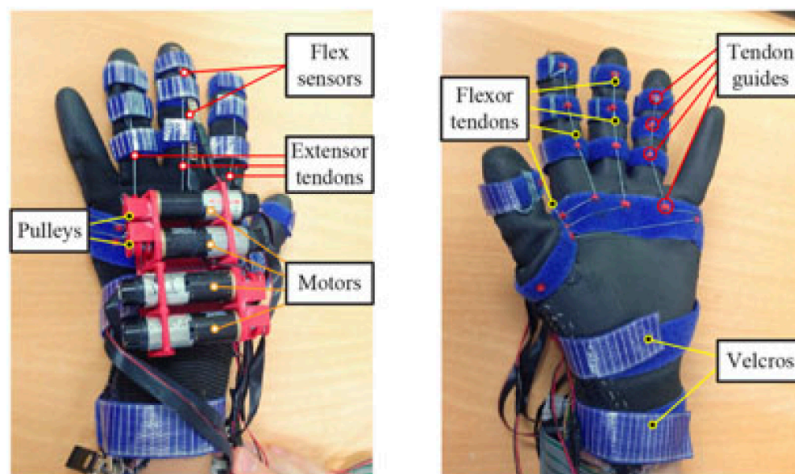


Figure 1-14 Grasp Glove dorsal and palmar view [25]

Wearable hand exoskeleton

This exoskeleton for exercising flexion/extension of the fingers was designed with a wearable and straightforward structure to assist during finger motions in 1 degree of freedom [26].

During this design procedure, a hand grasping experiment by fully-abled people was performed to investigate general hand flexion/extension motions to obtain the polynomial curve of general hand motions. The finger length and joint ROM of the user are used to adjust the polynomial equation and to optimize the design of the proposed structure to develop a suitable hand exoskeleton. In this way, the prototype of the wearable hand rehabilitation device was built to fit perfectly to the user's hand. Therefore, the structure was designed for guaranteeing natural finger motions with one active joint.

Comparing the line of the joint angles made by the exoskeleton in a graph shows it is very similar to the desired motion. It indicates that the optimized structure with 1 DOF guides the fingers to natural finger motions well.

A prototype divided into two parts, one part was developed for the thumb and the other part for the rest fingers. Each part is actuated by one linear motor for compact size and a light weight design. By using potentiometers to measure the motor stroke length, the finger posture can be estimated due to 1 DOF structure while maintaining the compact size and lightweight design.

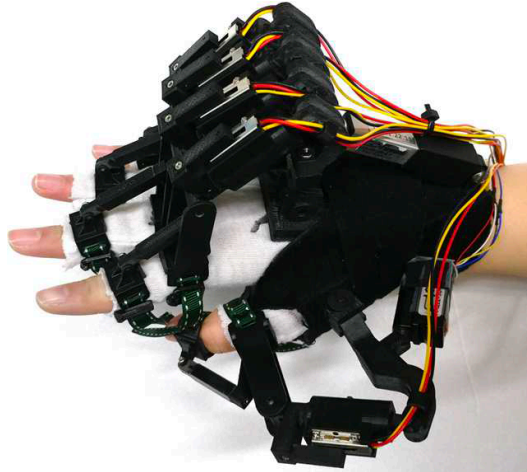


Figure 1-15 Design of the wearable hand exoskeleton [26]

Other designs

Another similar design of an external skeleton structure actuated by electric motors and a Bowden-cable transmission, including detailed kinetostatic analysis, is made by Cempini [27]. Also, this design addresses flexion and extension movement.

The total weight of the device is 500 grams. The actuation unit is remoted also because of its weight, around 1 kg. A Bowden-cable was used for transmission, which allows under-actuation strategies, and increases the flexibility and usability of the actuation block. The actuation system also includes a cable pretension system.

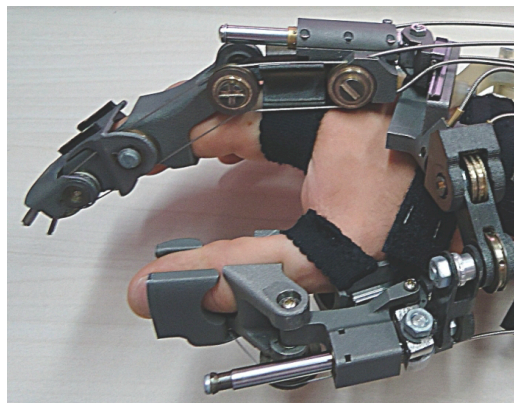


Figure 1-16 Hand exoskeleton prototype [27]

The next design is a combination of springs and an electric actuator in a jointless exoskeleton [28]. A tendon drive mechanism actuates all three joints using a single flexion wire. The proposed wearable robot design uses two wires as tendons for extension and flexion.

On the ventral side of the hand, flexion wires were connected to the actuator on the wrist. On the dorsal side, extension tendons were connected with a spring on the wrist to extend the fingers. The fingertip force of the design exceeds 18 N, which is enough to perform daily tasks.

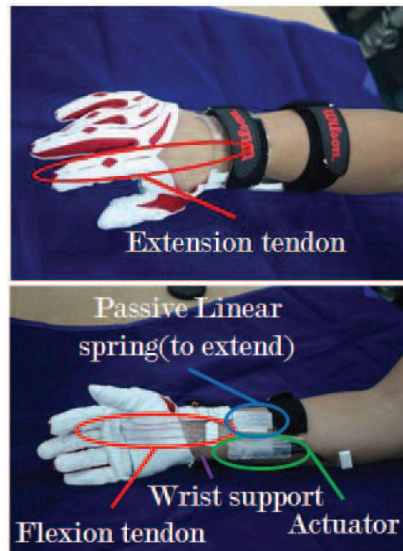


Figure 1-17 Prototype of wearable robotic hand [28]

A unique design with a single DOF actuation is the Vanderbilt hand exoskeleton [29]. It is a self-contained prototype which assists with both opening and closing of a power grasp. The hand exoskeleton actuates all fingers simultaneously. This manner of actuation simplifies the structure, volume of the device over the back of the hand, the number of drive units required, and total mass. Bidirectional actuation occurs via an under-actuated tendon system that offers equal flexion and extension forces on the hand. A test on a single subject showed this hand exoskeleton enabled a substantial reduction in the amount of time required to grasp the bottle (average 5.1 seconds instead of 25.9 seconds), which is the primary function of the paretic hand in this task.



Figure 1-18 Prototype of Vanderbilt hand exoskeleton [29]

1.3.3 Shape Memory Alloy (SMA) driven actuators

An SMA actuator (wire or spring) converts thermal energy into mechanical work by remembering and being able to return to its original shape. The SMA is heated when an electric current is flowing through the SMA; this is called the Joule effect. The heat triggers the SMA element to recover its original shape, resulting in mechanical work. An SMA wire can vary until 4% of its total length. Another feature of SMA is its pseudo-elasticity mode, which happens in the austenite phase. In this case, the alloy can tolerate high strains during loading and recovers once the stress is released.

Compared to a DC motor, an SMA actuator is more lightweight, has a reduced size, noise level, and complexity in a robotic application. Also, the power electronics and control system are relatively easy, and the costs for an exoskeleton application relatively low. On the other hand, the nonlinear behavior of the material due to hysteresis in cooling and heating processes makes controlling more complicated than that of DC motors. Also, it has a low actuation frequency because of the heating and cooling speed.

ASR Glove

The Advanced Service Robots laboratory (ASR) glove [30] is a shape memory alloy tendon-based actuated which can perform flexion and extension of the fingers and grasp objects efficiently. It can be utilized for both rehabilitation exercises and assistance for people with a hand disability. The total grasping force of more than 40 N can be produced at the tip of the fingers, in each fingertip being approximately generated 10 N force.

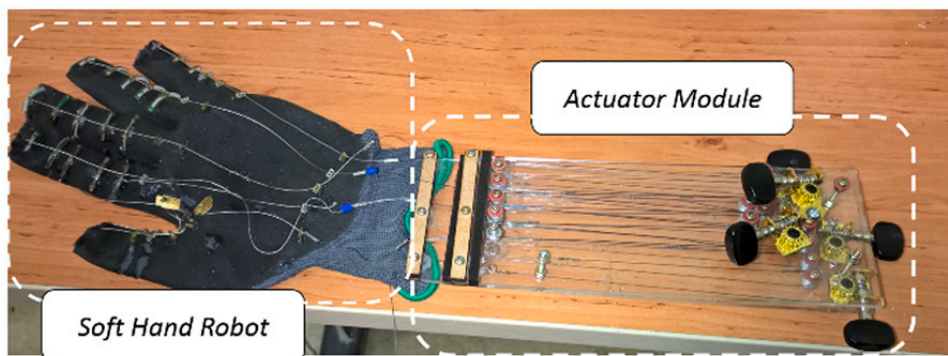


Figure 1-19 An overview photo of the actuator module and soft ASR glove [30]

Initially, the researchers intended to fasten a tendon to the proximal phalanx and another to the end of the distal phalanx of each finger. Due to the relatively high length of the SMA's (about 1 m), an independent module for placing five SMA wires has been designed. Each tendon is connected to an SMA actuator and each SMA being connected to a point on the module mounted on the forearm. A measurement with a load cell showed that the fingertip force is 0.35 of the tendon force. Consequently, the smart glove in which just five distal

tendons are actuated are sufficient, and adding the five proximal associated tendons is not vital.

At one end of each wire, a tuner is exploited on the module to include some pre-tension for improving system performance. One of the drawbacks of using these pulleys is the decreased fatigue life of the SMA's. Wire fatigue occurs due to the bending stress produced in the wires when passing through the pulleys. Therefore, in future research, the optimal size of the pulleys and the wire actuators should be studied.

Soft glove by Yao

This glove design is light-weight (85 g including an actuator and microcontroller) and very compact due to the low-mass and small-size SMA spring actuators [31]. The functionalities of tendons, pulleys, and muscles in the human hand are replicated by the soft structure of strings, bands and SMA spring actuators. It has 14 active degrees of freedom for four digits (the little finger is not involved). During a test, the glove could exert an 11N force on a hook produced by nine spring actuators. Also, it can achieve a functional thumb opposition.

Because the application has to be wearable, a Nitinol wire with an austenite temperature at about 60 °C was selected. A higher temperature would bring excess heat to the wearer. Also, the inactive SMA spring should be as easily stretched as possible, so that the wearer can move freely when the glove is off. The flexible sleeve, to which the SMA spring actuators are attached, is then made from thermal insulation textile to protect the user from excess heat. For the muscle glove, a low-mass and small-size SMA spring actuator with a large spring rate is used.

To reduce the energy consumption of the SMA spring actuator an adapted program of Pulse Width Modulation is chosen for the 'on' and 'hold' mode, respectively settings of 90% and 20% duty cycle.

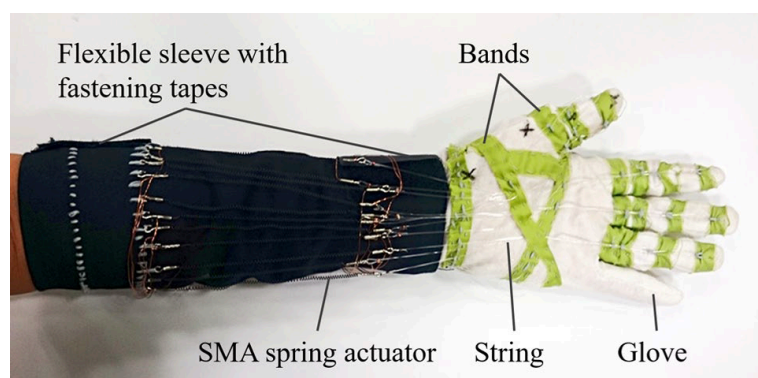


Figure 1-20 Soft glove design with SMA springs [31]

Exoskeleton system for hand rehabilitation by Tang

Instead of a tendon-like structure, this design [32] has a geared four-bar linkage mechanism as the main structure of the exoskeleton which can control five fingers separately. It is actuated by a rotational SMA actuator, which reduces the system's weight. The bar mechanism is mounted on the dorsal side of the hand and fixed with Velcro. Two actuators for each finger can perform a flexion and extension movement by rotating a linkage for the MCP joint and a pair of gears with two sets of linkages actuating the PIP joint. The motion of the most distal joint is neglected. The whole exoskeleton will bend when SMA-I spring rotates the first drive link. The second SMA-II spring is used for flexion.

A kinematic, static, and finite elements analysis were performed to optimize the linkage length, which is crucial for the performance of the exoskeleton structure. According to this analysis, an output force of 20N can be performed.

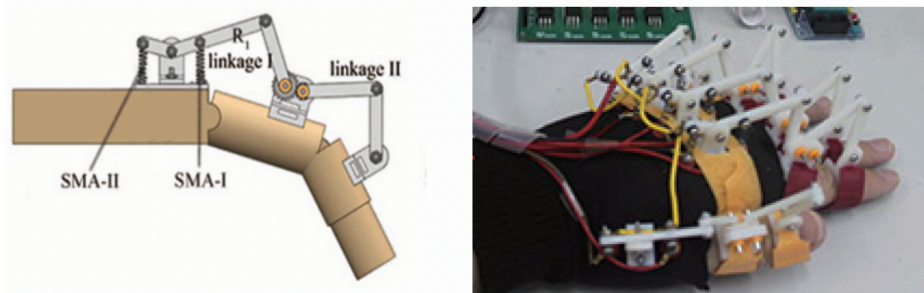


Figure 1-21 The linkage bar system actuated by two SMA springs, on the left a sketch for one single finger, on the right the complete exoskeleton with a separate system for each finger [32]

Other designs

Three other designs worth mentioning are the New SMA Actuator [33], Soft gripper [34] and wrist exoskeleton [35]. The first research is based on finding a way to substitute 13 bulky servo motors actuating a prosthetic hand. Every servomotor can be substituted by a mechanism of an SMA wire which can be used for flexion and extension. The control method consists of short pulses of milliseconds applied at high voltage in combination with a temperature monitoring to avoid overheating of the SMA wire.

The Soft gripper, however, shows a three-finger design for grasping objects using SMA-actuators with variable stiffness for adaptive grasping and holding of objects. It is developed by embedding thin SMA wires grouped mechanically in parallel as an SMA bundle.

The third model of the wrist exoskeleton is worth mentioning because of the SMA actuator's ability to be bent 180 degrees, providing more freedom of movements and therefore ideal for soft wearable robots.



Figure 1-22 The wrist exoskeleton [35] and the Soft gripper [34]

1.4 Shape Memory Alloys

Shape Memory Alloys, abbreviated to SMA, are a family of metallic materials that remember their original shape even when deformed. These alloys can return to their pre-deformed shape when heated above their transformation temperature. The SMA is heated when an electric current is flowing through the SMA, and this is called the Joule effect. The mechanical work done by the transition of shape can be used in robotic actuators like artificial muscles, tissues, and textiles. A particular advantage is that it can generate enough force to move up to thousands of times its weight. The most common shape memory material is a nickel and Titanium alloy called NiTiNol.

In this section, the general characteristics and mechanical properties of shape memory alloys are described theoretically. In particular, NiTiNol, the material used as an actuator for the hand exoskeleton, will be treated since it is an excellent candidate for the realization of wearable actuators.

In the 1930's the pseudo-elastic properties of an Au-Cd alloy gets discovered, but only in 1967, the shape memory effect of Nitinol means a breakthrough. Starting from the 1970s and 1980s, the first Nitinol implants are used in medical applications.

1.4.1 Austenite and martensite transformation

A shape memory alloy like NiTiNol has two stable states: martensite (cooled state) and austenite (heated state). When an SMA is below its transformation temperature (martensitic phase), it has a low yield strength and can be deformed quite easily and behaves like a pseudoplastic solid. When the deformed material is heated above its transformation temperature, there is a change in its crystal structure, which causes the return to its original shape (austenitic phase). This is called a Thermoelastic Martensitic Transformation (TMT).

During this transformation, the SMA element can generate a net force, behaving like an actuator. An SMA Nitinol wire can vary up to 4% of its total length and show a complete recovery of the impressed deformation, generating a considerable force during the return to the original form.

The austenitic phase is characterized by a Body Centered Cubic structure (BCC), with a nickel atom at the center of the crystallographic cube and Titanium atoms at the cube's corners. It is characterized by a hard, inelastic form which resembles Titanium.

The martensitic phase, however, consists of a rhombus alignment with an atom at each of the rhombus corners. It has a soft, inelastic form which has a more complex atom structure.

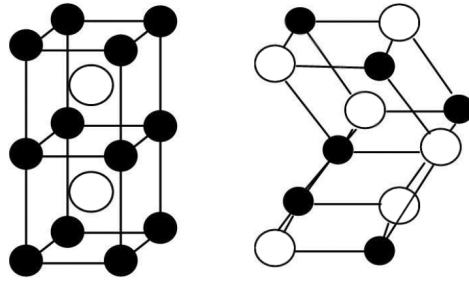


Figure 1-23 **Left:** Crystal structure of austenite (heated phase); **Right:** Crystal structure of martensite (cooled phase) [9]

On a macroscopic scale, the two crystal structures exhibit different technical properties, such as Young's modulus, electrical resistance, and damping behavior.

The graph in *figure 1-24* shows the temperature characteristics of NiTiInol by the percentage of martensite on the y-axis as a function of the temperature ($^{\circ}\text{C}$), highlighting the temperatures at which phase changes occur.

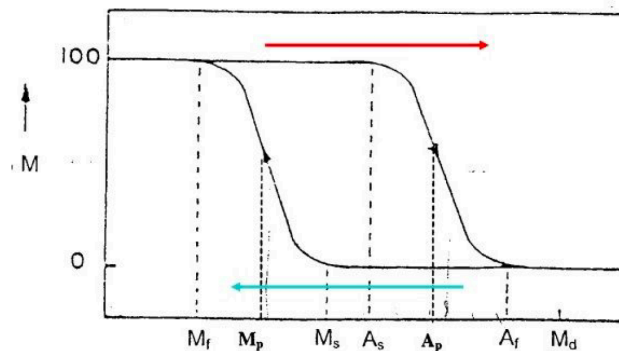


Figure 1-24 The graph shows the percentage of martensite as a function of the temperature and highlights the temperatures at which phase changes occur [9]

The red line from left to right shows the heating process while moving back from the right to the left the blue line is linked to the cooling process. Starting from the upper left and following the black curve, several specific temperatures can be distinguished:

- A_s The temperature at which, when heating the alloy, the phase transition from the martensitic to austenitic phase starts
- A_f The temperature at which, when heating the alloy, the phase transition from the martensitic to austenitic phase is finished
- M_s The temperature at which, when cooling down the alloy, the phase transition from the austenitic to martensitic phase starts
- M_f The temperature at which, when cooling down the alloy, the phase transition from the austenitic to martensitic phase is finished
- M_d The maximum temperature at which the alloy shows the shape memory effect. It is estimated as $A_f + 50^{\circ}\text{C}$ since this temperature is difficult to calculate

The temperatures A_p and M_p is where the peaks of the phase transformation between austenite and martensite are obtained during the heating and cooling process respectively; These characteristic phase transition temperatures can be regarded as material parameters, which depend on the alloy composition (the percentage of Nickel and Titanium in the composition) and the thermomechanical processing conditions. Alloys with a percentage of Titanium between 51% and 50,2% have an elevated A_f temperature, while for alloys with a percentage of Titanium between 49,8% and 49,4%, A_f is more similar to body temperature.

A peculiarity of the behavior just described is the hysteresis cycle which occurs during phase shifts. As can be seen from the graph shown in *figure 1-7*, the heating and cooling paths are different. Generally, hysteresis is defined as the difference between temperature to which the material is transformed to 50% in austenite, during the heating and the temperature at which the material is 50% martensite during cooling. The width of the hysteresis depends above all on the material; for NiTiInol alloys, the difference mentioned above also reaches 20-30 ° C. There are two temperature ranges for which a material model can describe the mechanical behavior of the alloy; below the temperature M_f (complete martensitic phase) and above the temperature A_f (complete austenitic phase). In these two conditions, inside the alloy is only one stable crystalline phase and therefore the macroscopic mechanical properties are known. In between these temperatures is a glass transition range of the NiTiInol, since there is no fixed temperature in which the phase changes as is the case with water.

1.4.2 Mechanical behavior

The fundamental properties of SMA's are essentially two; shape memory effect and pseudo-elasticity.

To explain these two principles, a short explanation of the stress-strain curve is necessary. When analyzing a deformation stress curve of a material like steel, it is possible to identify two distinct fields:

- The linear elastic field in which the stress-strain behavior is linear and is described by Hooke's law. In this field, when the force exerted on the material is removed, it recovers the entire deformation.
- The anelastic field in which the stress-strain behavior is no longer linear. Defects that are introduced between the crystalline planes of the metal irreparably deform the metal. The plastic deformation, due to the dislocation of the crystalline planes is therefore irrecoverable while the elastic deformation continues to recover.

Usually, when any metal is deformed, the rows of atoms of the crystal lattice affected by the deformation glide with respect to each other. It causes the breaking of interatomic bonds and the formation of new stable bonds, which give the material a different shape from the initial

one. In shape memory alloys, crystals alter their structure by moving on crystalline planes, without breaking interatomic bonds. Therefore the new deformed crystalline arrangement is not stable, and it is enough to heat the material so that the crystal lattice returns to its initial, more stable configuration.

1.4.3 Pseudo-elasticity

Pseudo-elasticity is the elastic behavior of shape memory alloys at constant load due to the phase transformation from austenite to martensite. The metal becomes pliable and can withstand strains of up to 8%.

It is obtained at a temperature higher than A_f , so when the alloy is in a complete austenitic phase. However, above the temperature M_d as highlighted in the right figure, the NiTiInol alloy behaves like a traditional material since the phase transformation is thermodynamically impossible. So pseudo-elasticity occurs in a range of temperatures comprised between A_f and M_d , as indicated in orange in the left figure.

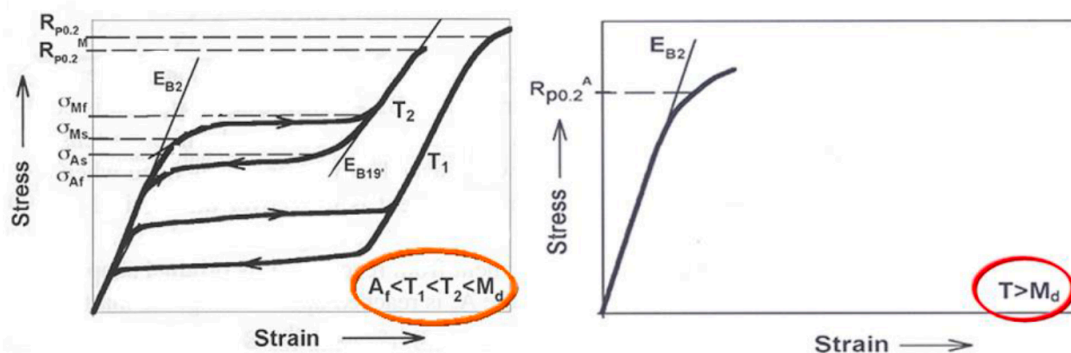


Figure 1-25 **Left:** The graph shows the principle of pseudo-elasticity during two different temperatures T_1 and T_2 , indicating the change of the stress value in a stress-strain graph during a load cycle on material above its austenitic temperature A_f . **Right:** the stress-strain graph if the material is above its maximum temperature for showing a shape memory effect, M_d [8]

In the left figure, the pseudo-elasticity principle is shown for two different temperatures. We will take a look at the upper curve during temperature T_2 . Above temperature A_f , NiTiInol is exclusively in the austenitic phase. If the alloy is subjected to a constant load, a transformation to the martensitic phase takes place which allows a shape transformation of the material (the stress during the transformation to the martensitic phase starts at M_{start} and reaches up to M_{final}). As soon as the load is taken away, the martensite, which above the temperature A_f is not thermodynamically stable, is rapidly transformed back into austenite (the stress starts at A_{start} and descends to A_{final}). The recovery of form is immediate. The area enclosed by the curves is the area of optimal superelasticity. This same loop is shown in another curve for a lower temperature T_1 .

1.4.4 Shape memory effect

The shape memory effect takes place when mechanically loading the alloy if it is below temperature M_f , so when in a complete martensitic phase. When a mechanical load is applied to the martensitic structure, stress-induced microstructural changes occur, so-called detwinning. The shape memory effect enables to recover all or part of the inelastic deformation (depending on the maximum deformation reached) if properly heated.

This property can be attributed to the combination of two microstructural changes; detwinning of martensitic phased materials and thermally induced phase transformation.

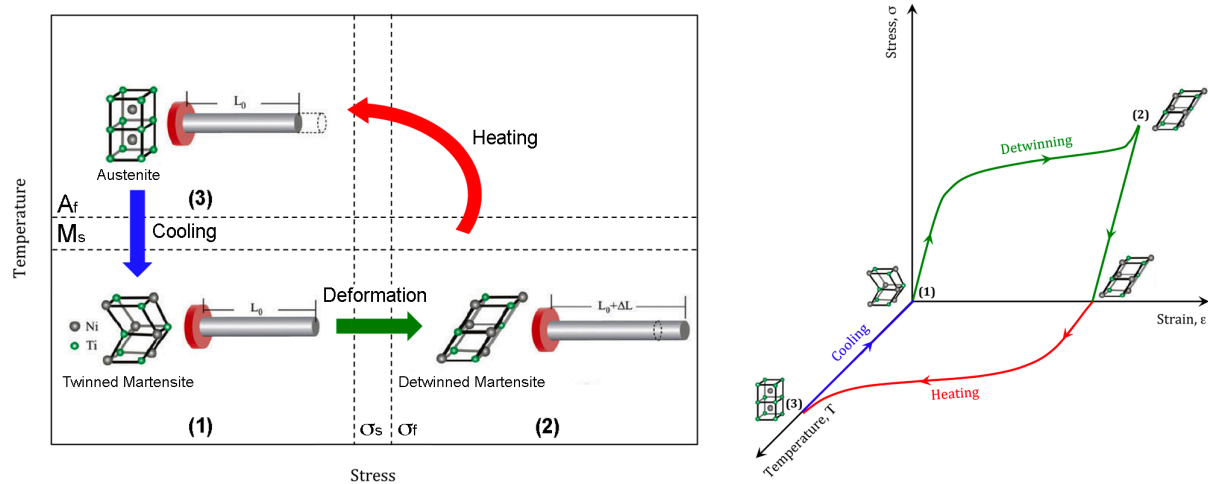


Figure 1-26 Process scheme of the shape memory effect in NiTiInol. First, plastic deformation occurs during detwinning. Then, heating the detwinned martensitic phase transforms it into austenite phase with a complete shape recovery. Lastly, it is cooled down to the twinned martensitic structure in its original shape.

The process will be explained with reference to *figure 1-26* above. If a mechanical load is applied to the twinned martensitic structure (1), detwinning occurs at a given critical stress value which corresponds to large plastic-like deformations (up to 10%) through a plateau in the stress-strain curve (2). These deformations persist after complete unloading because only the elastic recovery of the detwinned structure is observed.

If the material is heated up to the austenite finish temperature ($T > A_f$) a complete thermally induced phase transformation occurs (*red line*) from the detwinned martensitic structure to the austenitic phase (3) and, on the macroscopic scale, this transformation allows a complete shape recovery.

Finally, if the material is cooled down to the martensite finish temperature ($T < M_f$) it is able to remember its original twinned martensitic structure (1).

This unusual functional property is also known as one-way shape memory effect as it defines the ability of the material to remember and recover just one shape after being mechanically deformed.

Another property is the two-way shape memory effect, which is the possibility to return the alloy to its unstable deformed shape when it is cooled. It has two activation temperatures, one of which at high temperature pushes the material to its original stable form, while the second at low temperature forces it into the unstable condition in which it was deformed.

1.4.5 Application technologies

The fundamental peculiarity of the SMA, which has ensured that they are the object of attention in the scientific field, remains the high power/weight ratio that the material can provide. Concerning this last aspect, it is therefore natural that shape memory alloys are in the ascending phase of development. Consider also that the reliability is total since there cannot be malfunctions or wear since the movement is a consequence of the phase transformation of the alloy.

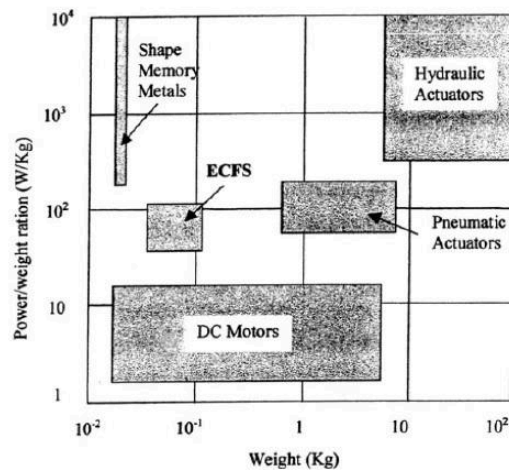


Figure 1-27 Comparison of different actuators: power/weight ratio [36]

Shape memory alloys can be used in a variety of shapes like rods, plates, ribbons, springs, and wires. Especially wires and springs are used often as actuators in this area of application.

Other significant areas of application are the aviation, civil, and automotive industry. In the medical field, most of the cardiovascular stents are made of NiTiInol. Also, it is useful for orthopedic fixation devices by cooling the metal before implanting it in bones. Once it heats up and returns to the smaller original state, it exerts a constant force on two bones which need to be pressed together.

In dentistry, it is a useful material for the construction of brackets to have constant forces on the teeth. In optometry, frames of eyeglasses which are made of shape memory alloys with transition temperatures below room temperature are more robust for accidental damaging because of pseudo-elasticity.

Weak points of the technology are energy inefficiency, slow response times, and large hysteresis. Also, their limited recoverable strain in the range of 4% requires them to have

lengths up to 25 times longer than their intended stroke length. By turning the SMA wires into springs, the actuation stroke can be significantly increased up to 200–1000% of their original actuation stroke, but the maximum force generated by the SMA is greatly decreased.

Another type of SMA is a ferromagnetic shape memory alloy (FSMA), which changes shape under strong magnetic fields. These materials are of particular interest as the magnetic response tends to be faster and more efficient than temperature-induced responses.

Also, shape-memory polymers (SMPs) are polymeric smart materials that have the ability to return from a deformed state to their original shape induced by an external trigger, such as temperature change, light or solution.

1.4.6 Technical specifications

Among the various materials characterized by this particular property, of considerable interest is NiTiNol (Nickel Titanium Naval Ordnance Laboratory, the laboratory in which it was first created). It shows a complete recovery of the impressed deformation and generates a considerable force during the return to the original form. It is certainly the most successful league thanks to its ability to recover up to 6-7% of its elongation. *Table 1-1* shows the properties of this alloy.

The Young's modulus of NiTi alloys depends on the phase that is considered. In particular, in the austenitic phase, it is $E_{\text{austenite}} = 75 \text{ GPa}$, while in the martensitic phase it is $E_{\text{martensite}} = 28 \text{ GPa}$.

Table 1-1 Properties of NiTiNol

Properties of NiTiNol	
Density	6.45 gm/cm ³
Thermal Conductivity	10 W/mK
Specific Heat	322 j/kgK
Latent Heat	24,200 J/kg
Ultimate Tensile Strength	750-960 MPa
Elongation to Failure	15.5%
Yield Strength (Austenite)	560 MPa
Young's Modulus (Austenite)	75 GPa
Yield Strength (Martensite)	100 MPa
Young's Modulus (Martensite)	28 GPa

When making a NiTi alloy it is of fundamental importance to pay attention to the percentages of nickel and titanium used. In commercial NiTi SMA's the percentage of titanium is between

49% and 50.7%, in particular, if this percentage is between 49% and 49.7% the alloy will have a purely pseudo-elastic behavior whereas if the percentage is between 49.8 and 50.7%, the behavior will be mainly in shape memory. If these percentages in the alloy exceed the range just described it would become biphasic, in particular, a phase will be composed of NiTi while the second phase will be composed of the element in excess. The result is an alloy that shows reduced or absent memory behavior. The main problem of these alloys is the variability of the finished product, in fact, 95% of the NiTi alloy is rejected due to defects or lack of homogeneity in the final acceptance checks; this is the reason for the high production cost.

For this prototype, the SmartFlex01 wire supplied by SAES GETTER was available. *Table 1-2* shows the main physical characteristics of the wire.

Table 1-2 Physical quantities of the specific NiTiNOL wire supplied by SAES GETTER

Physical quantity	Unit
Diameter	100 μm
Maximum strength	4,7 N
Suggested operating force	1,3 N
Maximum elongation	5%
Suggested operational lengthening	<3,5%
Young's modulus (martensite)	40 GPa
Young's modulus (austenite)	75 GPa

SAES GETTER recommends tensioning and stretching to avoid premature aging of the wire.

The martensitic low-temperature phase can be deformed similar to pure Titanium: it can be bent back and forth without strain hardening. Thus, the risk of breakage of a component made from martensitic NiTiNol is significantly lower than, for instance, in stainless steel. Finally, when heated into the austenitic phase, the alloy recovers its original shape. The metallurgical reason for the martensite deformability is the twinned structure of the low-temperature phase: the twin boundaries can be moved without much force and without the formation of dislocations, which can be considered as being the initiator of fracture.

The speed of shortening and that of relaxation depend on the size of the wire, the presence or absence of elements that dissipate the heat and the current that is used.

Chapter 2: Design goals and requirements

The goal for this thesis work is to improve the current prototype of a wearable hand orthosis made at LiSiN laboratory. Stimulated SMA wires work as actuators to regain finger muscle function with this wearable orthosis. Previously, multiple thesis works have been dedicated to this design [8], [9], [36]. Starting from scratch, in three thesis works a prototype for an actuator system has been presented. This prototype was only used on a wooden dummy hand for demonstrating feasibility.

In this chapter, the situation as at the end of the last thesis about this subject will be explained. Based on that, design goals will be set, which establishes the base of the design process. These goals will be translated to design requirements. From these requirements, specifications of the design can be distilled, and the design choices can be explained. Some of those specifications can be calculated as well, such as the kinematic and static analysis. Some choices had to be made immediately to proceed in the design and production of a prototype, but it was always tried to keep options open for future improvements that might need to be made.

A setup of the complete system will be given as well, to keep a complete overview of the prototype. Also, a more profound section will be dedicated to shape memory alloys, since this is used as the actuator in this orthosis prototype.

After that, the next chapter will describe the prototyping phase of this project.

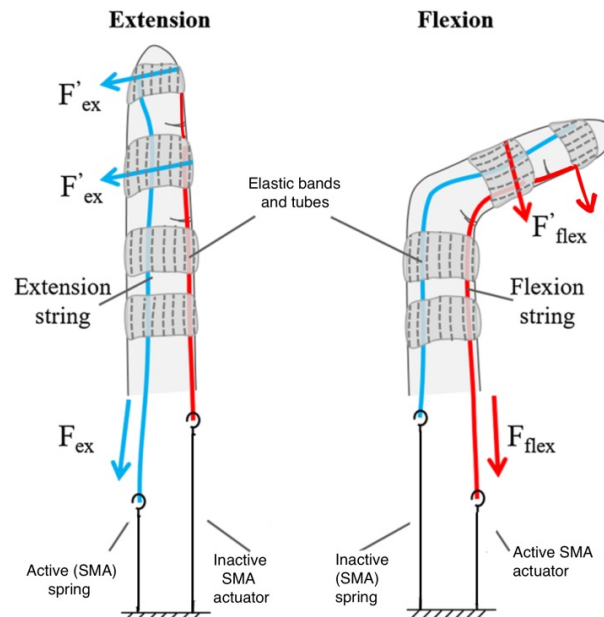


Figure 2-1 A sketch of a possible flexion and extension mechanism

2.1 Current situation

The design of the current prototype at the start of this thesis will be briefly explained to indicate the improvements that were necessary to proceed in the development of a useable prototype. The SMA actuators consisted of white sockets which are connected to the wooden dummy with adjustable straps. On the white sockets, pulleys are installed on a holder and connected to the black current cables attached to the SMA driver. An SMA NiTiNol wire is drawn zig-zag around these pulleys, in order to reach the amount of length of wire needed to obtain a sufficient shortening of the wire for a grasping movement.

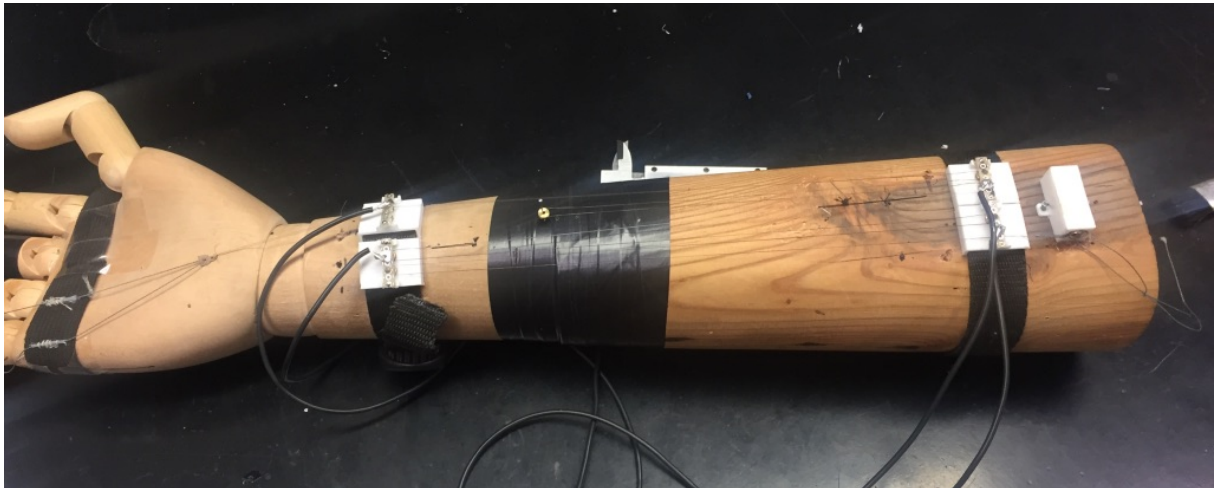


Figure 2-1 The prototype to improve, situating at the begin of the project

The wire is connected to a Kevlar wire which functions as tendon. The tendons run through annular tubes attached to the fingers with elastic straps. This prototype currently actuates only one degree of freedom, in this case, the flexion of the small finger.

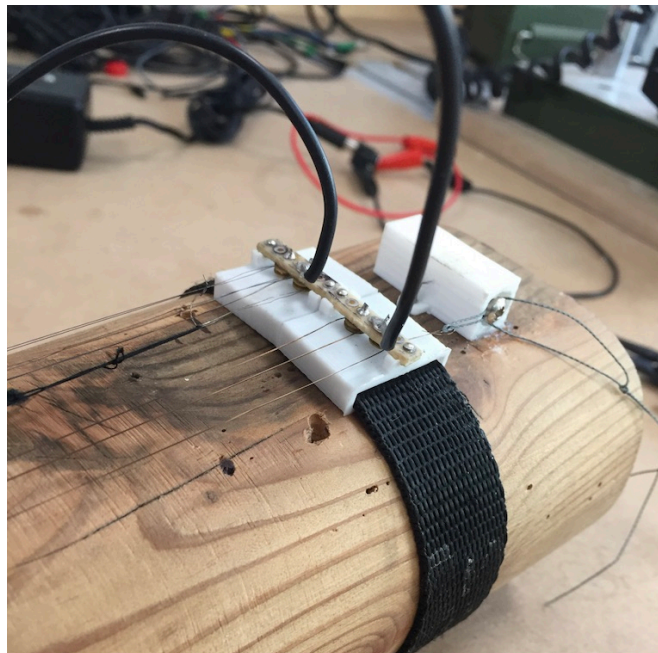


Figure 2-2 The holders for the pulleys containing the SMA wires. The black current cables are connected to the SMA driver.

The actuator consists of two modules, linked mechanically but isolated electrically. The SMA driver actuates the two modules in parallel by stimulating them through one channel. The two modules together are approximately 3.4 cm wide.

A small initial test was executed on the testing system created by Motta [36]. An SMA wire of 45 cm was stimulated at different current values, varying from 260 mA to 320 mA. The amount of shortening was on average 0,9 cm and did not differ a lot for different currents.

An important characteristic to note is the conservation feature of the memory effect of the wire. Previous tests show that the wire has a higher percentage of shortening if it is fed at a high current intensity before a test. The wire retains some memory effect due to a high-intensity current and thereby improves its relative shortening. Therefore, the wire needs to be supplied with a current stimulation greater than or equal to 300 mA before each test session, above all if this happens after a few days of inactivity of the wearable device.

2.1.1 Functional design requirements

Now, to proceed with an improvement of the prototype, the main points of improvement need to be stabilized. Some requirements are needed to extend the glove function while improving the current prototype.

1) *Wearability*

At the start of this thesis, it was not yet possible to test the prototype on persons. The current prototype is installed on a wooden hand and was not wearable during testing. Therefore, one of the main points of attention is wearability. The goal is to create a new prototype which can be moved around freely by a user while wearing the device.

2) *Adaptability/modularity*

Since there is a vast difference in arm and hand sizes, degree of disability, and amount of forces or shortening of the wire needed, adaptability was a requirement. In this way, one design can be fitted to many patients and therefore increase efficiency. Also, modularity makes part of this requirement, since linking multiple modules creates more possibilities for the requested shortening, which can be different for every patient. The orthosis should have the possibility to be adapted to different users, who have different hand size, different disorders, and require specific rehabilitation protocols.

3) *Movement function*

The system should preferably support an antagonism movement of both finger flexion and extension and be capable of controlling each finger separately. Another point of focus will be the extension of more degrees of freedom. Currently, the prototype is able to execute only one flexion or extension movement of a single finger.

4) *Weight and size*

The system should be lightweight since its intended use is during activities of daily living. A bulky device would result in difficulties for the user during use. SMA wires are very lightweight activators.

5) *Safety and comfort*

The device must be safe and comfortable for the wearer. For a safe design, there should be no rigid actuation systems attached to the fingers. The glove should be completely soft.

In the next sections will be focused on all the points of interest and choices encountered during the production and design procedure.

Functional specifications

Some functional specifications can be derived from the requirements above. These specifications can serve as tools during the design process.

1) *Wearability*

For the point of view of wearability and adaptability, a soft interface such as a lycra glove is a good choice. The glove is easy to put on and off and fits for different hand sizes. The wires should not be loose in the air like in the previous prototype. Therefore the module should be made of a rigid material. It will be an advantage if the patient is able to don and doff the device itself without the help of another person.

2) *Adaptability/modularity*

The length of the module should be adjustable to adapt to different test persons. Not only from a physical point of view but also to adjust the amount of SMA wire that is needed in the module to operate for a specific test person. During the design process, it has to be kept in mind that different modules have to be able to be linked together, even if they are set to different lengths. Also, as much as elastic material as possible has to be used for attaching modules or other parts to patients, to keep the system available for a vast range of different body sizes.

Specific rehabilitation protocols can require actuation of different fingers or specific movements. The module should be designed as a universal device which can be linked to different fingers while maintaining its artificial muscle function.

3) *Movement function*

For grasping, often the thumb, index finger, and middle finger are used. During this research will be focused on restoring the function of one or more of the four regular fingers. The movements of these fingers are similar to each other, which makes it easier to switch finger actuation, using the same modules but by simply linking it to a tendon on another finger. This improves the fluidity of the project during tests and satisfies the requirement of adaptability for different users.

These universal modules can also be used for an antagonism movement by putting it on the dorsal side of the arm and connecting the SMA wire to tendons on the dorsal side of the hand.

4) *Weight and size*

Lightweight materials should be used for the construction of the module. The SMA wires are very lightweight respect to other artificial muscles. The size and encumbrance of the system can be reduced if the modules can be piled up on each other, possibly with a click system. There should be a minimum number of actuated degrees of freedom (DOF) to reduce the weight, costs, and complexity of the system.

In fact, an underactuated system where one wire actuates multiple joints of a finger would be advantageous.

5) *Safety and comfort*

As seen during bibliographical research, many designs have a soft interface, which makes them more comfortable to wear. Therefore, a soft glove in lycra will be used as an inner layer, to cover the complete hand and give comfort to the user.

For a safe design, there should be no rigid actuation systems attached to the fingers. In case of a problem, this could cause damage to the user. A soft tendon system would be a better fit from a safety point of view.

A rigid container as a module wherein the wires are kept would be safer since the wires are separated from the patients' skin. Currently, the wires are in the open air, following their path between two small modules.

Also, the connection of the current wires to the SMA driver channels is ideally made with a closed connection, like a plug-and-play system. Unfortunately, this is not yet implemented.

A summary of the established requirements and functional specifications is shown in the table below.

Table 2-1 Summary of the established requirements and functional specifications

Requirements	Functional specifications
<i>Wearability</i>	Soft Lycra glove Rigid container Autonomous and easy donning and offing
<i>Adaptability/modularity</i>	Adjustable container length Use of elastic material if possible Possibility to link modules
<i>Movement function</i>	Actuation of one or more regular fingers, no thumb movement Universal modules for flexion and extension
<i>Weight and size</i>	Use of lightweight SMA wires Possibility to pile up modules Reduce the DOF, underactuated system
<i>Safety and comfort</i>	Soft lycra glove Soft tendon system Rigid wire container

2.1.2 Technical specifications

Kinematic analysis

Generally, there is a relation between the tendon length variation and rotation of each phalanx. If this relation is known, the required length of each SMA wire can be calculated.

In order to model applied forces on the finger, the following assumptions were used in the calculations:

- The metacarpal is fixed, and cable guide forces do not cause any rotation of the segment.
- Each joint is a pure revolute joint with 1 DOF.
- The cable passes through the cable guides with negligible friction.
- No movement of the cable guides occurs under force.

Under these assumptions, the finger is modeled as a planar three-link kinematic chain.

The relation between tendon displacement and joints angle can be extracted, as was done by the authors of another wearable glove design [30].

Tendon deflections during the closing of the hand can be computed based on joint angles:

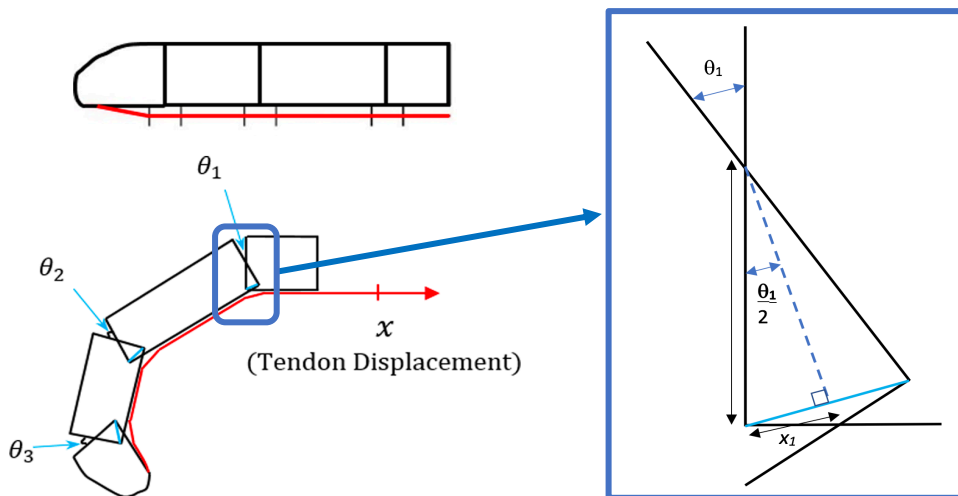


Figure 2-3 Sketch and detailed view of the finger anatomy with the indicated joint angles [3]

$$x = 2 \left(L_1 \sin \left(\frac{\theta_1}{2} \right) + L_2 \sin \left(\frac{\theta_2}{2} \right) + L_3 \sin \left(\frac{\theta_3}{2} \right) \right) \quad (1)$$

Where L_1 , L_2 , and L_3 denote the half of thickness of MCP, PIP, and DIP joints, respectively. For calculating the deformation distance x , we assume the thickness of the knuckles of an index finger for a 24-year-old man; 15 mm for DIP, 20 mm for PIP and 30 mm for MCP. The range of variation of each joint angle is $[0-80^\circ]$ for DIP, $[0-100^\circ]$ for PIP and $[0-85^\circ]$ for MCP joints.

$$x = 2 \left(\left(\frac{30}{2} \right) \sin \left(\frac{85}{2} \right) + \left(\frac{20}{2} \right) \sin \left(\frac{100}{2} \right) + \left(\frac{15}{2} \right) \sin \left(\frac{80}{2} \right) \right) = 46 \text{ mm}$$

This number is a good approximation for the given geometry. In case the patient has thinner fingers, less strain-length of the cable is necessary for actuating the finger. Vice versa, for bigger fingers more strain-length of the cable is necessary, and thereby also the total length of the SMA-wire. Differences between this theoretical model and practice could be due to the assumption made that the tendon is tightly attached to the finger during the whole movement. In practice that might not always be the case because of a minimal distance of the tendon wires respect to the skin, and deformations of the cable during bends of the phalanxes as shown in *figure 2-3* [37].

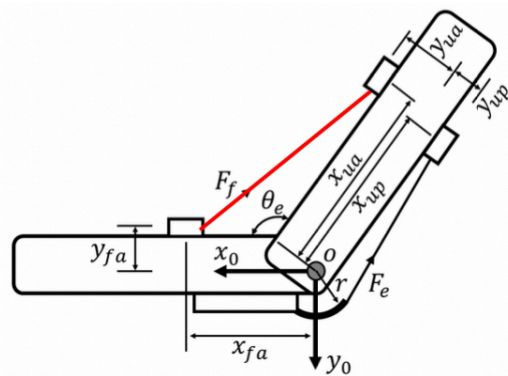


Figure 2-4 Distance of the tendon wire relative to the bending phalanx [37]

During a bend of two phalanxes, the tendon wire can take a different route relative to the skin of the two phalanxes. The obtained theoretical values give a good estimation during the design process for stabilizing the length of the SMA-wire that is needed for actuation.

Static force analysis

The force which is applied by the SMA wires to the tendons generates a force between the fingertip and objects during grasping. According to Hadi et al. [30], the relation between the tendon tension (T) and the grasping force (F_n) is proved to be that the grasping force is 0.35 times the wire tension.

Applying the virtual work principle leads to the relation between the tendon tension and the grasping force:

$$T * \delta x + F_n * \delta u + F_t * \delta u = 0 \quad (2)$$

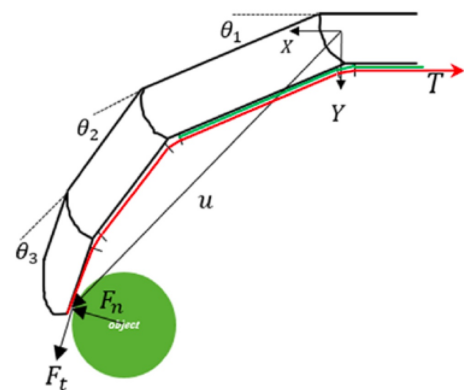


Figure 2-5 sketch of fingertip forces and position vector [30]

where δx represents the tendon displacement. Also, u denotes the position vector of the contact point. The relation between x and θ_1 , θ_2 , and θ_3 can be derived based on the previous equation:

$$d\vec{x} = -\left(l'_1 \cos\left(\frac{\theta_1}{2}\right)\delta\theta_1 + l'_2 \sin\left(\frac{\theta_2}{2}\right)\delta\theta_2 + l'_3 \sin\left(\frac{\theta_3}{2}\right)\delta\theta_3\right) \quad (3)$$

Similarly, the relation between δu and $\delta\theta_1$, $\delta\theta_2$, and $\delta\theta_3$ can be found by:

$$\begin{aligned} \vec{u} = & (l_1 \cos(\theta_1) + l_2 \cos(\theta_1 + \theta_2) + l_3 \cos(\theta_1 + \theta_2 + \theta_3))\hat{i} \\ & + (l_1 \sin(\theta_1) + l_2 \sin(\theta_1 + \theta_2) + l_3 \sin(\theta_1 + \theta_2 + \theta_3))\hat{j} \end{aligned} \quad (4)$$

and then deriving to:

$$\begin{aligned} \delta\vec{u} = & -(l_1 \sin(\theta_1)\delta\theta_1 + l_2 \sin(\theta_1 + \theta_2)(\delta\theta_1 + \delta\theta_2) \\ & + l_3 \sin(\theta_1 + \theta_2 + \theta_3)(\delta\theta_1 + \delta\theta_2 + \delta\theta_3))\hat{i} \\ & + (l_1 \cos(\theta_1)\delta\theta_1 + l_2 \cos(\theta_1 + \theta_2)(\delta\theta_1 + \delta\theta_2) \\ & + l_3 \cos(\theta_1 + \theta_2 + \theta_3)(\delta\theta_1 + \delta\theta_2 + \delta\theta_3))\hat{j} \end{aligned} \quad (5)$$

It should be noted that the application points of forces F_t and F_n are the same. Therefore, the same virtual displacement is considered for both. Substituting these equations in equation (2), the F_n and F_t can be extracted for a known T . And therefore, the results prove that F_n is approximately 0.35 times T . It should be noted that the above result is correct for an approximately straight posture of the hand where all the phalanxes have a zero degrees angle. This relation has been tested during an experiment by measuring fingertip and tendon forces with two load cells. The theoretical results had a good agreement with the experimental results.

Another research which confirms these results about hand forces is from Chao in 1985 [38]. It states that the tension of human's tendon, which is the primary source of the axial and shear force, reaches two or three times that of the fingertip force when performing a general pinch or grasp.

To grab a small bottle of water, weighing 522g and a diameter of 57mm, the forces on the five fingers, starting from the thumb and ending with the little finger, are 1.3 N, 1.0 N, 0.9 N, 0.8 N and 0.4 N [16]. Naturally, the contact forces of the other phalanges and the palm also intervene in a palm grip. During the research of Castro [39] however, for the same movement, the index and middle finger had an average force of 1.8 – 3 N.

Technical specifications of the SMA wire

Based on the kinematic and static analysis above, the first technical specifications for the SMA wire can be stabilized. Based on the Nitinol wire that is at our disposition, the required length and amount of wires can be calculated.

In order to obtain a shortening of 4.6 cm, while considering a 3.5% shortening of the SMA wire, means a wire of 132 cm is needed. The requested fingertip force on the index finger according to the previously mentioned research is more or less 2 N. The fingertip force is approximately 0.35 of the tendon force. That means a tendon force of 6 N is needed. The Nitinol wires that are used in this prototype can exert up to 3 N force. That means a double Nitinol wire of 132 cm is needed to obtain the requested shortening and force. A single SMA wire is folded to form two parallel branches so that the force that the wire exerts is doubled.

The electrical resistance of a wire can be calculated with the second law of Ohm formula:

$$R_{wire} = \frac{\rho * L}{S}$$

Where ρ is the electrical resistivity, L the length of the wire (132 cm), and S the surface ($d = 100 \mu\text{m}$). The electrical resistivity of an SMA wire varies between $1,05 \times 10^{-6} \Omega \text{ m}^{-1}$ in the martensite phase and $0,85 \times 10^{-6} \Omega \text{ m}^{-1}$ in the austenite phase. The total resistance of a single wire results between 176 Ω and 143 Ω . In parallel these values are halved;

$$R_{//2 \text{ wires}} = \frac{1}{\frac{1}{R_{1 \text{ wire}}} + \frac{1}{R_{1 \text{ wire}}}} = \frac{R_{1 \text{ wire}}}{2}$$

If all fingers, except the thumb, need two wires to perform a flexion and extension movement, at least 10 meters of NiTinol wire needs to be stored within the system.

To avoid having a bulky SMA actuator because of the long wire, wrapping the wire around a miniature pulley array in an N-shaped layout is a common approach. In this way, even if a long wire is needed to obtain the requested shortening of the wire due to the limited stroke length, the dimensions of the actuator can be reduced and fitted into a wearable module. The disadvantage of this solution is that if the length of the wire increases, more pulleys are needed to keep the actuator compact, increasing the complexity and weight of the actuator and its frictional losses.

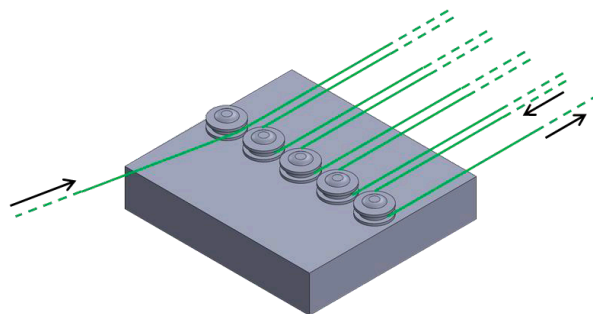


Figure 2-6 Visualization of a miniature pulley array to wrap the wire around in order to reduce the actuator size. [8]

Finger choice

During the design process, multiple options for the tendon strategies as well as the actuation method have been reviewed. It can be stated that most importantly for stabilizing a path for the design, is to determine which hand or finger function needs to be replicated with this wearable orthosis. From literature research, several options were found, varying from two up to five functioning fingers. For this, it is essential to study human anatomy and finger functions during activities of daily living. A lot of the projects considered in the literature research assumed restoring the function for three fingers; mostly thumb, index finger and middle or ring finger.

Restoring the thumb function would be a good but also complicated choice. The opposition movement between the thumb and index finger is a very natural movement used in most grasping movements. Though, the thumb does not consist of three phalanxes linked by joints with a single DOF like all the other fingers. The thumb CMC joint has three DOF's: abduction/adduction, flexion/extension and opposition/reposition [40]. It is hard to mimic these degrees of freedom of the thumb in a natural way using a single wire system. In future research restoring the thumb function, should be considered to achieve the most natural hand function possible.

This prototyping process is focused on the other four fingers since their actuation is easily interchangeable and extendable between the different fingers. For grasping, two or three fingers generally should be enough. The more fingers are actuated, the more complex the system becomes. Also, the amount of controllable fingers depends on the number of channels available to control the system. Currently, four control channels are available to actuate the hand orthosis. In the future, the control unit (also called SMA driver) which will be explained later in this chapter, is extendable to more channels.

The aim is to initially start the design with an index finger function, after that it possibly can be expanded to the middle finger or the ring finger. The small finger has the fewest use in regaining the strength and use of the hand and will not be considered in the current design. During literature research, almost no design was found where the small finger was actuated. In most of the designs, the choice for a specific finger was not specified.

Further, the required movements of each finger should be chosen. It is possible to use the available control channels for both flexion and extension movements. For example, two channels are used to control wires for the flexion movement of the fingers separately, while the other two available channels control the flexion of each of the fingers. Another solution would be to use springs placed on the dorsal side of the hand for the extension of the fingers. In any case, the muscle function will be replicated by contracting an SMA-wire connected to the finger, like in the current prototype.

2.2 System's architecture

The system consists of four parts; SMA driver, SMA wire modules, EMG system, and software. The figure below shows the functioning scheme of the complete system.

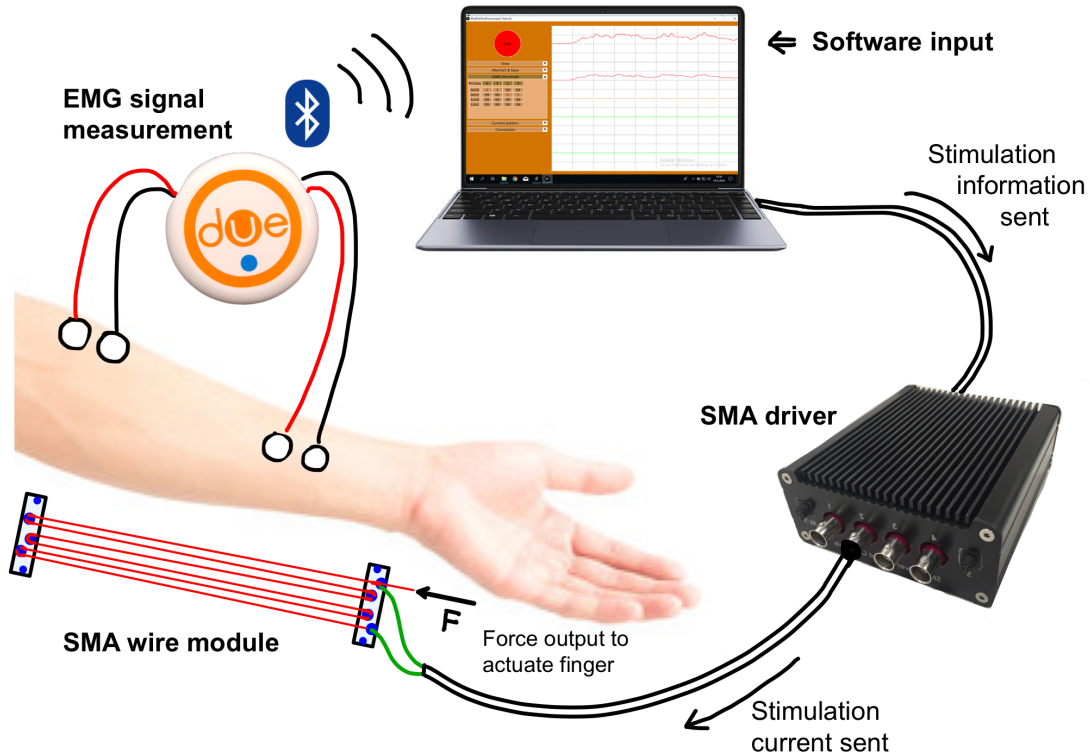


Figure 2-7 Scheme of the system which consists of four parts; SMA driver, SMA wire modules, EMG system, and software

2.2.1 SMA driver

The SMA driver is a constant current generator which can be controlled from the computer where it is linked to. It has four channels to deliver current to the SMA-wire modules. The SMA driver is designed and developed in the LISiN lab together with the orthosis. The new version which is available since the development of the new orthosis prototype also has a modular connection, and therefore the number of channels can be increased. For now, only four channels will be used. It is connected to a 60V power supply and a computer through an USB-port.



Figure 2-8 SMA driver unit, four cables can be connected to the channels to actuate the SMA wire modules.

2.2.2 SMA wire modules

The SMA wire modules are the main point of interest during the prototyping process treated in this thesis. The modules are small plastic sockets which contain the amount of SMA wire needed to actuate the patients' fingers. These modules are installed on the forearm of the patient and connected to the tendon system installed on a soft glove worn by the patient. The prototyping process will be explained in chapter 3.



Figure 2-9 SMA wire module as at the end of the prototyping process. This module contains all the needed SMA wires which are actuated with the red current cables coming from the SMA driver.

2.2.3 EMG system

During a regular test on a test person, it is not clear whether the test person is using muscle force or not. In order to exclude this uncertainty during tests, the EMG signal can be measured to make sure the forces are generated by the actuator only.

Residual EMG signal of the muscles responsible for closing the hand can also be used to control the actuation system, for example functioning as a switch if the signal reaches above a specific set value.

Also, this muscle signal can be used if only one side of the body is affected by post-ictus complication, such as reduced muscle control. In that case, the EMG signal of the healthy arm can be used to make the affected arm mirror its movements.

In previous thesis works, the EMG signal was already implemented in the software, but not used in a very extensive way. The functioning of the EMG measurement and implementation and the improvements made in the software will be briefly explained. In chapter 4, the results of some functional tests which are useful for verifying the usability of the improved prototype are described.

Due Pro system

The same software as in previous thesis work is used to control the actuation of the SMA wires. Furthermore, the DUE probe of the Pro system (OT Bioelettronica, Turin) will be used to measure the EMG signal. In the manual of the Due system is a vast explanation for installing the software and drivers. The probes are wirelessly connected to the computer through a USB receiver for transmitting the EMG signal. This signal can be analyzed and converted in real time to use it as a driving mechanism for the SMA actuators. Two pairs of bipolar electrodes

placed on the forearm are connected to a probe and measure the muscle activity under the electrodes.



Figure 2-10 The Due pro system and a Due probe

The superficial flexor of the fingers is chosen as the muscle to take the EMG signal from. Since it is a superficial and large muscle, that also facilitates the task of positioning the bipolar electrodes on the forearm.

2.2.4 Software

The software installed on the computer has a Graphic User Interface, which is used to set the current regulation in terms of pattern, current level, current duration, and channel. The selected channels can be stimulated by sending the set current and pressing the try_stim button. Also, during this research, two other buttons were added with whom all channels could be stimulated at the same time (try_all) or in a predefined pattern, switching channel every 2 seconds (try_pattern).

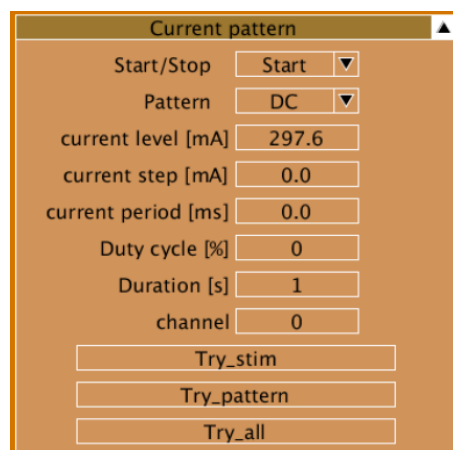


Figure 2-11 Parameters to be set for the current pattern used for actuation.

Once the two pairs of electrodes have been placed, and the system is connected to the PC, the values of the threshold can be set in the user interface. Some screenshots of the actual control software are shown in the figures below. In the software, the raw EMG signal is processed by taking the RMS value and envelope function to obtain a useful signal which can be compared with the threshold.

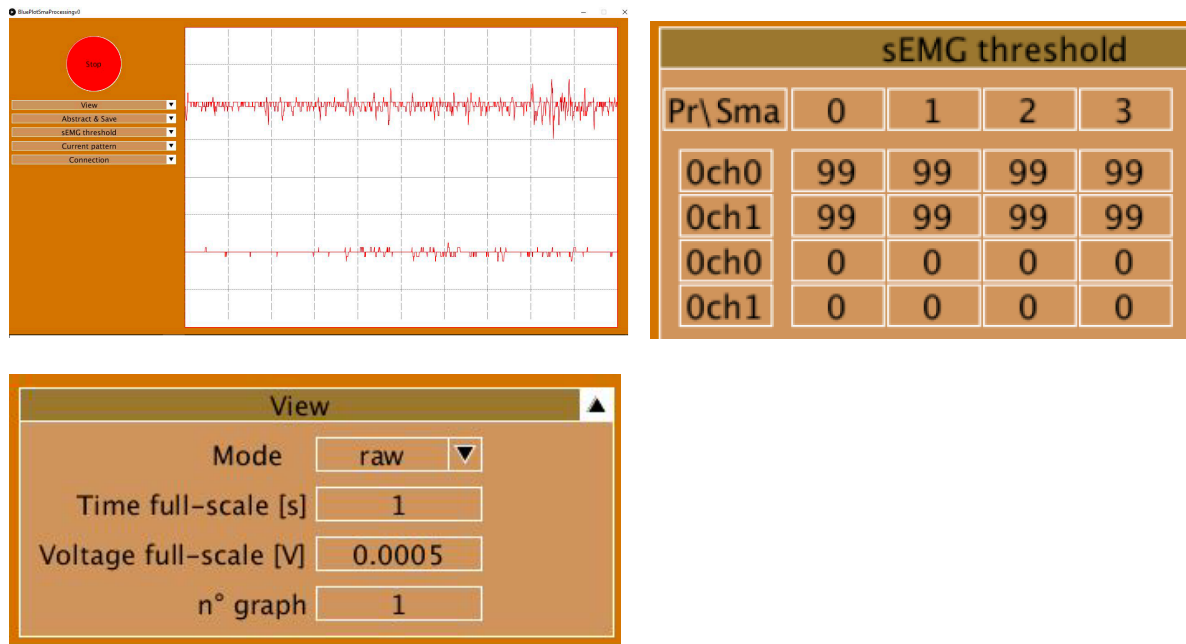


Figure 2-12 Upper left; visualization of the EMG signal. Upper right; upper and lower threshold matrix for each channel. Below; parameters to be set for the visualization of the EMG signal

When the threshold is set to 1 for both the distal channel and the proximal channel, good results are obtained. In order to control the device with an EMG signal, the electrodes need to be correctly positioned, to have a correct reading of the EMG signal. Then, on the right moments when the signal exceeds the threshold, the current can be supplied in the correct order on the channels. So the device leads the closing of the finger according to the myoelectric signal taken from the muscle in the actuated arm or the muscle in the other arm. In order to improve the software and implementation of the EMG signal, two extra functions are inserted in the software.

Probe number box

The first one contains a box where the number of the Due probe can be inserted, also called the probe ID. Every Due probe has a color code and thereby an own number. If a different probe is used during an experiment, this had to be changed in the software code before the experiment started. If the probe ID did not correspond to the probe that was used, the EMG signal was not visible. With this simple box, the probe number is immediately updated without having to search in the code to set the correct value of the probe ID.

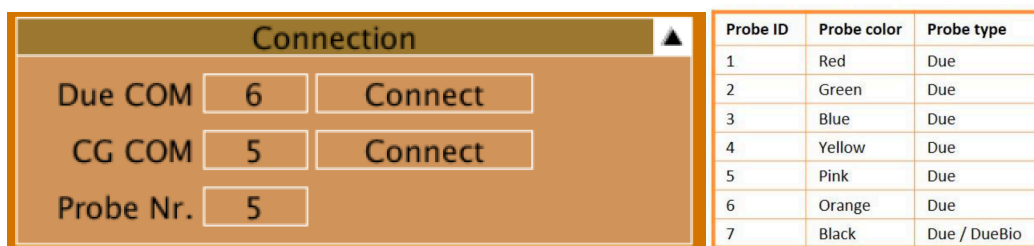


Figure 2-13 The box where the number of the Due probe can be inserted, which is based on the color code of the probe. In this case, the pink Due probe was used.

Hysteresis cycle

Also, a hysteresis threshold is inserted to have a more smooth transition between the activation and deactivation of the SMA wire. If the envelope of the signal reaches the upper threshold of a channel, the channel is activated, and the set current is sent. This activated mode continues for as long the signal remains above the set minimum threshold. This hysteresis cycle prevents the activation of a channel from changing rapidly. The activation will only be interrupted if the EMG envelope signal goes under the lower threshold.

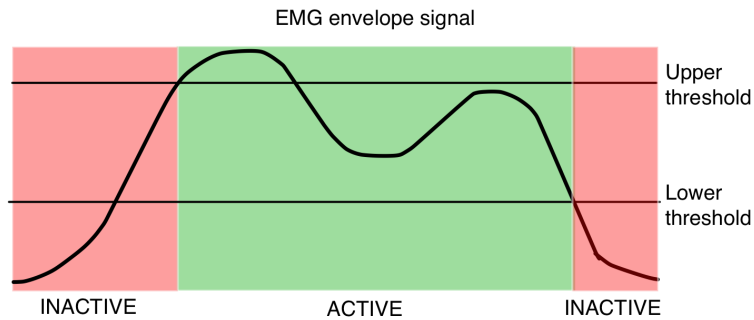


Figure 2-14 Example of an EMG envelope signal and the upper and lower threshold that can be set. As soon as the signal exceeds the upper threshold, the stimulation is active until the signal is inferior to the lower threshold.

The values for the upper and lower threshold can be set in the user interface. In the upper two lines, the upper threshold for each of the two EMG signals is set for each SMA driver channel (0 / 1 / 2 / 3). In the lower two lines, the lower threshold is set. In this case, SMA driver channel 0 and 1 are activated by the EMG signal from the first probe channel, which higher and lower thresholds are set to 1 and 0.5 respectively.

		sEMG threshold					
		Pr\Sma	0	1	2	3	← SMA driver channel
Probe CH. 1	0ch0		1	1	99	99	→ Upper threshold
	0ch1		99	99	1	1	
Probe CH. 2	0ch0		0.5	0.5	0	0	→ Lower threshold
	0ch1		0	0	0.3	0.3	

Figure 2-15 User interface for the setting of the lower and higher threshold for each probe channel, to activate the SMA driver channels (0 / 1 / 2 / 3)

Chapter 3: Design and prototyping

In this chapter, the prototyping process of the wearable orthosis will be described and guide through the practical side of the design and improvement phase of this project. The process consists of an improvement of the previous prototype, which is described in chapter 2. It was a trajectory of design choices, crafting of the prototype, verifying tests, and improvements. Several design features and choices which were encountered will be described.

During the prototyping process, also some practical matters and design choices are introduced and explained. Some of the subjects addressed in this chapter are of a practical nature and are necessary steps to go through in the design process. Many choices had to be made, and they did not only depend on the best options but also on the availability and specific applications which were considered important in this project. Some choices had to be made immediately to proceed in the design and production of a prototype, but it was always tried to keep options open for future improvements.

The prototyping is split up in a part about the modules, which contain the SMA wire, and a part about the glove with a built in tendon system. These are two separate parts but can be easily connected by linking the tendon wire to the SMA wire. The situation of the design of the SMA module will be highlighted during two stages of the process, also referred to as the first and second prototype.

3.1 Prototyping of SMA-wire module

An SMA wire socket is needed to store the SMA wire which is used as an actuator. The main goal is to design a socket that is modular, safe, and compact. The socket needs to be able to store at least 130 cm of NiTiNol wire which can be tensioned and directed to the finger tendon system. In the socket, the SMA wire needs to be connected to wires coming from the control unit. In that way, the SMA wire can be controlled with a current coming from the control unit to obtain a Joule effect and thus shortening of the wire. The most obvious solution is to continue with and extend the current prototype according to the functional and technical requirements. The previous prototype was installed on a wooden hand and consisted of 2 sockets on each side. The wire is tensioned loose in the air between the sockets. Wearability is key in the next step since it needs to be wearable for a patient to use the system. The most basic solution at this point is to make a 'container' to keep the SMA wires under tension. In order to improve modularity, the containers can be piled upon each other, expectedly two stacks high. Also, their compactness can be improved by narrowing the width, for example, by making a single socket for the pulleys instead of the current double socket.

3.1.1 First prototype

An important point to start with while designing a new module for containing the SMA wire was safety. The current prototype did not have any support surface between the wire and the arm, in this case being the wooden dummy arm. So the system was not wearable for a person to test the system. The most basic solution at this point is to make a 'container' to keep the SMA wires under tension. If these containers are smooth enough, they could be piled up on each other, expectedly two stacks high to improve modularity. Also, a container would be more resistant during experiments than two separate holders attached to the arm with all the SMA wires hanging loose around.

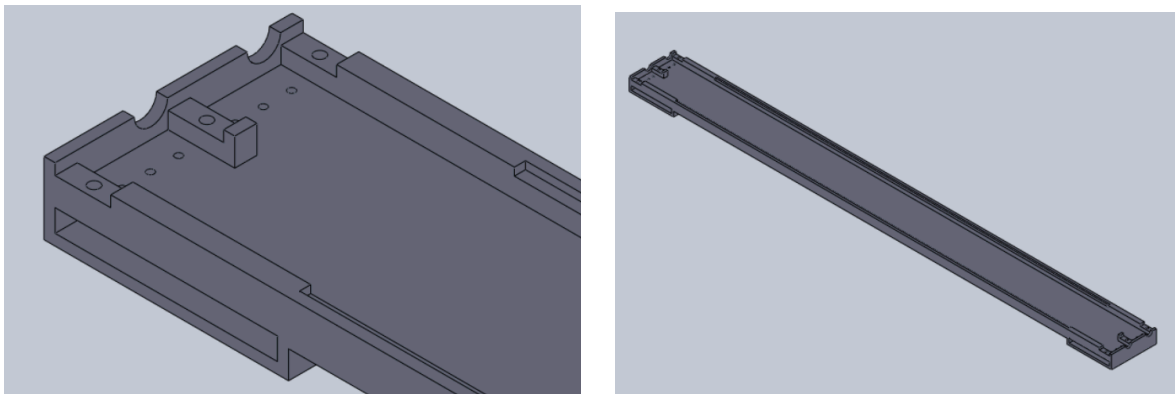


Figure 3-1 Design of a double socket for containing the SMA wires

The prototype first consisted of one piece and was, therefore, is not variable in length. The requirement of adaptability to different users is therefore not met. This feature had to be added immediately, by splitting the container into two pieces and adding a rail system which could make them slide into each other.

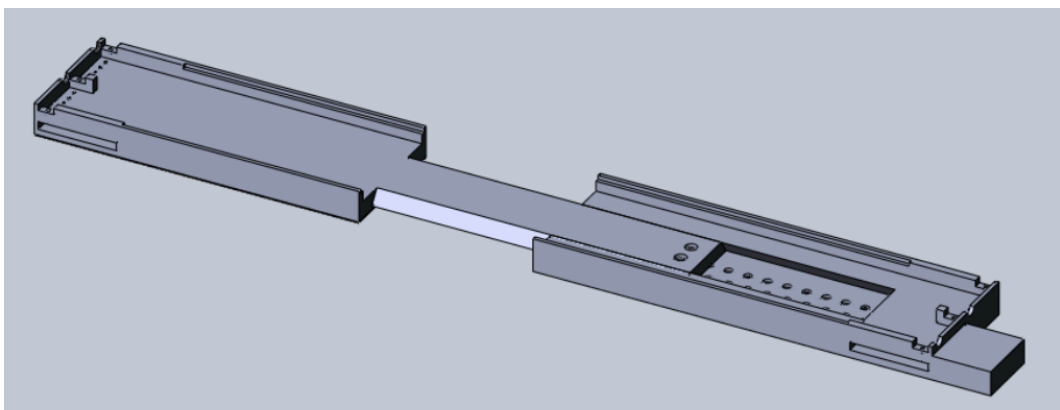


Figure 3-2 First prototype with a sliding connection system

The container is very broad and is divided in the middle by a small step, which gives extra support and creates space for a connection between two SMA wires.



Figure 3-3 First prototype installed on the dummy hand

After 3D printing the pieces, post-processing them, and installing the SMA wires, the prototype looked like shown in the picture above. There are two different SMA wires, connected electrically isolated with a combination of cotton and nylon thread, as described in the previous thesis work [9].

A sketch and electrical scheme of the first prototype where two wires are linked electrically isolated is shown in the figure below.

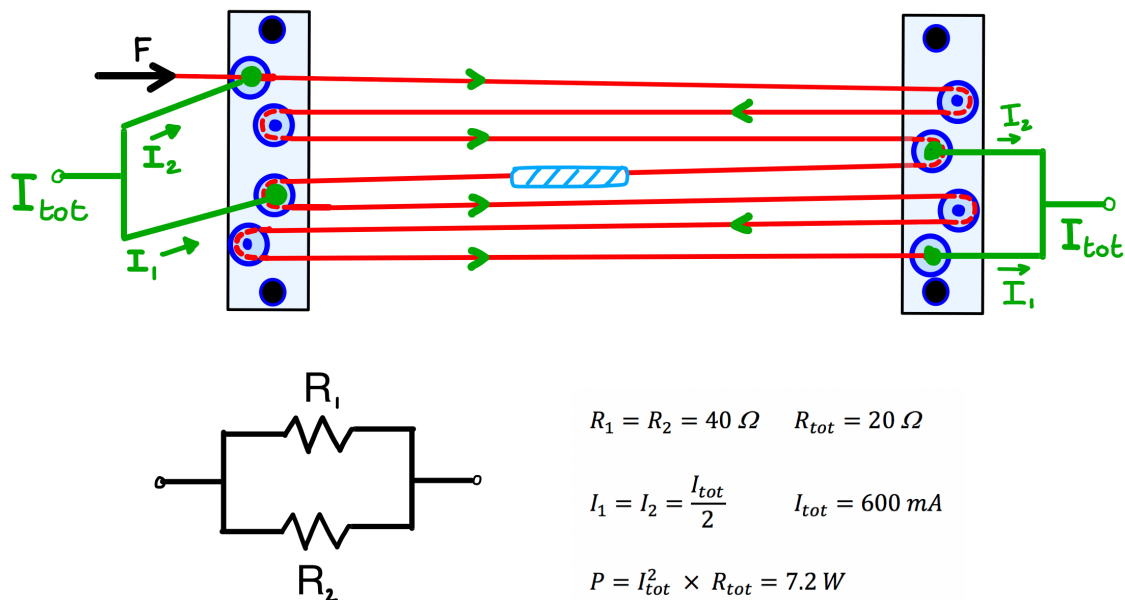


Figure 3-4 Sketch and electrical scheme of the previous situation, where two wires of 66 cm each are linked through an electrically isolated link (signed in blue). The current divides equally over the two wires, which are shown as resistances R_1 and R_2 . A current of 600 mA is needed to obtain a power of 7.2 Watt for the Joule effect.

This prototype is an improvement compared to the previous situation, but some things still have to be changed regarding the size of the module, and a closer look has to be taken at the mechanical and electrical infrastructure of two separate SMA wires.

From a modular point of view, it is better to have a separate module for each electrical connection. Also, checking the electrical schemes of both in parallel and series connected resistances shows it is advantageous to connect them in series because of the reduced current that is needed to obtain the same Joule effect. The Joule effect is the resistance times the square current. The improved set up with one wire with twice the length of the old wire needs only half the current to obtain the same Joule effect. This is shown in the sketches and calculations below. The current is equal in both resistances, and therefore the Joule effect has also a power of 7.2 Watt, using only half the current as in the previous situation.

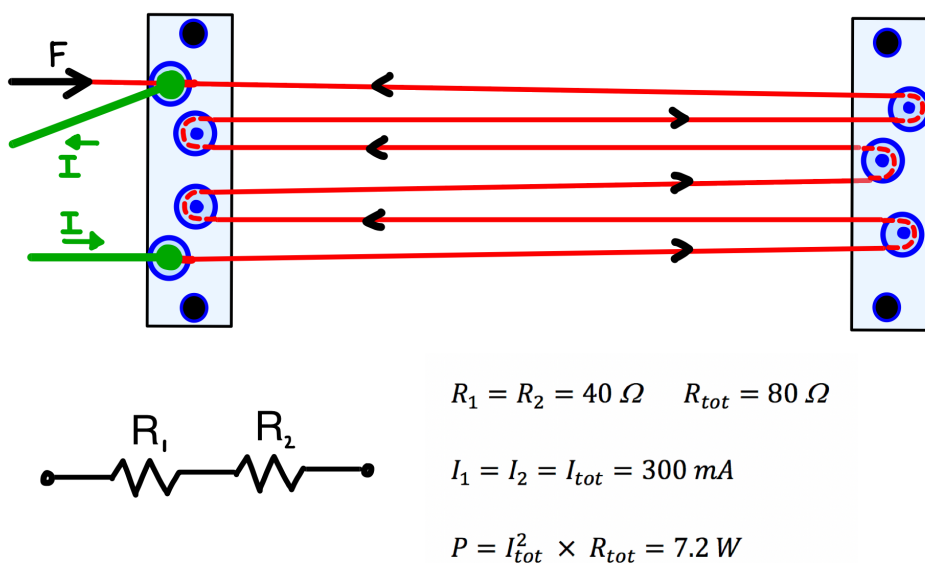


Figure 3-5 A sketch and electrical scheme of the new situation, where the wire is twice as long as the previous wires (and therefore indicated as two resistances in series). The current is equal in both resistances, and therefore the Joule effect has also a power of 7.2 Watt, using only half the current as in the previous situation.

3.1.2 Second prototype

The second prototype is considerably smaller, because of the calculations made regarding the needed SMA wire length, control, and connection. The mechanical electrically isolating link is eliminated, now the SMA is a long double wire instead of two separated double wires. The advantage is the reduced current needed to operate, as explained in the previous section. Fewer pulleys are needed in this new design, which drastically reduced the width and therefore increased portability.

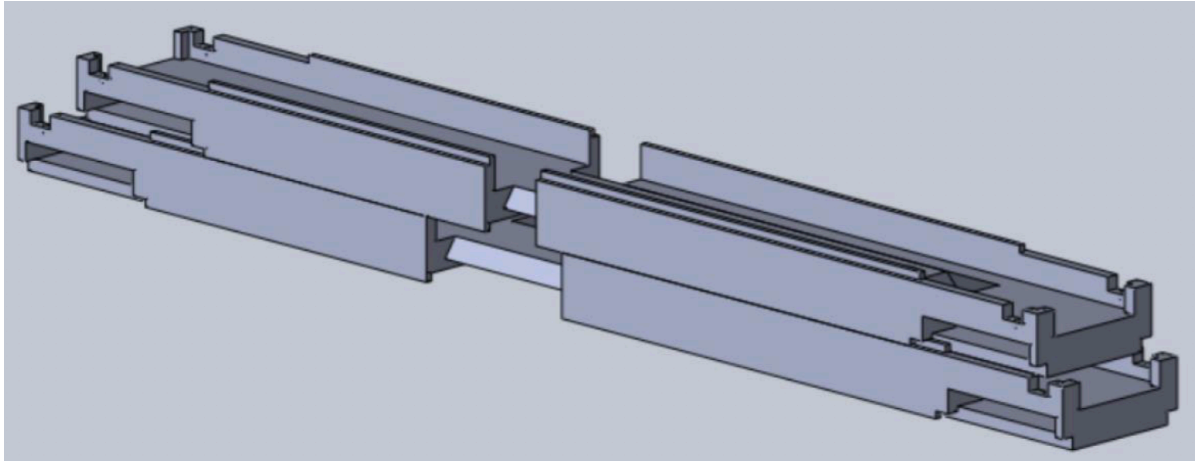


Figure 3-6 Solidworks CAD design of two double modules on top of each other

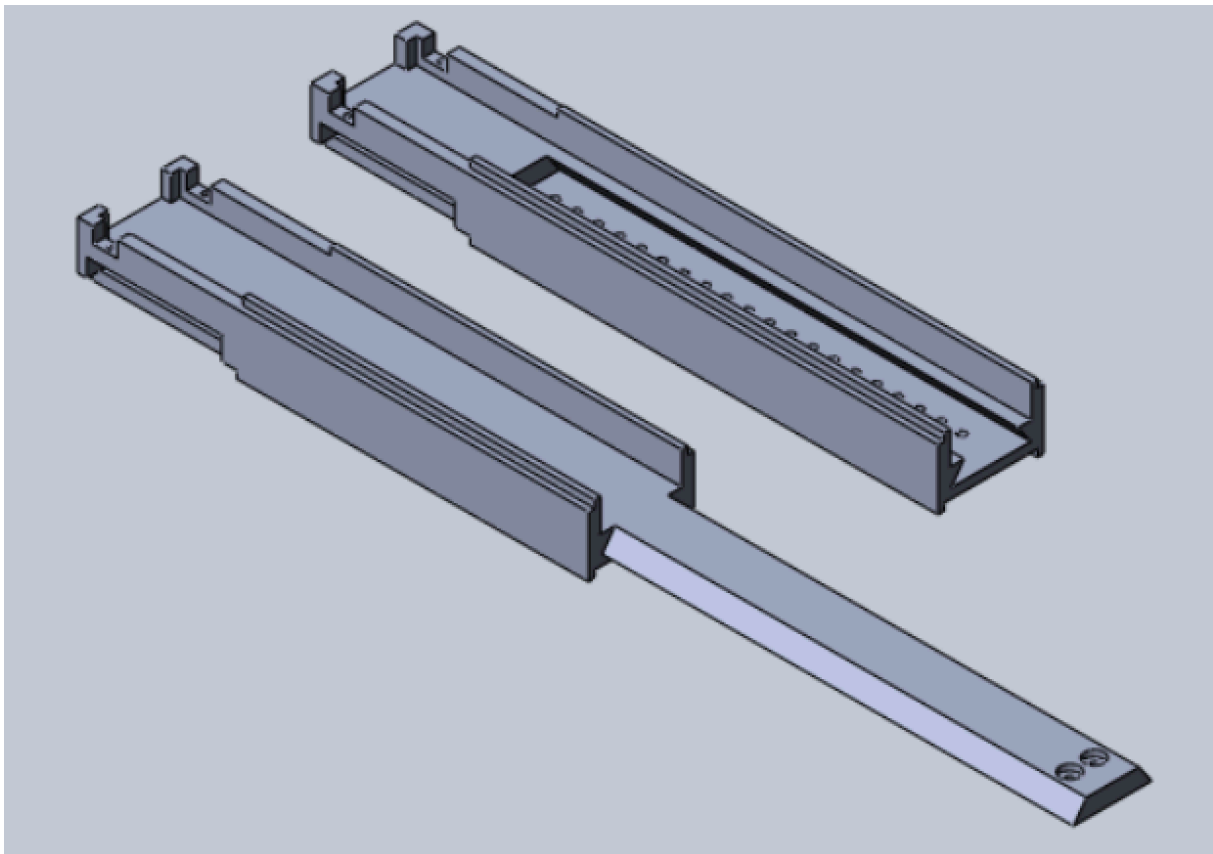


Figure 3-7 The two parts of the second prototype

Also, in the first prototype, post-processing actions like filing took a long time because of the surface roughness. In the new prototype, a distance of 0,2 mm margin between two sliding surfaces is made to reduce the post-processing time.

In the first design screenshot, the modularity of the container is visible. Two modules with variable length can be placed on top of each other. In this way, adaptability and reduced size as a design requirement are met.



Figure 3-8 Second prototype installed on the dummy hand

This picture of the new prototype shows how the size of the module has been improved. The system to adjust the container length is clearly visible. The part on the right has a pin which can slide in the left part and fixed with a small bolt and nut at a point of choice. Each hole is on a 3.5 mm distance. The SMA wire is zig-zagged 6 times. So changing the bolt with one position, changes the SMA wire length with $6 \times 3.5 = 21$ mm.

The length can be changed from 21,5 cm up to 24 cm, giving a total 11% more length to the wire if necessary. With this system, the module is adjustable for more different patients, each having different arm lengths.

As soon the functionality of the new prototype has been proven, also a cover for the module was designed, and 3D printed to improve safety. With a cover on top of the module, the SMA wires which get heated are less exposed, and therefore the risks of burning are confined. The cover is shown attached to one of the modules in the picture below.

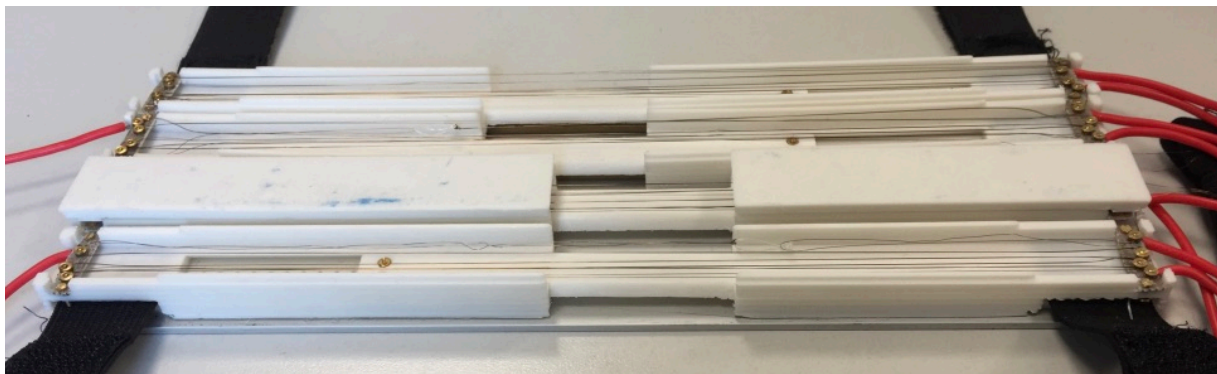


Figure 3-9 The cover, which improves safety for the user, is attached to the second module from below

Pulleys

In order to store and tension a long SMA wire in a limited amount of space, pulleys are needed to make it go back and forth in a container. In a previous thesis [8], silicon tubes, nylon screws, iron screws, and plastic tubes are tried as previous options, but best results were obtained with metal pulleys. The current which is needed to control the SMA wire through the Joule effect can be applied to the wire through these pulleys. If the wire is wrapped around a pulley and tensioned adequately, it has good contact with the pulley and is therefore ideal for applying current. So one requisite for the pulleys is electrical conductivity. Also, they have to be of small dimensions to reduce the space needed in the container. Previously, Adatto already researched different materials which can be used for this purpose [9]. Silver seemed to be the best material but is discarded because of the high costs. Another good option which is conductive and readily available is brass. These brass pulleys can be found with a 2.5-millimeter diameter (Amati modellismo, Turin). These are the smallest size available and suits the SMA wire container, and therefore will be used during the prototyping. First, bigger sized pulleys of 4-millimeter diameter were used during the design. Later, the smaller 2.5 mm pulleys became available and thus were used in the final design.



Figure 3-10 The 4mm and 2.5 mm pulleys from Amati modellismo Torino

The width of the pulleys largely influences the width of the actuator container. In the section which explains the attachment system for the pulleys to the container, it becomes clear the 2.5mm pulleys are a better choice than 4mm.

They will be mounted on the topside of this attachment system to facilitate easier installation of the SMA wires. Also, the wires will be more distant from the PLA material, which is not very heat resistant.

Power linkage to container

The power cables coming from the SMA driver are connected to the wire through the electrically conducting pulleys, which are attached to a holder. This holder is made of stripboard, which consists of a matrix of small holes. The distance between each hole on the used stripboard is 1.27 mm.

The ends of the stripboard are attached to the container, while the pulleys and the electric cables are soldered to the board in the middle. To increase the distance between the pulleys, they are attached alternately to the board, to avoid the pulleys touching each other, which would cause a short circuit.

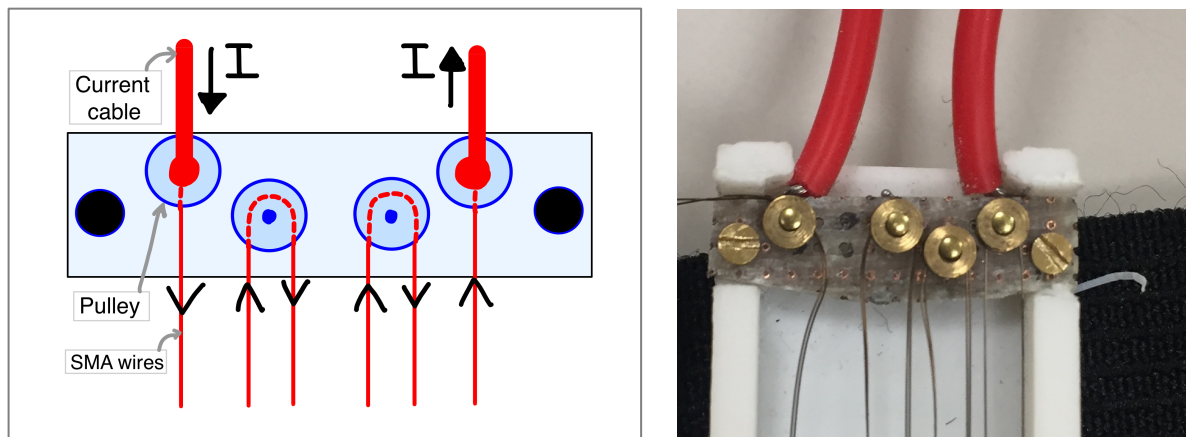


Figure 3-11 Sketch and a picture of the pulleys attached to the stripboard. The current is coming from the SMA driver through the red current cable on the left. The current then passes the pulleys zigzagging back and forth before closing the circuit back to the SMA driver through the current cable on the right.

The soldering is very precise since there should not be any mechanically conducting linkage between two pulleys, despite the pulleys being very close to one another. Also, for this reason, both sides of the stripboard had to be filed to take away the metal layer covering each hole of the board. The holes where the pulleys were inserted with a pin had to be drilled out because of the reduced diameter.

Linked modules

One module contains 132 cm of Nitinol wire. The modules are designed to have the possibility to be connected to each other, and thus longer the length of the SMA wire. In that case, the wire can be double the length and continue its path through a second module.

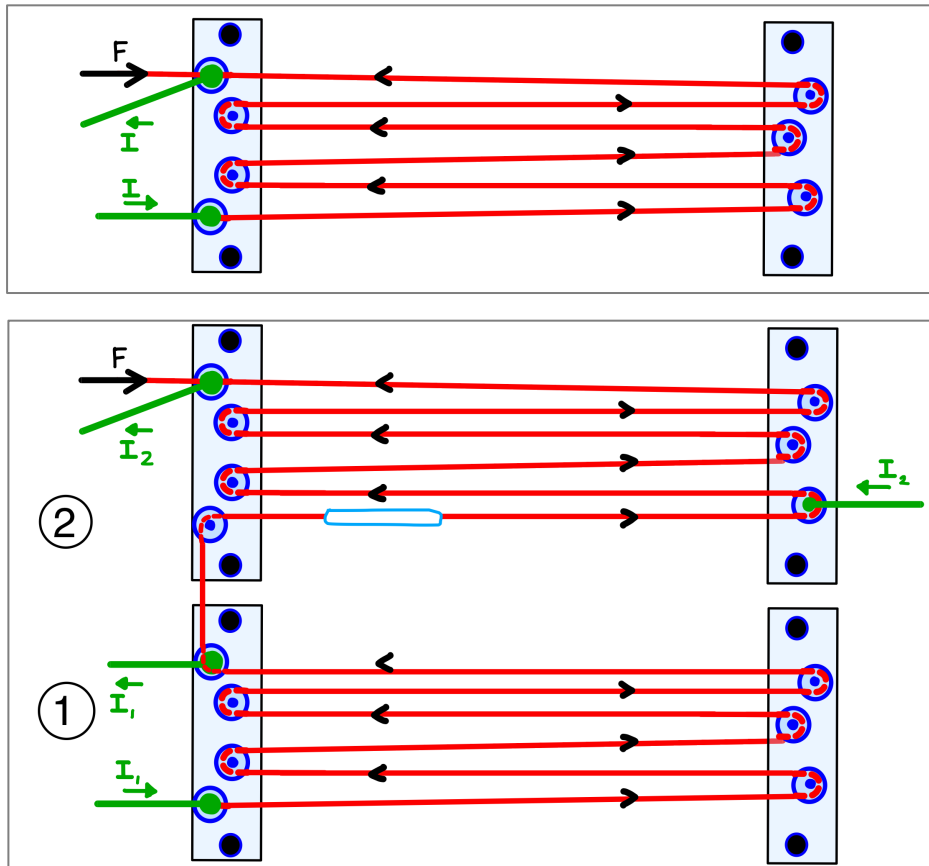


Figure 3-12 The upper design shows a standard connection of the green current cable to the red SMA wire. The figure below shows an electrically isolating mechanical link between two modules, which increases the shortening with 50%, even if the length of the SMA wire is doubled.

The wire can also be mechanically linked to another SMA wire with an electrically isolating link such as nylon (shown in blue). In that case, the two modules can be controlled separately, for example, to have one module pretension the wire to let the other module become more effective.

As will be described in the next chapter about tests, using a double linked module increased the shortening of the wire with 50%. This is less than the expected double shortening, because of the increased friction due to the added pulleys. However, this shortening was necessary to obtain a sufficient closing of the finger.

3.1.3 Final design

In the final situation, four modules are attached side by side to the forearm with two elastic straps. A brass rod for reinforcement is attached on the bottom of each module, to avoid them from bending when the SMA wire is activated. In this case, every two modules are linked mechanically with an electrically isolating link in nylon. One module pretensions the wire once activated; the second one makes the finger flex.

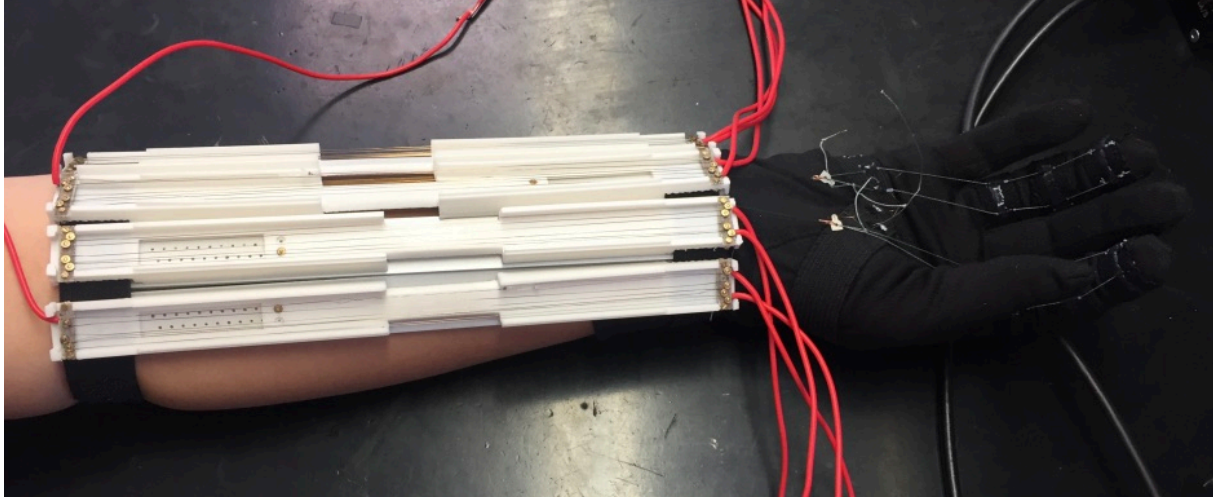


Figure 3-13 Final design of the SMA wire modules, connected to the tendons of the annular and index finger.

The first two modules are linked together and actuate the index finger. The other two linked modules are connected to the ring finger. Each module is separately connected with the red cables to one of the four channels on the SMA driver.

3.2 Prototyping of glove

The glove consists of multiple layers. A soft glove in lycra will be used as an inner layer, to cover the complete hand and give comfort to the user. The second layer is made up of some elastic straps, attached to the soft layer. This is more rigid material and therefore more suited to attach tubes onto it which serve as cable guides. In order to achieve a soft design, actuation is provided to individual joints via a flexible cable. The third layer is the actual tendon system of cables running through the cable guides, which actuates the fingers. This whole glove with all its additions can then be attached to actuators which are placed on the forearm.

3.2.1 Tendon system

In this design, two separate cables are used as tendons for extension and flexion, which is guided along the central axis of the finger. During flexion, all three finger joints are actuated using one single flexion wire. This approach was inspired by flexor digitorum profundus tendons that perform simple grasp and pinch motions. The flexor strings can be split into two slips over the phalanges to avoid high pressure on the finger and have a more stable flexion motion. Also, with cables running on both sides of the finger, the palmar side of the finger is free while grasping objects.

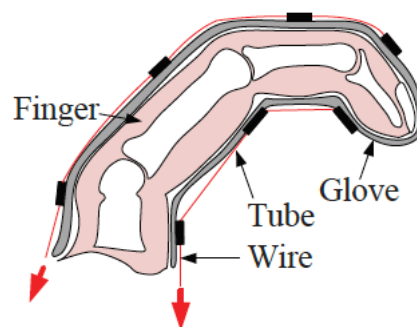


Figure 3-14 Tubes design for passing through the tendon mechanism [28]

Tubes attached to elastic straps will keep the tendons in place and will function as cable guides. For each finger, the cable guides are located on the metacarpal bone, proximal phalanx, and medial phalanx with fixation of the cable on the distal phalanx. This routing mimics the tendon function of the flexor digitorum profundus. The elastic straps prevent possible stretching of the glove material and hold the soft structure together like human skin does.

For extension movement, a single cable on the dorsal side of the hand would be sufficient. The extension tendon should be attached to the second-last most distal phalanx of any finger, which is the natural situation in hand anatomy. If the mentioned cable is aligned correctly, it should not generate any undesired abduction or circumduction finger motions.

The tendon path is usually severely curved in a soft tendon routing system, and this curvature increases friction. In addition, the friction is increased proportionally to the tension of the tendon. The NiTiNol wire, which is used as actuator will break when too much tension is applied. If the same wire is also used as tendon, the wire might break because of a highly concentrated force at the tube edge. Therefore, the tendon wire should be made of a material with a small friction coefficient, a high yield strength, and a small Young's modulus for better performance and durability. This tendon wire will be connected to the Nitinol wire of the actuator with a pin that is hooked to the wire.

The chosen tendon material is Kevlar, a very strong synthetic fiber which has excellent resistance to heat and flame. Because of its resistance characteristics, it is used as reinforcement fiber for the construction of bullet-proof vests, equipment for extreme sports and components used in airplanes, boats and racing cars.

A high tensile strength characterizes these fibers (3600 MPa, comparable to that of carbon fibers and about ten times higher than that of steel), low specific weight and high resistance to impact and shear strength. It has low adherence to the cable guides and thus low friction losses.

Teflon tubes with a diameter of 0,5 millimeter were attached to the elastic straps around the phalanges and palm to make paths for the wires. The low friction coefficient of Teflon is an advantage for this application. Also, the electrical isolation, chemical inertia, and insolubility are useful characteristics regarding the contact of the glove with any external object.



Figure 3-15 Final glove design with tendon system. Kevlar wires pass through tubes which are attached to elastic straps around the phalanges. The SMA wire can be hooked onto the small metallic part at the end of the tendon.

Two different sizes of gloves were made, one typically for women's hands and one for men. Since the material is elastic, the glove is a good fit for a wide range of hand sizes.

Chapter 4: Tests

Tests on a wooden dummy hand and four subjects are done to have a characterization of the developed prototype. Finally, a functional test with the implementation of the EMG signal will be conducted to evaluate functionality.

4.1 Final test on dummy hand

4.1.1 Test protocol

The goal of this test is to measure the range of motion and repeatability of the small finger motion, conducted by a single SMA wire module. The information that needs to be retrieved from these measurements is the x and y position of the three joints in the finger in time. Once having retrieved these positions, it is possible to calculate the angular displacement, angular velocity, and angular acceleration of the phalanges. For retrieving data about the movement of the dummy hand, it is necessary to design an optometric measurement system. An optometric system is a good option since it is non-invasive, relatively easy to implement and sufficient for the data that needs to be retrieved.

A GoPro 7 black which is available will be used to film the finger while conducting flexion and extension movements in several positions. The video material will be processed in software called Tracker (Douglas Brown). Tracker has the advantage of being free opensource software. Also, Dartfish was tried for a 15-day trial but was not satisfying in use and costs 20 up to 100 euro per month.

During a pre-test, the finger motion will be measured for several input configurations of the SMA-driver, such as duration (2, 3 or 4 seconds) and current (300 or 320 mA).

From previous visual registrations, it turns out that pretensioning has a big influence on the capacity of bending the finger. During the experiment, the pretensioning of the SMA-wire will be done by hand, every time in the best way possible to achieve results which can be checked for repeatability.

The input configuration, which offers the best results in terms of angular movement will be repeated ten times, to retrieve data for statistical analysis of the movement.

All of these measurements will be repeated in 3 different positions of the hand: supination, neutral, pronation. The neutral position is expected to be the easiest to achieve good motion results since gravity is not working in the plane of the movement.

A supinated position of the arm (palm facing upwards) will be used to check the flexion motion of the finger while it has to overcome gravity.

A pronated position of the arm (palm facing downwards) will be used to check the extension motion of the finger while it has to overcome gravity.

GoPro settings

For a 2.7K measurement, the GoPro video frequency can be set to 60, 30, or 24 frames per second (fps). Since the movement will be executed in a few seconds and a maximum movement of 180 degrees can be obtained, the accuracy of a measurement can be quickly calculated to determine the minimum frequency of the video registration.

Assume that the movement is executed within 2 seconds and measured at 30 fps. The video will provide 30 images which can be used to make a calculation. If the finger motion is 180 degrees within this timeframe, position accuracy of 3 degrees can be stabilized, which is not precise enough. While filming at 60 fps, the accuracy can be 1,5 degrees. Doubling the number of frames is still acceptable for data storage, so it will be set to 60 fps.

Another setting to consider is the angle of view of the GoPro. In older GoPro models, it was only possible to film with a fisheye effect, which gives a distortion to the image in order to obtain a large field of view. This is useful to capture an object while filming on a short distance. The fisheye distortion effect can also be removed during post-production of the video. During this experiment, it does not need to be filmed on an extremely short distance or capture a wide field of view, and thus it is better to avoid the image distortion which is created with this effect. Therefore the angle of view is set to linear mode. However, it will be better to avoid any possible distortion by filming the subject in the center of the camera view.

The points of interest for this measurement are fixed rotation points, which are clearly visible during the motion of the finger. To improve the recognition of the three points of rotation, these are highlighted in fluorescent green to improve visibility during data processing.

Measurement setup

The wooden dummy arm needs to have a fixed position during the measurements. A wooden construction to rest the arm on is built.



Figure 4-1 The wooden armrest construction built to obtain a fixed and stable position during the measurements

The background surroundings of the experiment should be preferably in one fixed color, possibly with thin squared lines to check for image distortion. A checkerboard image is used for calibration of the tracking software.

During the test, the GoPro is connected to an iPad which can be used to start and stop recording and see a preview of the recorded image. This is convenient to avoid touching the camera and thereby changing the setup. Also, with the internal calibration app of an iPhone, the position of the GoPro is checked for banking to avoid a distorted image.

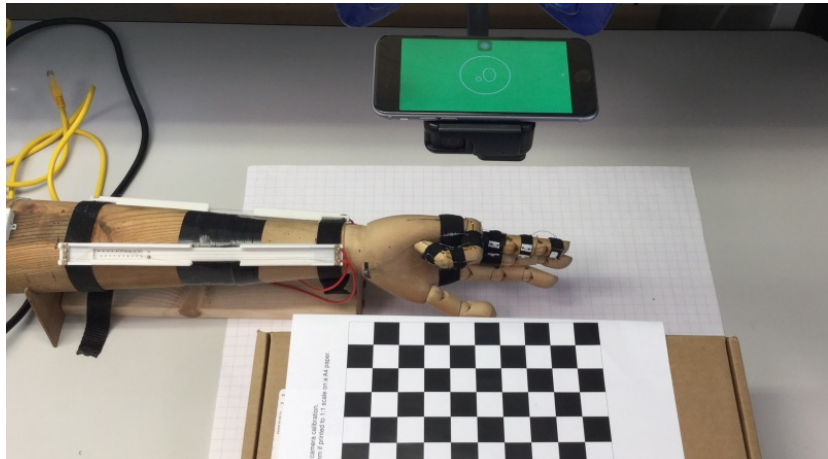


Figure 4-2 The calibration setup to avoid a banked installation of the GoPro

In the Tracker software, each video test needs to be calibrated by selecting the origin, markers, and calibration stick manually. An automated tracking system will recognize the selected markers in each frame automatically. This is more precise than selecting markers by hand in every frame and therefore reduces measurement inaccuracies.

The begin and end frame are selected, and then the software automatically calculates the requested parameters. Useful parameters for this research would be the x and y - position of each marker and the angle with respect to the origin. This information can be saved and further processed in Matlab (MATLAB 2016b, The MathWorks, Inc., Massachusetts, United States) for statistical analysis or visualization of all data.

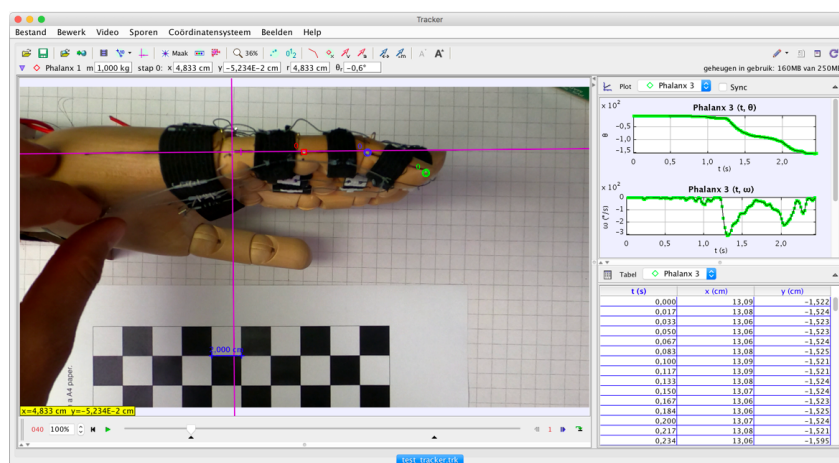


Figure 4-3 Tracker software interface, in the main frame the video is showed frame by frame, the markers are automatically recognized. The required data is extracted and graphed immediately on the right.

Supplies

- GoPro 7 Black
- Charging cable for GoPro
- iPad with internet connection
- SD-card reader
- GoPro mounts
- Markers
- Background paper with squares
- Checkerboard image for calibration
- Armrest
- Wooden dummy arm with module installed
- SMA driver with alimentation
- Computer to control SMA-driver
- Extra light
- iPhone for calibration

Outline of the test

The setup is made, with the GoPro mounted on the test table, hanging above the armrest with the wooden dummy arm on top of it. The background (under the dummy arm) is white with squares. The GoPro is connected to an iPad to control the registration of the movies. Each video will take more or less 5 seconds.

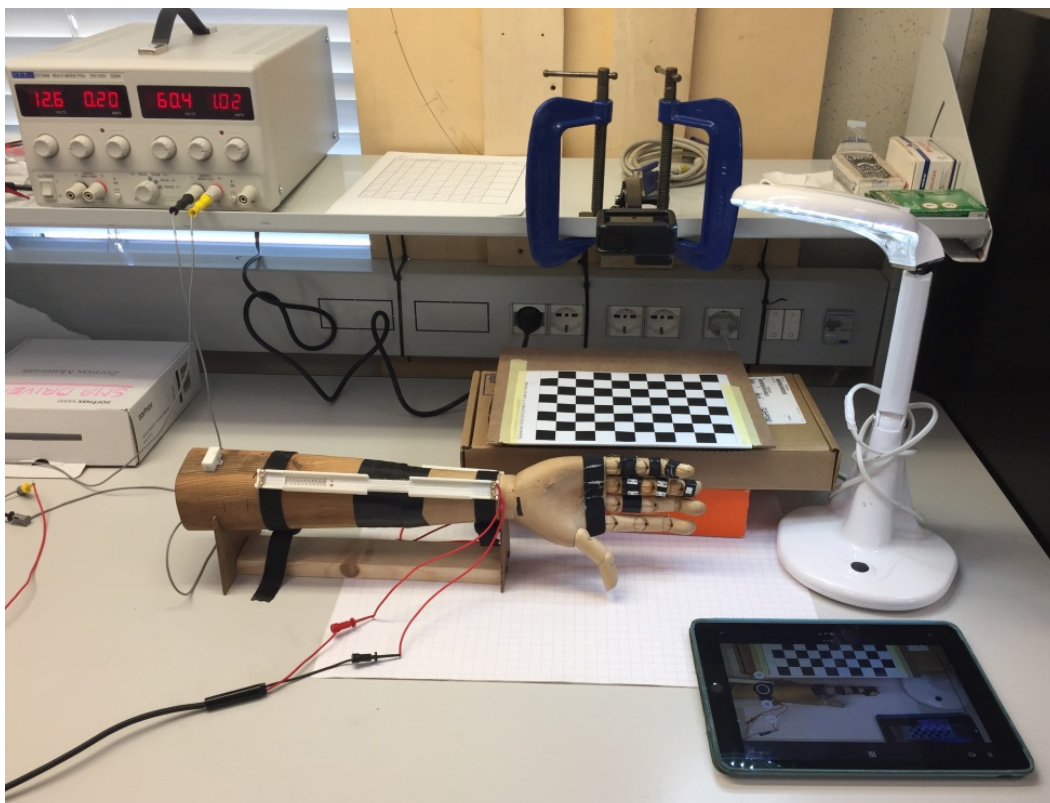


Figure 4-4 Test setup with the iPad to control the GoPro

A pretest in a neutral position is performed to find the best settings for current and duration. During pretest, best results were obtained with a 320 mA setting for 3 seconds. This will be the setting used to repeat this experiment 10 times each for flexion and extension. After that, the arm is changed to supination position, where the finger will perform ten times an anti-gravity flexion. As the last test, the arm is changed to a pronation position which measures the extension of the finger in anti-gravity position for another ten times.

With the chosen software, all these videos will be processed to retrieve the position, angular displacement, angular velocity, and angular acceleration of each marker respect to the origin. During all these experiments, the same SMA wire is used. The SMA wire will be 'preheated' to activate the conservation feature of the memory effect by stimulating it a couple of times on a current higher than 300 mA.

4.1.2 Test results

Range of Motion

The range of motion is almost the same for all tests; the anatomy of the hand rather limits it. The movement of the finger is already completed to a closed position before the stimulation has ended. The data angles that are achieved are useful for comparing the functionality with the tests on human hands. *Figure 4-6 and 4-7* show the position and angle of the three markers at each joint during a flexion movement in a neutral position, while *figure 4-5* shows the initial and final position of the hand.

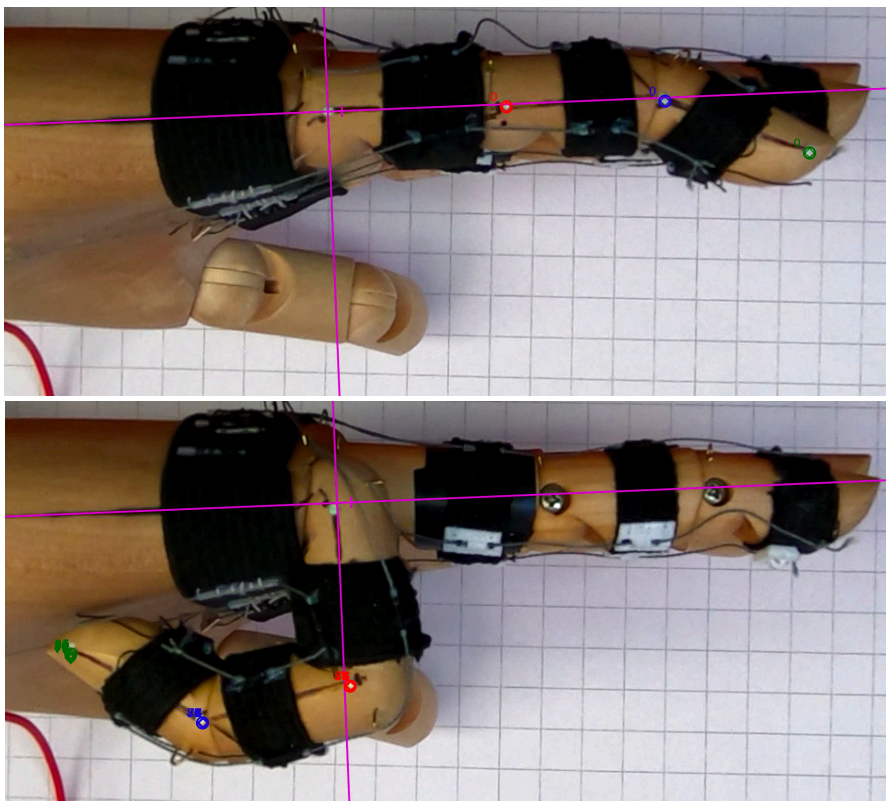


Figure 4-5 End position during a flexion movement in a neutral position

The movement of the finger starts in an extended position, as shown in *figure 4-5* above. The three colored lines show the position of the markers on each phalanx during the movement. During flexion, each joint follows a curved track and stops at the left end of each line. The last position of the green line corresponds to the final angle of the fingertip (phalanx 3).

Figure 4-7 shows that it is bent almost 160 degrees, which was the maximum reachable position, reaching a complete closure.

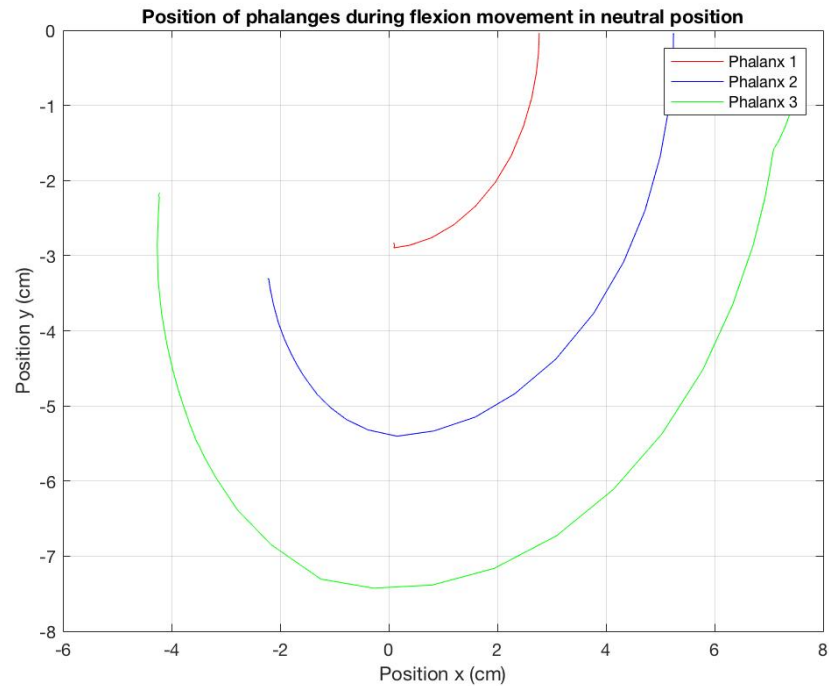


Figure 4-6 Position of phalanges during flexion movement in a neutral position. The movement starts up near the 0 on the y-axis and follows the curve to a closed position of the finger at the left end of the line.

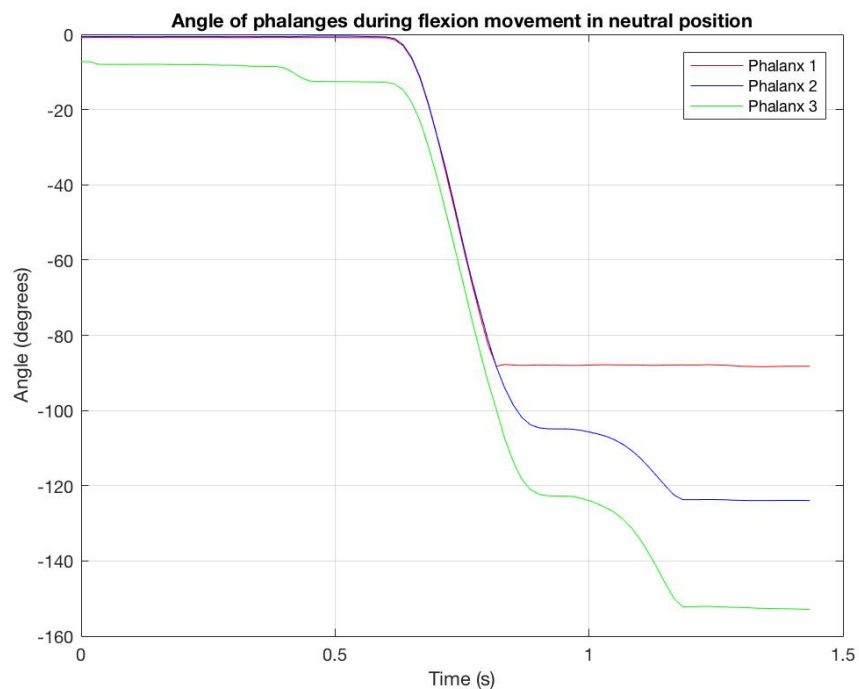


Figure 4-7 Angle of phalanges during flexion movement in a neutral position of the hand. The final position of the line shows the angle of each joint respect to the origin

The angle of the third phalanx, which is the fingertip, respect to the origin is calculated for each experiment to establish a Range of Motion (ROM). All values are similar since every experiment led to a complete closure of the finger. During a flexion with the hand in a neutral position, the mean value of the angle at closure is 153.9 degrees with a standard deviation of 0.72 degrees (0,46 %). That means the closure of the finger is practically always the same.

Repeatability results

Since the Range of Motion is almost constant at its maximum closing value, another parameter needs to be found for comparing different situations of movement. Since the x and y position of each rotation joint is extracted during data processing, the angular speed and acceleration can be calculated for each phalanx and is shown below

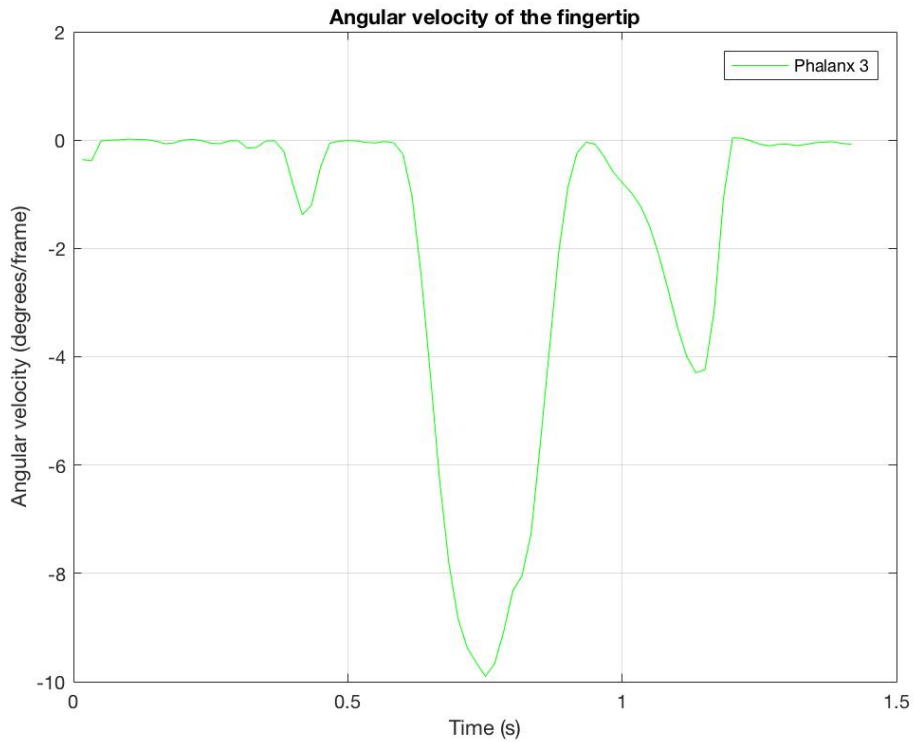


Figure 4-8 Angular velocity of the fingertip during flexion movement in a neutral position of the hand.

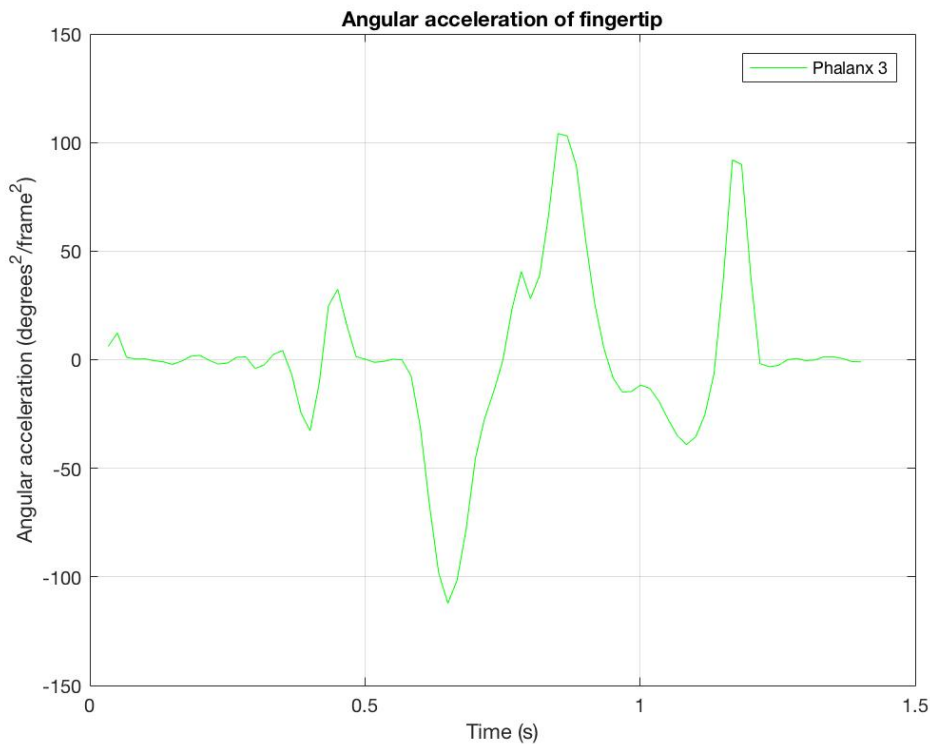


Figure 4-9 Angular acceleration of the fingertip during flexion movement in a neutral position of the hand.

The extracted data for every experiment shows constant features. At almost every test, a clear peak is visible for the angular velocity of the fingertip. Also, for the angular acceleration, three peaks can be distinguished.

The figure below shows a plot of the angular velocity plots of all ten neutral flexion experiments together. Not all data is perfectly aligned, and that makes it harder to confront several outcomes of the test.

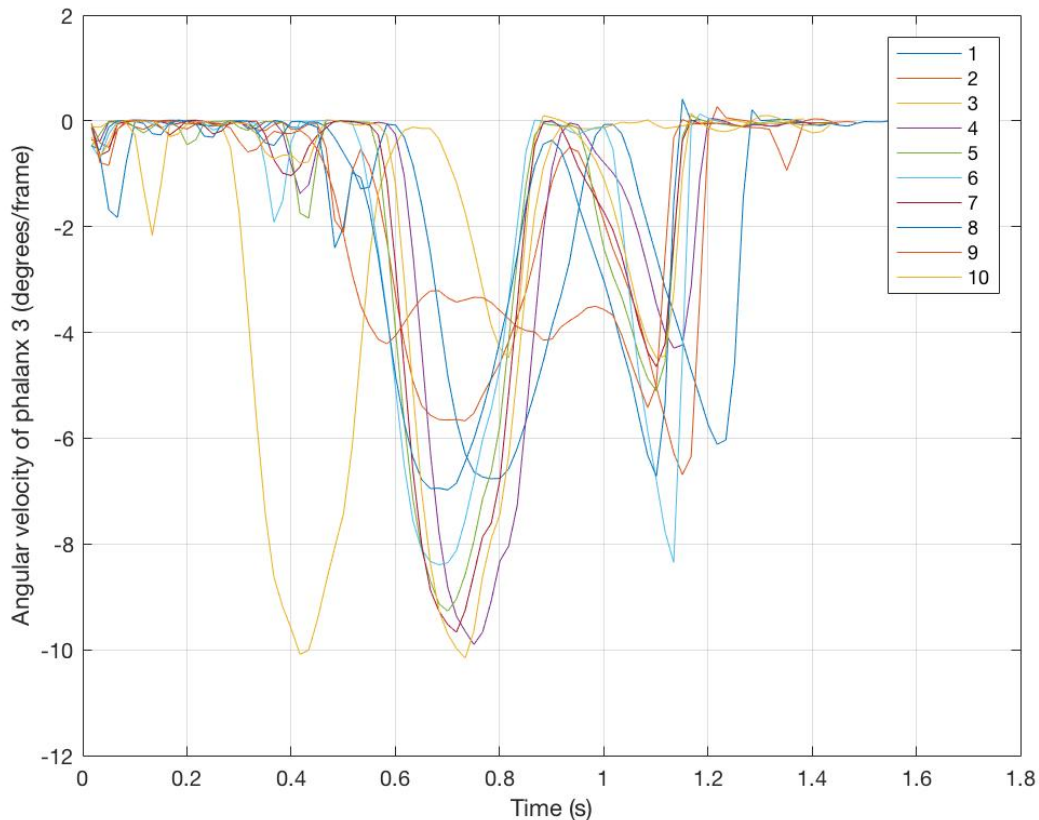


Figure 4-10 Angular velocity plots of all ten neutral flexion tests. Almost every test shows a typical angular velocity peak that can be identified and used for comparing with other tests.

To avoid aligning of the data, peak values can be used for comparing. For almost every test, a typical angular velocity peak can be identified. For acceleration, this is harder since there are more peaks to compare, which can lead to wrong identified peaks. Repeatability is checked by calculating the minimum value of the typical angular velocity peak at the third phalanx.

A boxplot of the absolute minimum values for the angular velocity of the fingertip is made and shown below. The average and standard deviation of these peaks are calculated as well. Low standard deviation indicates good repeatability. With this data, the motion in the neutral or open palm facing upwards position can be compared.

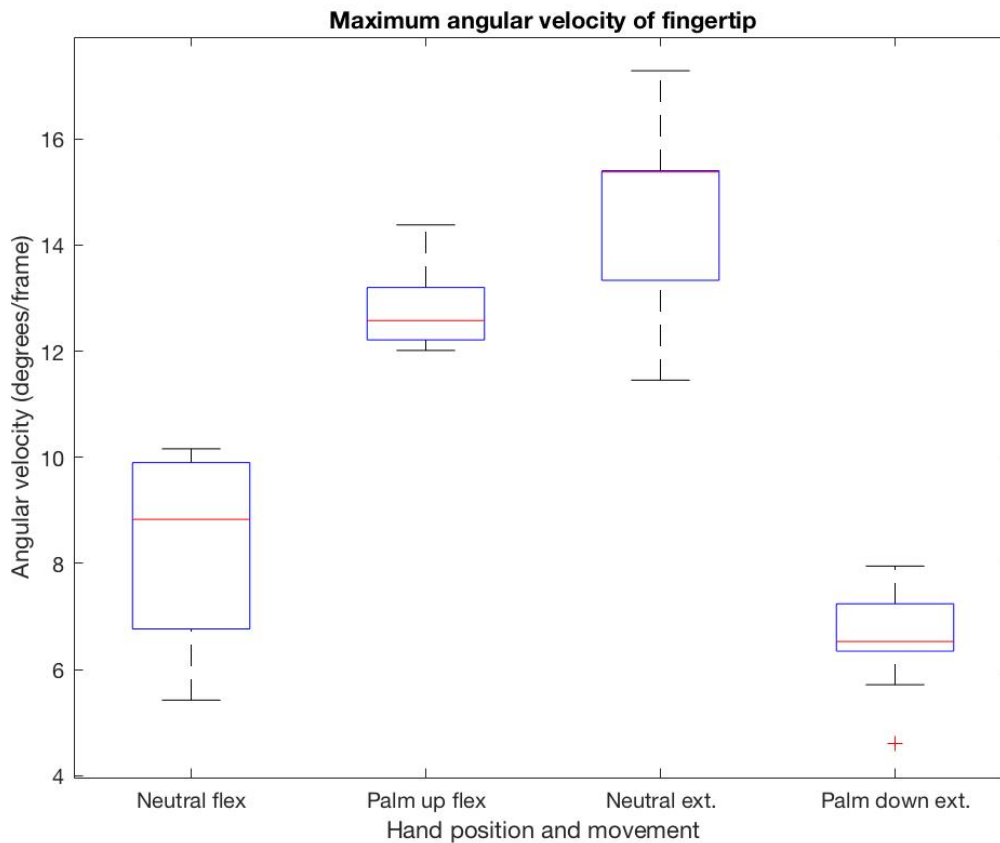


Figure 4-11 Boxplot of the maximum angular velocity peaks for the different tested hand positions

The boxplot above shows the maximum values of the angular velocity of the fingertip for the different tested hand positions. It has a mean of 8.3 °/frame with a 20,8 % standard deviation in a neutral position. If the dummy hand is in a position with the open palm facing upwards, the medium angular velocity increases to 12.8 °/frame with a 6 % standard deviation. Now, this can be compared with the extension motion in neutral position and palm facing downwards position. The angular velocity plots show the same characteristic peak, only as a maximum instead of a minimum, since the motion is in the opposite direction. The average angular velocity during extension in a neutral position is higher than during flexion, namely 14,8 °/frame with an 11,2 % standard deviation. The velocity during extension of the finger with the palm facing downwards is considerably lower with a typical peak at only 6.6 °/frame with a standard deviation of 15,1%. This can be explained by the gravity that needs to be overcome during the whole motion.

Noticeable is the increased angular velocity of the 'palm up' (antigravitational) in comparison with the neutral position during flexion. The actuators have to overcome gravity working on the finger; that is why it takes a bit longer before the actuator accumulates enough force to bend the finger. Once it does, there is more force actuating and thus velocity because of the building up of the force by the actuators. Then, when the phalanges bend over the dead point, gravity is a benefit while continuing the motion.

This can also be seen in the position plotting of some of the experiments with the open palm facing upwards. The position contours are not perfectly smooth; the second and third phalanx show a point of pause before continuing the trajectory.

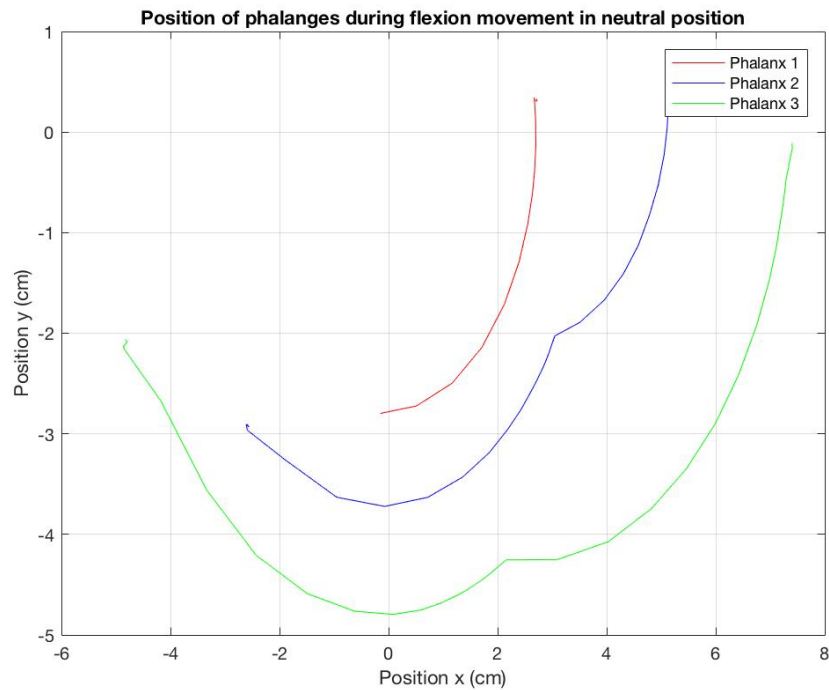


Figure 4-12 Typical trajectory of the phalanges during flexion movement in neutral position of the hand

4.2 Final test on subject

After successfully having tested and gained data with the wooden dummy hand, we will proceed to test on subjects. Some pretests have been conducted to check the feasibility of single or double modules actuation on single or multiple fingers, thereby adding the software function of stimulating multiple channels at the same time or in a pattern. Actuating one finger with a single module gave unsatisfactory results. Therefore two modules were linked as explained in the previous chapter.

Double module linked preparation

A single module did not give a sufficient closing of the finger, so two modules were connected to obtain better results. Only a minor adjustment of soldering an extra wire had to be made, which keeps all future options of linking modules open.

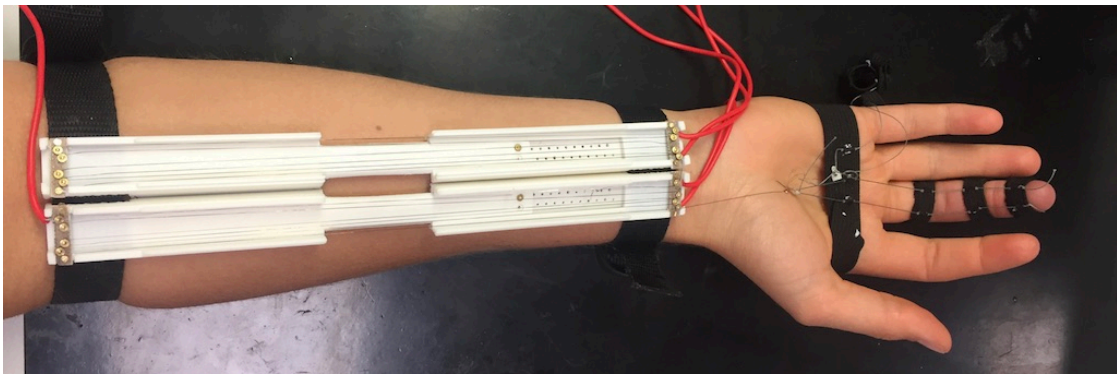


Figure 4-13 Double module connected in series with an electrically isolating nylon wire

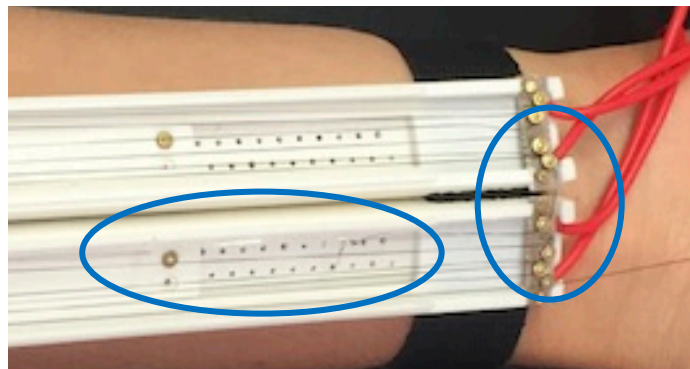


Figure 1-14 Close up of the nylon and Nitinol connection between the two modules

The wires of both modules are mechanically connected with a nylon wire to keep both modules electronically isolated (visible in the left blue circle *in figure 2-14*). During stimulation, two channels are used in a predefined pattern mode. First, the most distal module was stimulated with the set current. Two seconds after the start of stimulation, the other module was stimulated with the set current. In this way, the most distal module pretensions the other.

The double module was first tested in a test setup without a subject. The SMA wire is kept tensioned collinear with a ruler during stimulation, and the difference in length is measured. Depending on the pretensioning of the wire, a shortening of 3 cm up to 3,5 cm is obtained.

In order to compare these results with a single module, the same test is repeated. For a single module, a shortening of 2 up to 2,5 cm is obtained. So doubling the length of the SMA wire does not double the obtained shortening. This is probably because not only the length of the SMA wire is doubled, also the amount of pulleys, which creates friction, is doubled.

Also, another loss can be due to the stretching of the nylon connection wire. Nylon can be stretched a bit if a lot of force is put on it. To minimize this influence, the length of the nylon connection wire is shortened to a minimum.

The results of each experiment are very variable, and it depends very much on the pretensioning of the most distal module. If only one module is used, this can be tensioned simply by stretching the finger. For a double module, the friction of the wire is too elevated to reach tensioning of the most distal cables by stretching the finger to whom it is attached. In this case, the pretensioning of the most distal module has to be done by hand.

Another modification was to try several other configurations by changing the number of pulleys involved. During a test with only six pulleys on each side, which means a combination of one complete module and two pulleys of the distal module in use, shortening of the wire is not significantly increased compared to using only one module.

Using seven pulleys on each side, a combination of one complete module and three pulleys of the distal module, during a test setup without a subject shortens the wire with 3 cm. The proportion of the amount of pulleys and shortening is more or less linear. Two fully equipped modules would be most resistant during use and most easy in setup.

Multiple double modules

The pretest is extended to actuation of two fingers by two double modules. A glove does the transmission of motion with an internal tendon system installed on the ring finger and the index finger. While actuating these fingers, the middle finger moves along as well in the grasping movement. This can be changed to any finger, based on the tendon system installed on the glove. Changing between fingers is done by simply attaching the hook at the end of the SMA wire to the pin at the other finger.

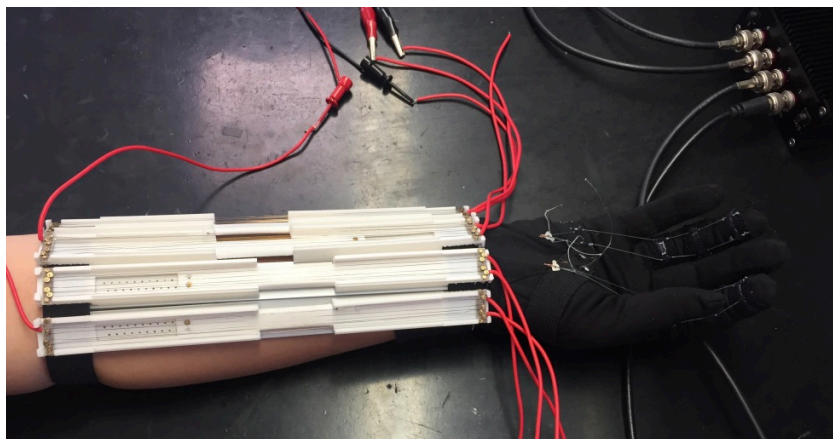


Figure 4-15 Overview of two double modules, each one attached separately to a finger

Since the requirement of modularity is met, this system can be expanded to all fingers. Modules can be placed on top of or next to each other and be connected to the other fingers. During the functional EMG test, also two double modules will be used to actuate two fingers.

Test on subjects

Now the double modules are successfully prepared for testing on subjects. Also, some data needs to be obtained to have a characterization of the actuation of the index finger to confront the test results of the wooden dummy hand. The same optometric system will be used in the same settings (GoPro 7 black, 60 fps, 2.7k, linear field of view). The hand of the subject will be put in the same position as the wooden hand, and the finger will be positioned horizontally in front of the camera. In this case, the index finger will be filmed since the hand can be held in a neutral position while the camera has a clear field of view to film all the markers on the joints from above. Since the index finger is larger than the small finger, the Range of Motion and repeatability results are expected to be less satisfying. Expectedly, there is less friction in the fingers of the wooden hand compared to the anatomical resistance of a real human hand during movement.

Especially the end position will be considered during the evaluation of the test. During the test, the hand needs to be relaxed, so the test is not influenced by muscle force.

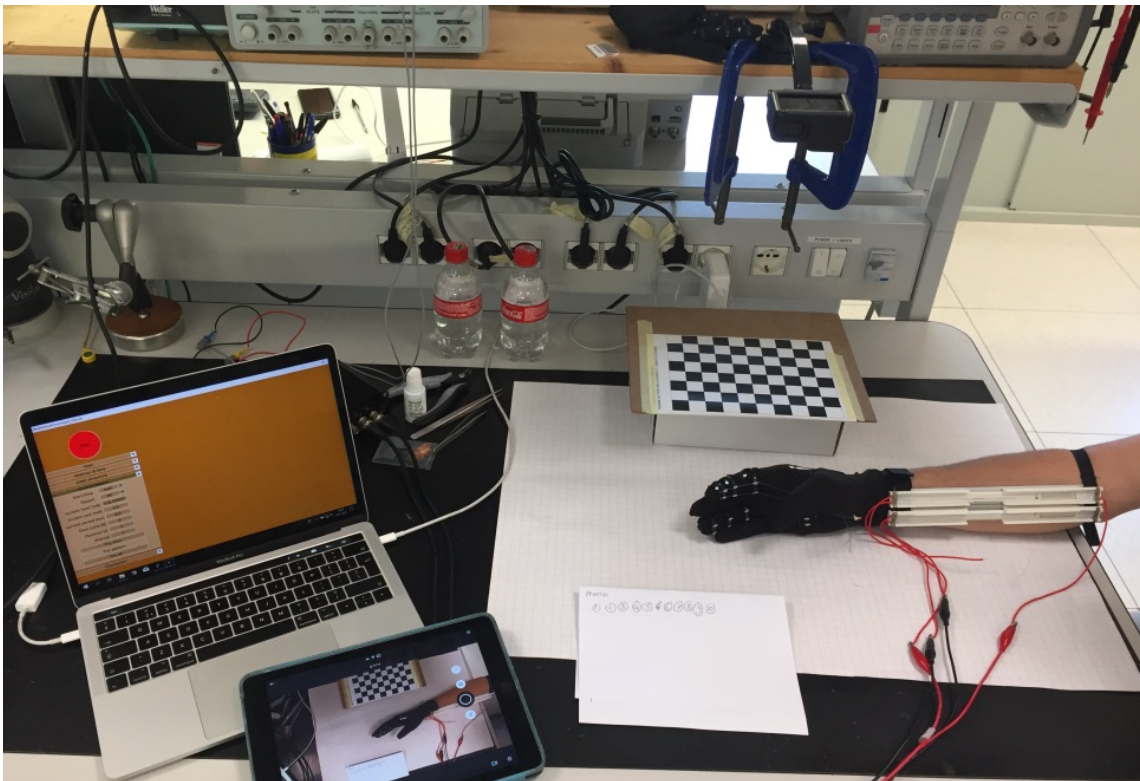


Figure 4-16 Test setup to obtain data for characterization of the use of a double module to actuate the index finger.

The test is conducted on four test persons (two female, two male) and repeated five times each. Three markers are placed on the joints and the fingertip of the index finger. Then, in

the software, the x and y position in time, angular speed, angular velocity, and angular acceleration are extracted.

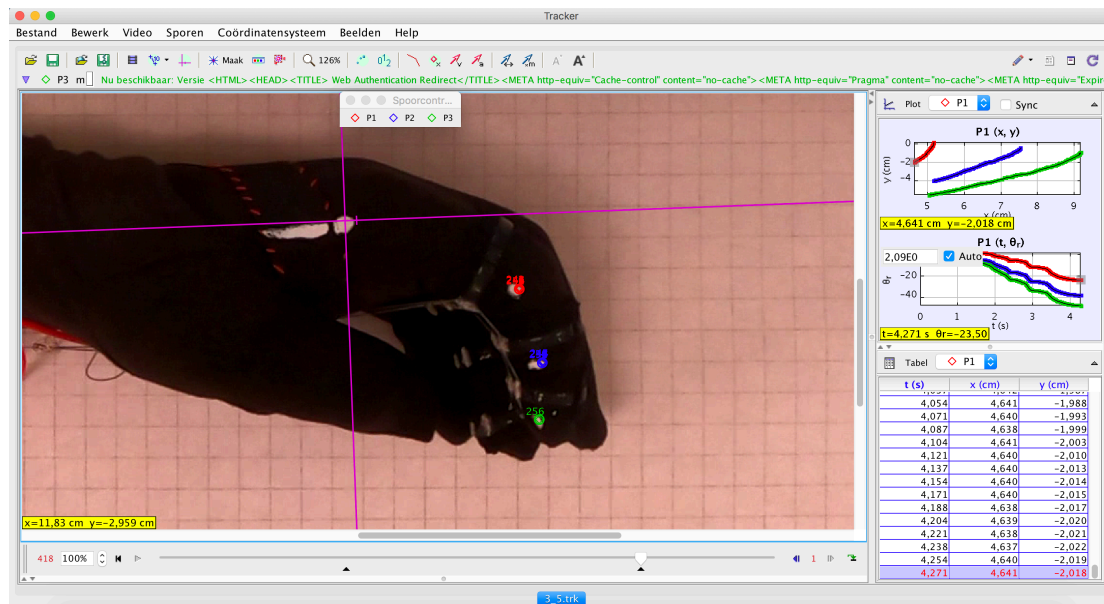


Figure 4-17 Interface of Tracker software, each marker position gets tracked during the movement and saved

Some typical graphs of position, angles, and velocity which are extracted are shown in the figures below. The plots of the angular acceleration were not useable for confronting since there was too much noise in the plot. No particular peaks or information could be extracted from those graphs so they will be discarded.

In the meanwhile, the position of the phalanges is shown in the plot below, and shows a reduced path, only arriving at approximately 65 degrees of flexion.

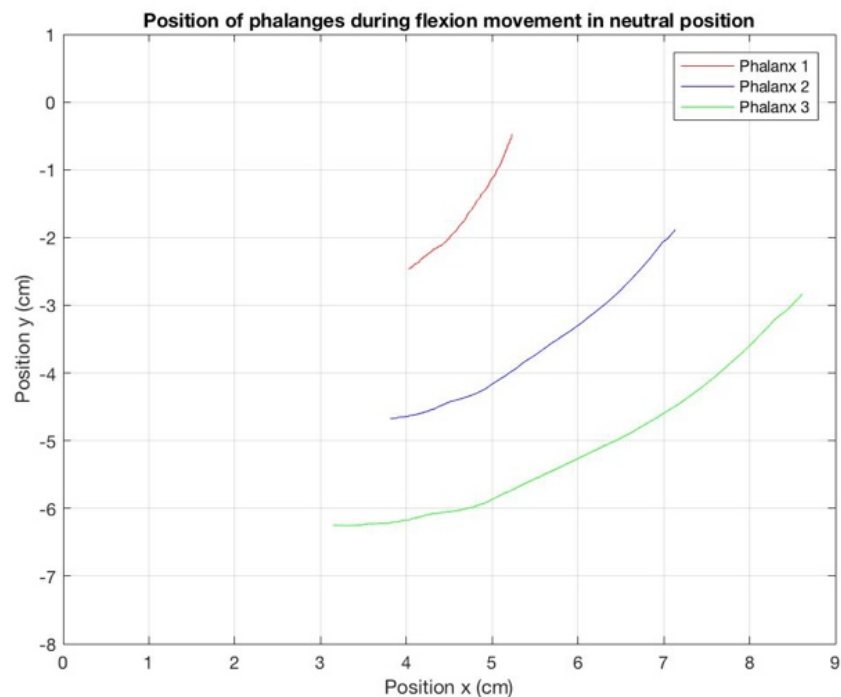


Figure 2-18 Plot of the x and y position of the markers on each phalanx during flexion

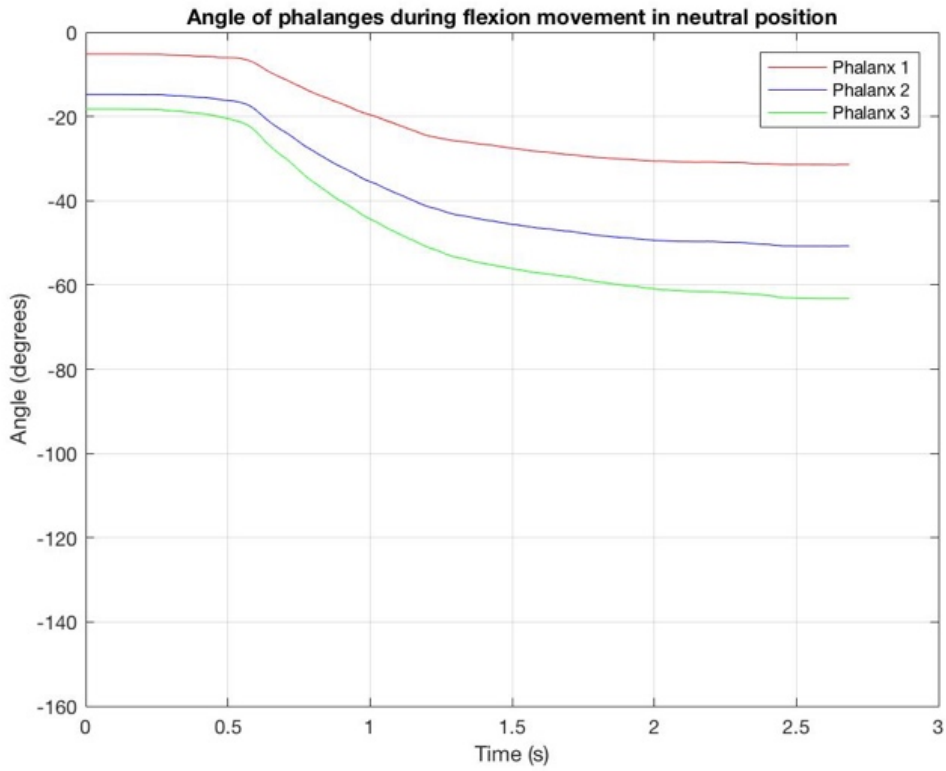


Figure 4-19 Plot of the angular displacement of the markers on each phalanx during flexion

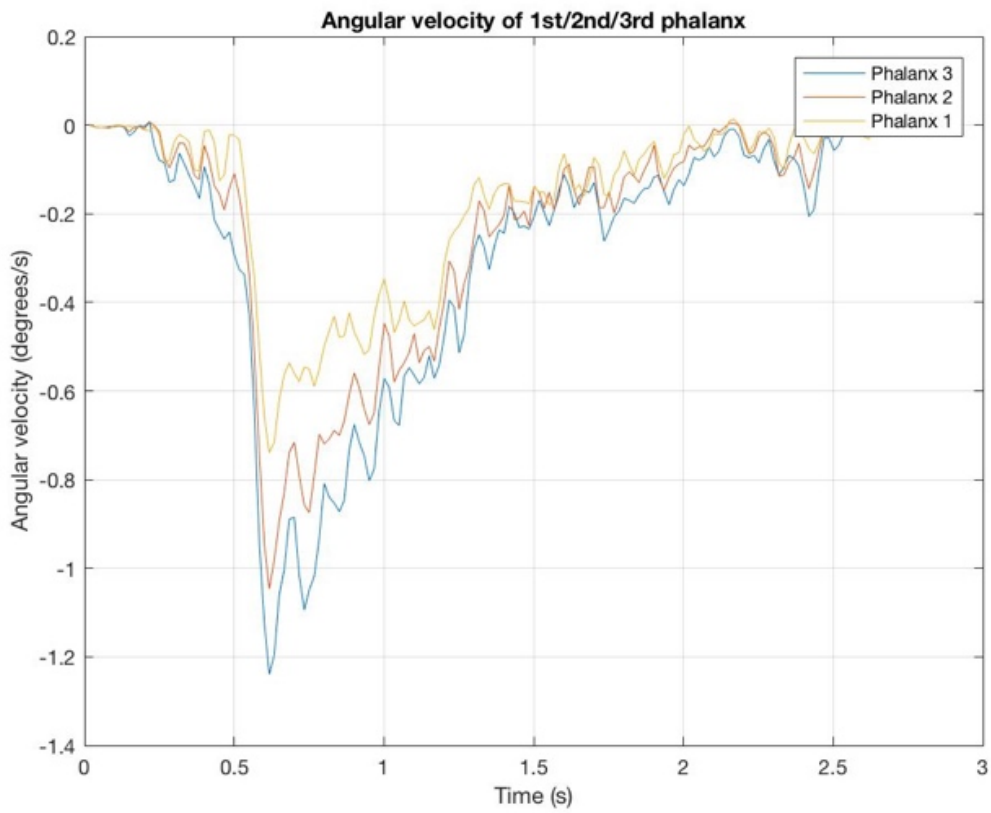


Figure 4-20 Plot of the angular velocity of the markers on each phalanx during flexion

The y-axis in the angle graph is scaled to the y-axis from the experiment on the wooden dummy hand, to show the difference in maximum obtained angle of the fingertip clearly. The maximum angle of the fingertip is obtained for every experiment, and the mean value is calculated for each test person separately. The mean maximum angle of all test persons together is 58.5° . The first two test persons are female, number three and four are male. Test person number three had larger hands than the other test persons, which could explain the reduced maximum angle since more force is needed to overcome the rigidity of the anatomical hand structure.

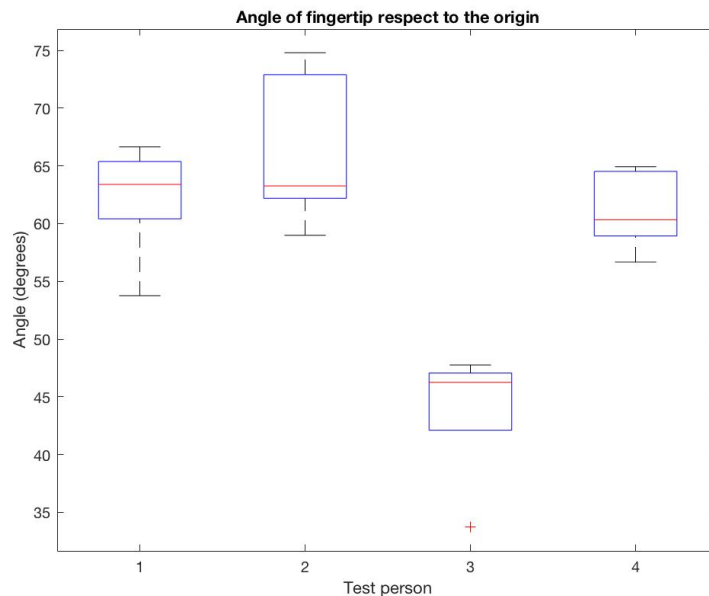


Figure 4-21 Boxplot of maximum angles of the fingertip for each test person

In the angular velocity plot, a clear peak is still visible and can be used to confront both situations. The maximum value of the peak of the angular velocity is calculated for every test person separately. Mean maximum angular velocity of all test persons is 1° /frame (which is considerably lower than 8.6° /frame on the wooden hand!)

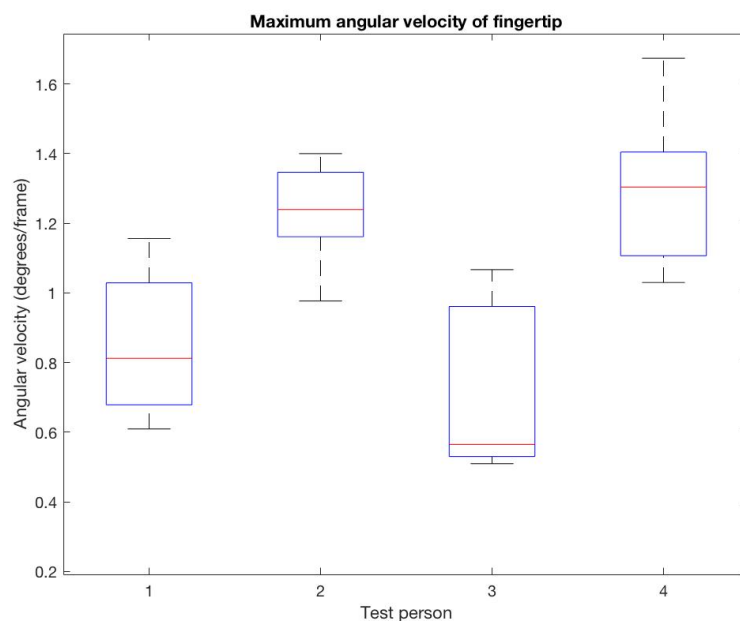


Figure 4-22 Boxplot of the angular velocity peaks of the fingertip of every test person

4.3 EMG Test

The final goal is to proceed to a functional test where implementation of the EMG signal in the control system will be tested. The goal is to demonstrate a final functional implementation of still usable muscle signal during the revalidation process. The EMG signal will be measured on the test persons' left arm and used to actuate the right arm as a mirror movement. An example of an activity of daily life is grasping a water bottle. In this test, the test person will grab a bottle with the left hand, while two actuated fingers on the right hand will follow this movement and mirror the movement while grasping a bottle which is placed near the palm of the right hand. After that, the test person will try to lift the bottle of the actuated hand to see if the grip is sufficient to keep the bottle lifted.

Test protocol

These measurements will be filmed from above and aside with a GoPro to show functionality. Currently, the orthosis is controlled by software on the computer. Characteristics of the current such as step, amount, and mode can be set and send to the SMA driver, which sends the current to the SMA wires. In this case, the current is set to 300 mA for 0.2 seconds of stimulation if the EMG signal activates the channel.

In this experiment, on the test persons' left forearm will be placed electrodes and connected to the Due module. The EMG signal will be measured and send in real-time through Bluetooth to the computer. The superficial flexor of the fingers is chosen as the muscle to take the EMG signal from. Since it is a superficial and large muscle, that also facilitates the task of positioning the bipolar electrodes on the forearm. The electrodes are placed as shown in the picture. The two electrodes on the right are connected to channel one and detect flexion of the index finger, while the two electrodes on the left are connected to channel 2 and detect flexion of the ring finger. The EMG signal of the two channels can be easily distinguished for a flexion movement of one of those two fingers.

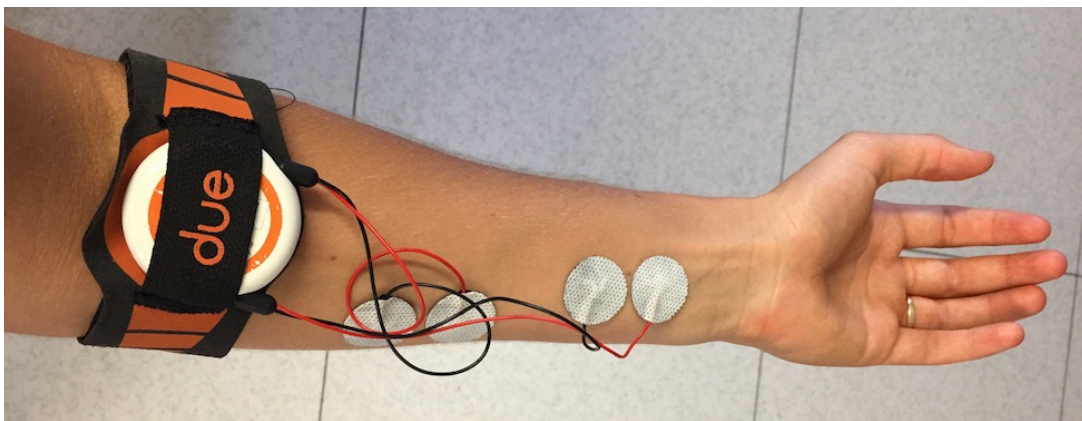


Figure 4-23 Placement of the surface electrodes. The left electrodes detect flexion of the ring finger, the electrodes on the right detect flexion of the index finger

Once the electrodes have been placed, and the system is connected to the PC, the values of the threshold can be set. In the software, the raw EMG signal is processed by taking the RMS value and envelope function to obtain a useful signal which can be compared with a lower and upper threshold, as explained in chapter 2.2. Once the signal exceeds the thresholds, the SMA driver will send current to the actuators. The lower and upper thresholds are set to 0.6 and 1 for the index finger, while they are set to 0.3 and 1 for the ring finger. Those values lead to a correct succession of exceeding the thresholds; therefore the current is supplied in the correct order on the channels. The EMG signal of each separate movement is easy to distinguish, which is a sign of correct positioning of the electrodes. These device settings lead to the flexion of the correct finger according to the signal read from the muscles.

Then, after having found useful threshold values, the setup of the test was as the previous test on a test person. The test person put on the glove, attached the actuator modules to the forearm, and connected the wires to the SMA driver. The screenshot below is of a video where an autonomous module fastening to the forearm is demonstrated. The patient is able to autonomously put on the glove and attach the modules in less than 20 seconds.

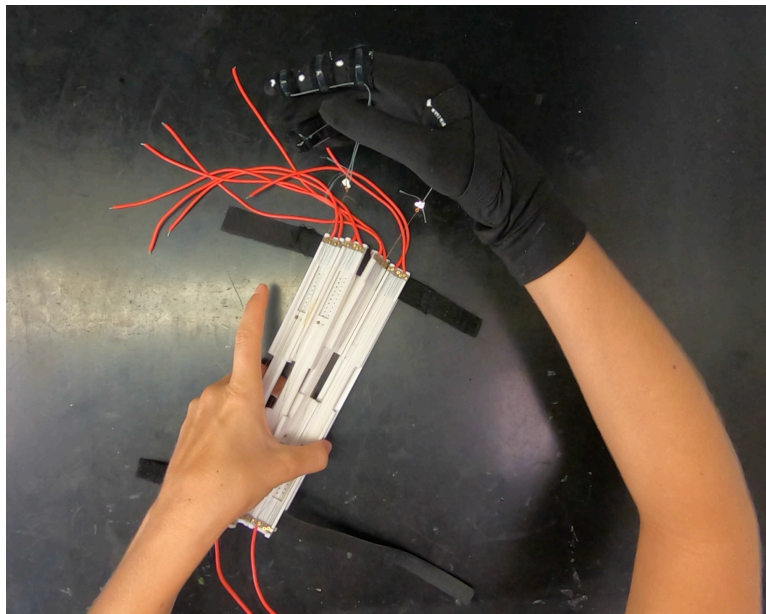


Figure 3-24 Screenshot of a video where autonomous donning is demonstrated

Two fingers will be actuated by four modules, two each mechanically linked. Initially, two fingers can be moved separately, stimulated by the EMG signal. Two different finger movements can be distinguished in the signal, which can be used to actuate two double modules separately.

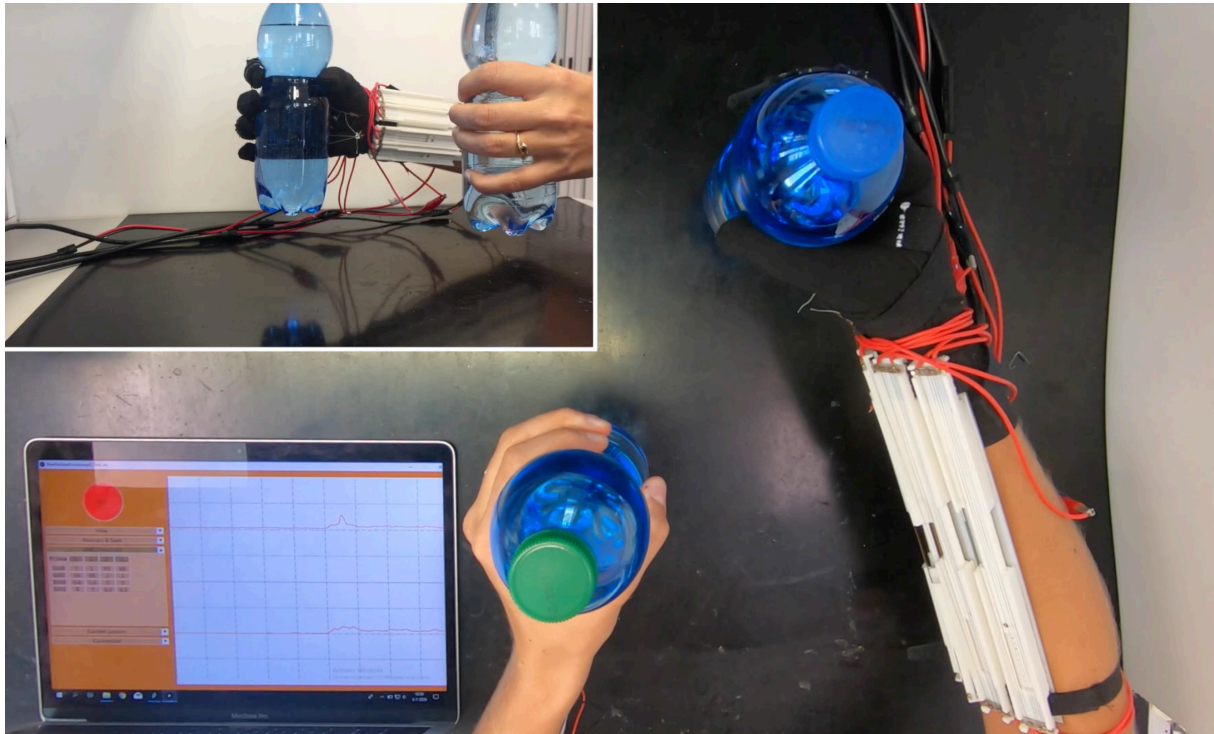


Figure 4-25 Final test to show the functionality of the orthosis by mirroring the movement of the left hand by using the EMG signal

The test is filmed from above and aside to have a clear view of the grasping movement and the ability to lift the bottle. This final test has a satisfying result, with an immediate stimulation of the modules on the right hand when the left hand grasps the bottle. The modules create sufficient grip to lift the bottle. When the grasp of the left hand finishes and the muscles are relaxed, the stimulation of the channels stops immediately. It takes a moment for the SMA wires to cool down and get back to their original state, losing grip on the right bottle which is then dropped.

Chapter 5: Conclusion and recommendations

This paper presents the prototyping of a glove for the rehabilitation of the hand piloted through the EMG signal taken from the forearm. The orthosis actuator is based on NiTiNol wires with a diameter of 0.1 mm. The design process of the prototyping started with a list of requirements and functional specifications. In this chapter, the fulfillment of these requirements will be checked after seeing a brief summary of the final prototype and results. Finally, recommendations for future improvements will be listed.

5.1 Conclusions

During the prototyping process, in particular, the following problems have been developed:

1) Realization of a modular mechanical actuator capable of flexing two fingers

The modules can be attached to the forearm with two elastic straps. Actuator pulleys are mounted on the modules to keep the SMA wire in an N-shaped configuration. It was decided to use a double wire for each actuator in order to produce more force which is needed to actuate the finger. When a stimulation current is sent from the SMA driver, the SMA wires in the module shorten and create an actuation force to bend the finger.

2) Realization of the glove with a tendon-like structure

The glove is made in lycra and reinforced with elastic bands near the sheaths that contain the nylon threads where the tendons pass. The actuators can be easily connected to the tendon system. At this moment only the tendons for the flexion of index and ring finger are realized, but this can easily be extended to the other two fingers, also for flexion movement. Two different sizes of gloves are made, typically for a men's and women's hand.

3) Improvement of the software interface between the EMG signal acquisition device and the SMA driver

The software is created in Processing and processes the EMG signal, takes the envelope function of the raw signal, compares it to a threshold and sends the stimulation signal to the SMA driver.

In the software have been added two functions, namely a button to stimulate all channels at the same time, and a button to stimulate the channels in a pattern with a 2-second break in between. Also, an option to insert the Due probe number based on the color code is now part of the software, to avoid changing it by hand before running the script.

Finally, a hysteresis cycle is introduced to compare the EMG envelope channel with a double threshold. This cycle will make the EMG driven system more smooth in its stimulations that are sent to the SMA driver.

Finally, it was possible, by driving two double actuators by utilizing the EMG signal taken from the DUE system, to perform the flexion movements of two fingers. The EMG signal measured

on the forearm could be distinguished for the movement of the index and ring finger separately. A flexion of these fingers triggered a stimulation to be sent to the modules linked to the same fingers on the other hand. With this movement, during the final test, a bottle could be grasped and lifted with the actuated fingers.

Also, some characterization tests have been conducted on a wooden hand and test persons. During tests on a wooden dummy hand, the finger always had a complete closure during a flexion movement. The average maximum velocity was $8.3^\circ/\text{frame}$ for a flexion movement in a neutral position.

However, during tests on test persons occurred that a double actuator placed in series allowed the fingertip to flex 58.5° , which is 38% of the movement respect to the dummy hand. The loss of efficiency is due to the increase in frictions of the human anatomy respect to wooden joints. The same typical peak at the angular velocity occurred, which was on average $1^\circ/\text{frame}$ for all test persons.

Control of the established specifications can be checked according to the functional requirements. For every requirement is evaluated whether the prototype satisfies the functional specifications.

1) Wearability

The new prototype can be moved around freely by a user while wearing the device. The soft interface of the glove makes it easy to put on and off and fits for different hand sizes. The wires are inserted in a rigid container and therefore are not anymore loose in the air. As shown in a video registration of the procedure of putting the device on, a patient would be able to don and doff the device itself within a limited amount of time. Therefore we can say that the requirement of wearability is fulfilled.

A significant improvement would be easier cable management, a plug-and-play system for the current cables would improve wearability even more. For a complete wearable solution, the system should be portable without any cable attachments to the power supply. In that case, a portable power source which is not too cumbersome is the biggest concern.

2) Adaptability/modularity

The newly designed modules are adjustable in length, and therefore adaptable to different test persons. Changing the length, also the amount of used SMA wire is different, which can be applied for different requested shortening of the cable or needed force for actuation. With a bolt and nut, the two different sliding parts of the module can be fixed at a certain length. The modules have a connection interface with edges on top and below to be clicked together to other modules. All connections and fabrics are made of elastic material to keep the system available for a vast range of different body sizes.

The modules are universal devices which can be linked to different fingers. This design can be fitted to many patients and can be adjusted for specific rehabilitation protocols.

3) Movement function

The final prototype can be attached to any finger, except the thumb. Currently, two fingers can be actuated at the same time. The modules are universal and can be easily switched to another finger by merely connecting the SMA wire to another tendon. For actuation of four fingers with double modules, the SMA driver has to be extended to 8 channels.

During an experiment on test persons, however, complete closure was not reached.

4) Weight and size

The final module weighs almost 50 grams, the complete set of 4 modules for two fingers and the glove weighs 200 grams, which is lightweight. Most of this weight is added last-minute because of the extra attached reinforcing brass rod to avoid bending of the module. If the module would be made of more stiff material, this weight can be significantly reduced by removing this rod. The container is made of PLA, which is very light, the SMA cables are extremely thin and have a negligible weight in the total construction.

The modules have an interface which makes them suitable to click one on top of another, this reduces the size of modules around the forearm.

The system is underactuated since the wire actuates one finger with 3 Degrees of Freedom, and therefore the complexity of the system is reduced.

5) Safety and comfort

The requirements for safety and comfort have been addressed since the glove has a soft interface with a joint-less interface. There is no rigid actuation system which can cause damage to the human hand. The container is rigid and creates a layer between the human skin and the wires which tend to become very hot because of the Joule effect.

Unfortunately, the current wires are still connected to the SMA driver with a clamp connection. If four modules are connected with eight different cables, this causes a chaotic situation where easily a short circuit could appear. This could be improved with a closed plug-and-play connection.

5.2 Recommendations

Many works are still to be investigated and developed to improve the orthosis. For every part of the system, a few suggestions are written as points of attention for improvement.

SMA Modules

- Insert a **plug & play system** to improve cable management.
- **Reduce friction** on the pulleys. This will improve the amount of force that is available and transferred to the fingers. The force lost by friction can be quantified by using a load cell.
- **Increase shortening** of the SMA wires. This could be done by increasing the amount of SMA wire available for shortening. If one single module could reach a sufficient

shortening for actuating one finger, doubles modules would not be needed anymore, resulting in only half of the SMA channels needed.

- Make the system **more robust**, since many parts are handmade and fragile if not handled well by inexperienced users.
- **Change the support material** of the modules since PLA is not rigid enough to avoid bending when the SMA wires are activated. Currently, brass and aluminum rods are used to strengthen the construction. Therefore, the modules can no longer be stacked on top of each other.

SMA Driver

- Ideally, the SMA driver is **miniaturized and made portable** for the patient to have a completely portable device which can be used everywhere. The biggest concern is to have a portable power source which is sufficient for autonomous use for a limited amount of time.
- **Increase** the number of **channels** for stimulation. Currently, four channels are available to stimulate the SMA wire modules, where for every movement two channels are needed. The infrastructure to link multiple SMA drivers and thereby increasing the number of channels is already available but only needs to be enabled by means of a number of adjustments.

Glove

- **Extend tendon infrastructure** to all fingers, for both flexion as extension movement. Currently, the tendons are only attached to the index and ring finger. This can be easily extended but is a precise and intensive work by hand.
- Create an option for **thumb movement**. Currently, only the other fingers are available for actuation. The thumb has a more complex anatomical interface and requires a different kind of actuation which is harder with an underactuated tendon-like and jointless system.

EMG signal

- Ideally, the EMG surface signal can be measured on the forearm that needs to be actuated. Currently, the modules are attached to the forearm and therefore the intended place to attach the electrodes is already occupied.

Acknowledgements

I would like to express my deep gratitude to Professor Gazzoni and Dr. Gigi Cerone, my research supervisors, for their guidance, assistance, and useful critiques of this research work. Also, a special thanks to Davide for all the help with the hardware related questions and helping me to find my way around the laboratory. I would also like to thank all the staff and people at LISiN for having supported me throughout the year. Not only for the nice moments, coffee and cake we have shared in the laboratory, but also for being test persons for the experiments in this research.

During my master degrees I could not have missed the support of my colleagues Maria, Mayra, Antonio and Giovanni, not in the last place for extending my Italian vocabulary with their local expressions which helped me to go incognito in this beautiful country.

A special thanks to my dear friend Christian who made me feel at home in Turin and was always available to go out for adventure and talk about anything but study. Also my Argentinian colleague Maxi was always available and thanks to him I was not the only foreigner in class. Thank you to my roommates Beatrice and Clarissa, for all the good advice and making me feel at home.

My special thanks to my friends and colleagues who all took the effort, even multiple times, to visit me but also support me on a distance, Tobias, Rebecca, Laura and Amanda.

Last but not least, thank you to my wonderful family for giving me the occasion to study in Turin and the non-stop support and love I received.

Bibliography

- [1] S. Katz, "Assessing self-maintenance: activities of daily living, mobility, and instrumental activities of daily living," *J. Am. Geriatr. Soc.*, vol. 31, no. 12, pp. 721–721, 1983.
- [2] G. Mackay, Judith; Mensah, "The atlas of heart disease and stroke," in *The atlas of heart disease and stroke*, Geneva: World Health Organization, 2004.
- [3] SPARC The Partnership for Robotics in Europe, "Robotics 2020 Multi-Annual Roadmap for Robotics in Europe," 2015.
- [4] Ministero della Salute, "www.salute.gov.it," 2013. [Online]. Available: http://www.salute.gov.it/portale/salute/p1_5.jsp?lingua=italiano&id=28&area=Malattie_cardiovascolari. [Accessed: 22-Oct-2018].
- [5] K. Bütefisch, C; Hummelsheim, H; Denzler, P; Mauritz, "Repetitive training of isolated movements improves the outcome of motor rehabilitation of the centrally paretic hand," *J. Neurol. Sci.*, vol. 130, no. 1, pp. 59–68.
- [6] G. B. Prange, M. J. A. Jannink, C. G. M. Groothuis-Oudshoorn, H. J. Hermens, and M. J. IJzerman, "Systematic review of the effect of robot-aided therapy on recovery of the hemiparetic arm after stroke," *J. Rehabil. Res. Dev.*, vol. 43, no. 2, pp. 171–184, 2006.
- [7] H. M. Feys *et al.*, "Effect of a therapeutic intervention for the hemiplegic upper limb in the acute phase after stroke: A single-blind, randomized, controlled multicenter trial," *Stroke*, vol. 29, no. 4, pp. 785–792, 1998.
- [8] J. Filippi, "Prototipazione di un'ortesi tendon-like a controllo mioelettrico attuata da fili nitinol," Politecnico di Torino, 2017.
- [9] A. Adatto, "Prototipazione di un'ortesi a controllo mioelettrico per la mobilizzazione assistita del singolo dito," Politecnico di Torino, 2018.
- [10] R. Drake, A. W. Vogl, and M. Adam, *Gray's Anatomy for Students*, 2nd ed. Churchill Livingstone, 2009.
- [11] P. Heo, G. M. Gu, S. jin Lee, K. Rhee, and J. Kim, "Current hand exoskeleton technologies for rehabilitation and assistive engineering," *Int. J. Precis. Eng. Manuf.*, vol. 13, no. 5, pp. 807–824, 2012.
- [12] A. Hollister and D. J. Giurintano, "Thumb Movements, Motions, and Moments," *J. Hand Ther.*, vol. 8, no. 2, pp. 106–114, 1995.
- [13] F. Netter, *Atlas of human anatomy*. 2014.
- [14] A. B. Swanson, I. B. Matev, and G. de Groot, "The strength of the hand.," *Bull. Prosthet. Res.*, pp. 145–153, 1970.
- [15] NASA, "NASA-STD-3000 Man-System Integration Standards," 1995.
- [16] A. Kargov, C. Pylatiuk, J. Martin, S. Schulz, and L. Döderlein, "A comparison of the grip force distribution in natural hands and in prosthetic hands," *Disabil. Rehabil.*, vol. 26, no. 12, pp. 705–711, 2004.
- [17] C. Y. Chu and R. M. Patterson, "Soft robotic devices for hand rehabilitation and assistance: A narrative review," *J. Neuroeng. Rehabil.*, vol. 15, no. 1, pp. 1–14, 2018.
- [18] P. Polygerinos, K. C. Galloway, S. Sanan, M. Herman, and C. J. Walsh, "EMG controlled soft robotic glove for assistance during activities of daily living," *IEEE Int. Conf. Rehabil. Robot.*, pp. 55–60, 2015.
- [19] P. Polygerinos, Z. Wang, K. C. Galloway, R. J. Wood, and C. J. Walsh, "Soft robotic glove for combined assistance and at-home rehabilitation," *Rob. Auton. Syst.*, vol. 73,

- pp. 135–143, 2015.
- [20] H. K. Yap, J. H. Lim, F. Nasrallah, and C. H. Yeow, “Corrigendum: Design and preliminary feasibility study of a Soft Robotic Glove for hand function assistance in Stroke Survivors,” *Front. Neurosci.*, vol. 11, no. 547, pp. 1–14, 2017.
- [21] B. Wang, A. Mcdaid, M. Biglari-abhari, and K. C. Aw, “Design and Development of a Glove for Post - Stroke Hand Rehabilitation,” *IEEE Int. Conf. Adv. Intell. Mechatronics*, pp. 1047–1051, 2017.
- [22] L. Connelly, Y. Jia, M. L. Toro, M. E. Stoykov, R. V Kenyon, and D. G. Kamper, “A Pneumatic Glove and Immersive Virtual Reality Environment for Hand Rehabilitative Training After Stroke,” vol. 18, no. 5, pp. 551–559, 2010.
- [23] B. B. Kang, H. Lee, H. In, U. Jeong, J. Chung, and K. J. Cho, “Development of a polymer-based tendon-driven wearable robotic hand,” *Proc. - IEEE Int. Conf. Robot. Autom.*, pp. 3750–3755, 2016.
- [24] B. H. In, B. B. Kang, M. Sin, and K. Cho, “A Wearable Robot for the Hand with a Soft Tendon Routing System,” *IEEE Robot. Autom. Mag.*, no. March 2015, pp. 97–105.
- [25] D. Popov, I. Gaponov, and J. Ryu, “Portable Exoskeleton Glove With Soft Structure for Hand Assistance in Activities of Daily Living,” *IEEE/ASME Trans. Mechatronics*, vol. 22, no. 2, pp. 865–875, 2017.
- [26] I. Jo, S. Member, J. Lee, Y. Park, and S. Member, “Design of a Wearable Hand Exoskeleton for Exercising Flexion / Extension of the Fingers,” in *2017 International Conference on Rehabilitation Robotics (ICORR)*, 2017, pp. 1615–1620.
- [27] M. Cempini *et al.*, “Kinematics and Design of a Portable and Wearable Exoskeleton for Hand Rehabilitation,” in *2013 IEEE International Conference on Rehabilitation Robotics*, 2013.
- [28] H. In, K. Cho, K. Kim, and B. Lee, “Jointless Structure and Under-Actuation Mechanism for Compact Hand Exoskeleton,” in *2011 IEEE International Conference on Rehabilitation Robotics Rehab Week Zurich, ETH Zurich Science City, Switzerland*, 2011.
- [29] B. W. Gasser, D. A. Bennett, C. M. Durrrough, and M. Goldfarb, “Design and Preliminary Assessment of Vanderbilt Hand Exoskeleton,” in *2017 International Conference on Rehabilitation Robotics (ICORR) QEII Centre, London, UK, July 17-20, 2017*, 2017, pp. 1537–1542.
- [30] A. Hadi, K. Alipour, S. Kazeminasab, and M. Elahinia, “ASR glove : A wearable glove for hand assistance and rehabilitation using shape memory alloys,” *J. Intell. Mater. Syst. Struct.*, vol. 29, no. 8, pp. 1575–1585, 2018.
- [31] Z. Yao, C. Linnenberg, A. Argubi, R. Weidner, and J. P. Wulfsberg, “Biomimetic design of an ultra - compact and light - weight soft muscle glove,” *Ger. Acad. Soc. Prod. Eng.*, vol. 11, pp. 731–743, 2017.
- [32] T. Tang, D. Zhang, T. Xie, and X. Zhu, “An exoskeleton system for hand rehabilitation driven by shape memory alloy An Exoskeleton System for Hand Rehabilitation Driven by Shape Memory Alloy,” in *Proceeding of the IEEE International Conference on Robotics and Biomimetics (ROBIO) Shenzhen, China*, 2013, no. December.
- [33] C. S. Loh, H. Yokoi, and T. Arai, “New Shape Memory Alloy Actuator : Design and Application in the Prosthetic Hand,” in *Proceedings of the 2005 IEEE Engineering in Medicine and Biology 27th Annual Conference Shanghai, China*, 2005, pp. 6900–6903.
- [34] W. Wang and S. Ahn, “Shape Memory Alloy-Based Soft Gripper with Variable Stiffness for Compliant and Effective Grasping,” *Soft Robot.*, vol. 4, no. 4, pp. 379–389, 2017.
- [35] A. Villoslada, M. Bionics, A. Flores-caballero, D. Copaci, and D. Blanco, “High-

- displacement flexible Shape Memory Alloy actuator for soft wearable robots High-displacement flexible Shape Memory Alloy actuator for soft wearable robots,” Madrid, 2014.
- [36] C. Motta, “Fili SMA come attuatori indossabili: uno studio di fattibilità,” Politecnico di Torino, 2015.
- [37] C. J. Nycz, M. A. Delph, and G. S. Fischer, “Modeling and design of a tendon actuated soft robotic exoskeleton for hemiparetic upper limb rehabilitation,” *Proc. Annu. Int. Conf. IEEE Eng. Med. Biol. Soc. EMBS*, vol. 2015-Novem, pp. 3889–3892, 2015.
- [38] K. N. An, E. Y. Chao, W. P. Cooney, and R. L. Linscheid, “Forces in the normal and abnormal hand,” *J. Orthop. Res.*, vol. 3, no. 2, pp. 202–211, 1985.
- [39] M. C. F. de Castro and A. Cliquet, “An artificial grasping evaluation system for the paralysed hand,” *Med. Biol. Eng. Comput.*, vol. 38, pp. 275–280, 2000.
- [40] T. Chen and P. S. Lum, “Hand rehabilitation after stroke using a wearable, high DOF, spring powered exoskeleton,” *Proc. Annu. Int. Conf. IEEE Eng. Med. Biol. Soc. EMBS*, vol. 2016-Octob, pp. 578–581, 2016.

